

## Chemistry, structure and properties of rare-earth containing Si-Al-O-N glasses

**Citation for published version (APA):**

Graaf, de, D. (2004). *Chemistry, structure and properties of rare-earth containing Si-Al-O-N glasses*. [Phd Thesis 1 (Research TU/e / Graduation TU/e), Chemical Engineering and Chemistry]. Technische Universiteit Eindhoven. <https://doi.org/10.6100/IR571796>

**DOI:**

[10.6100/IR571796](https://doi.org/10.6100/IR571796)

**Document status and date:**

Published: 01/01/2004

**Document Version:**

Publisher's PDF, also known as Version of Record (includes final page, issue and volume numbers)

**Please check the document version of this publication:**

- A submitted manuscript is the version of the article upon submission and before peer-review. There can be important differences between the submitted version and the official published version of record. People interested in the research are advised to contact the author for the final version of the publication, or visit the DOI to the publisher's website.
- The final author version and the galley proof are versions of the publication after peer review.
- The final published version features the final layout of the paper including the volume, issue and page numbers.

[Link to publication](#)

**General rights**

Copyright and moral rights for the publications made accessible in the public portal are retained by the authors and/or other copyright owners and it is a condition of accessing publications that users recognise and abide by the legal requirements associated with these rights.

- Users may download and print one copy of any publication from the public portal for the purpose of private study or research.
- You may not further distribute the material or use it for any profit-making activity or commercial gain
- You may freely distribute the URL identifying the publication in the public portal.

If the publication is distributed under the terms of Article 25fa of the Dutch Copyright Act, indicated by the "Taverne" license above, please follow below link for the End User Agreement:

[www.tue.nl/taverne](http://www.tue.nl/taverne)

**Take down policy**

If you believe that this document breaches copyright please contact us at:

[openaccess@tue.nl](mailto:openaccess@tue.nl)

providing details and we will investigate your claim.

# **Chemistry, Structure and Properties of Rare-Earth Containing Si-Al-O-N Glasses**

PROEFSCHRIFT

ter verkrijging van de graad van doctor  
aan de Technische Universiteit Eindhoven,  
op gezag van de Rector Magnificus, prof.dr. R.A. van Santen,  
voor een commissie aangewezen door het College voor Promoties  
in het openbaar te verdedigen  
op woensdag 14 januari 2004 om 16.00 uur

door

Dennis de Graaf

geboren te Purmerend

Dit proefschrift is goedgekeurd door de promotoren:

prof.dr. G. de With

en

prof.dr. S. Hampshire

Copromotor:

dr. H.T.J.M. Hintzen

Druk: Universiteitsdrukkerij Technische Universiteit Eindhoven

Kaftontwerp: J.W. Luiten, JWL Producties

CIP-DATA LIBRARY TECHNISCHE UNIVERSITEIT EINDHOVEN

Graaf, Dennis de

Chemistry, structure and properties of rare-earth containing Si-Al-O-N glasses / by Dennis de Graaf. – Eindhoven : Technische Universiteit Eindhoven, 2004.

Proefschrift. – ISBN 90-386-2805-6

NUR 913

Trefwoorden: keramische materialen; glas / aluminiumsilicaten; Si-AL-O-N / zeldzame aardmaterialen / luminescentie / siliciumnitriden

Subject headings: ceramic materials; glass / aluminosilicate glasses; Si-Al-O-N / rare earth metals / luminescence / silicium nitrides

*The rare earths perplex us in our researches, baffle us in our speculations, and haunt us in our very dreams. They stretch like an unknown sea before us, mocking, mystifying and murmuring strange revelations and possibilities*

*Sir William Crookes, 1902*



# Table of contents

---

Chapter I	Introduction	7
	1.1 General Introduction	8
	1.2 Si-Al-O-N glasses	8
	1.3 Synthesis of oxynitride glasses	12
	1.4 The rare earths and luminescence	14
	1.5 Scope and outline of this thesis	15
Chapter II	EPMA/WDS as a tool to analyze the local chemical composition of Si-Al-O-N glasses	17
	2.1 Introduction	18
	2.2 Principles and problems for the analysis of Si-Al-O-N glasses using EPMA/WDS	18
	2.3 Experimental procedure	21
	2.4 Results and discussion	24
	2.5 Conclusions	28
Chapter III	Redox behavior of iron in Si-Al-O-N melts; formation of iron silicides	29
	3.1 Iron and the transparency of Si-Al-O-N glasses	30
	3.2 Experimental procedure	30
	3.3 Results and discussion	31
	3.4 Conclusions	33
Chapter IV	Determination of the oxidation state of Eu by magnetic measurements	35
	4.1 Introduction	36
	4.2 Experimental	38
	4.3 The oxidation state of europium	39
	4.4 Conclusions	41

Chapter V	Eu <sup>2+</sup> luminescence in Si-Al-O-N glasses	43
	5.1 Introduction	44
	5.2 Experimental	45
	5.3 The oxidation state of europium	47
	5.4 Optical properties of (Eu,Y)-Si-Al-O-N glasses	47
	5.5 Conclusions	51
Chapter VI	Ce <sup>3+</sup> luminescence in Si-Al-O-N glasses	53
	6.1 Introduction	54
	6.2 Experimental	55
	6.3 Results and discussion	56
	6.4 Conclusions	61
Chapter VII	Tb <sup>3+</sup> distribution and luminescence	63
	7.1 Introduction	64
	7.2 Experimental	65
	7.3 Results	67
	7.4 Discussion	70
	7.5 Conclusions	71
Chapter VIII	Mixed oxidation states of Yb and Sm	73
	8.1 Introduction	74
	8.2 Experimental	75
	8.3 Results	76
	8.4 Discussion	81
	8.5 Conclusions	83
Chapter IX	Hardness and indentation size effect in Si-Al-O-N glasses	85
	9.1 Introduction	86
	9.2 Experimental	88
	9.3 Results and discussion	89
	9.4 The influence of the modifier cation	94
	9.5 Conclusions	95

Chapter X: Slow crack growth in Si-Al-O-N glasses	97
10.1 Introduction	98
10.2 Experimental	98
10.3 Results and discussion	100
10.4 Conclusions	104
Chapter XI: Thermal properties of Si-Al-O-N glasses	105
11.1 Introduction	106
11.2 Experimental	106
11.3 Results and discussion	109
11.4 Conclusions	117
Summary	121
Samenvatting	125
Dankwoord	129
List of Publications	131
Curriculum Vitae	133





# Chapter I

---

Introduction

## 1.1 General introduction

Most people recognize glass as a useful companion in their everyday life. They are able to name a number of large-scale see-through applications such as windows, bottles, television screens, etc. From that perspective it is hard to understand that there is a need for new glasses. Especially if you realize, that the basic recipe for commodity glass has not changed in the past thousands of years. But glass is an evolving material and so are the demands on it. New applications ask for glasses, which are stronger, which are less likely to deteriorate in aggressive chemical environments or which have advantageous optical properties. One example can be found in the field of communication. Fibre optics have enabled us to transfer large quantities of data with the speed of light. With that glass fibre network comes a whole range of glassy optical devices in order to manage and distribute these data flows. In order to increase the capacity and reliability of that data transport systems new glasses have to be developed. Another example can be found among the glasses for lighting applications. As lamp envelopes are become smaller and the light output higher, the working temperature increases. This means that the glasses have to be able to withstand higher temperatures and yet remain unaffected by the aggressive chemical environment within the lamp envelope.

A glass basically consists of cations and anions. One can alter the properties of a glass by changing the chemical composition, by adding new components or by replacing one component for another. In the pursuit of new glasses many researchers have worked on the effects that different types of cations have on the various properties of glass. In these investigations oxygen is the sole anion present in the glass. At this moment we are reaching the limits of what can be achieved by cation replacement, so our effort is shifted towards the anions. In this thesis we create oxynitride glasses by partially replacing the oxygen in the glass by nitrogen and try to stretch the limits of glass a bit further.

## 1.2 Si-Al-O-N glasses

The first publications on oxynitride glasses started to appear in the late 60's. It was accidentally discovered that oxygen, which is present in the glass structure, could be replaced by nitrogen by a reaction between molten glass and  $\text{NH}_3$ , hence producing an oxynitride glass [1,2].

It cannot exactly be said that discovery of the existence of oxynitride glasses shook the scientific world; in fact it was hardly noticed. Nor did anyone at that time realise the potential of such glasses, so research towards these glasses was more or less abandoned for a while. It was only in the seventies that large-scale investigations towards the properties and structure of such glasses were started [3]. Curiously enough it was not the glass-, but the ceramic world, which provided justification for the research. In that period the interest in ceramic materials for technological applications was rapidly growing and it was realized that ceramic materials based on silicon nitride are very interesting since they show an excellent mechanical performance at high temperatures.

On the downside these materials generally show a poor sinterability. Using high temperatures can solve this, but then the nitrogen pressure has to be increased to prevent thermal decomposition of the silicon nitride, which makes the process unattractive for commercial purposes. In order to facilitate the sintering process, one often has to turn to sintering aids such as  $Y_2O_3$  and  $Al_2O_3$  [4]. Together with the present silicon nitride and silicon oxide (oxidation product from silicon nitride) an oxynitride melt is formed which acts as a transport medium during sintering. This melt is very stable and partly remains as a glassy phase at the grain boundary, as is illustrated in figure 1.1.

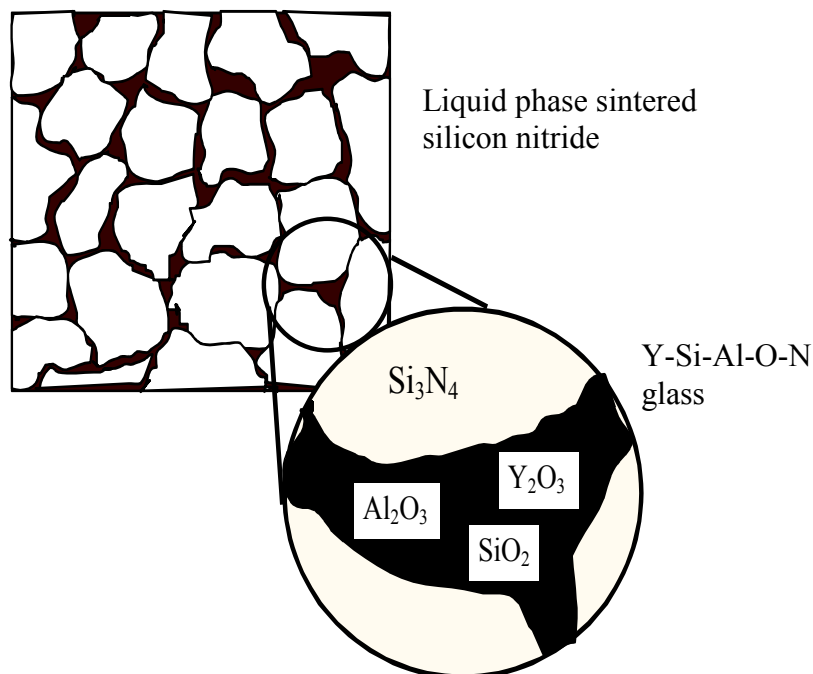


Fig. 1.1 *Schematic representation of liquid-phase sintered silicon nitride and the intergranular oxynitride phase.*

This residual glass phase has a negative effect on the mechanical properties of the ceramics, because the mechanical resistance of the glasses is by far inferior to that of the silicon nitride. This was the reason for a number of groups to start investigating the properties of these glasses. Improvement of the mechanical resistance of these glasses would have a beneficial effect on the mechanical properties of the sintered silicon nitride.

Very soon it became apparent that the mechanical properties of oxynitride glasses differ considerably from the properties of oxide glasses. Generally speaking these glasses display an enhanced mechanical, thermal and chemical durability upon nitrogen incorporation. The glass becomes less susceptible to chemical attack by acids, bases and water [5]. In contrast to oxide glasses the oxynitride glasses are susceptible to oxidation, but this is only a problem at temperatures approaching the glass transition temperature [6,7].

The most pronounced effects can be found in the mechanical properties. Oxynitride glasses display a rigidity [8], hardness and fracture toughness [9], which is far higher than for the conventional oxide glasses. Moreover the glasses show to be extremely resistant against water-assisted subcritical crack growth, which is a major cause for failure among the oxide glasses [10]. The thermal properties are also affected by the incorporated nitrogen resulting a very high glass transition temperature and a low thermal expansion coefficient [11]. The origin of this effect can be found in the structure of these glasses.

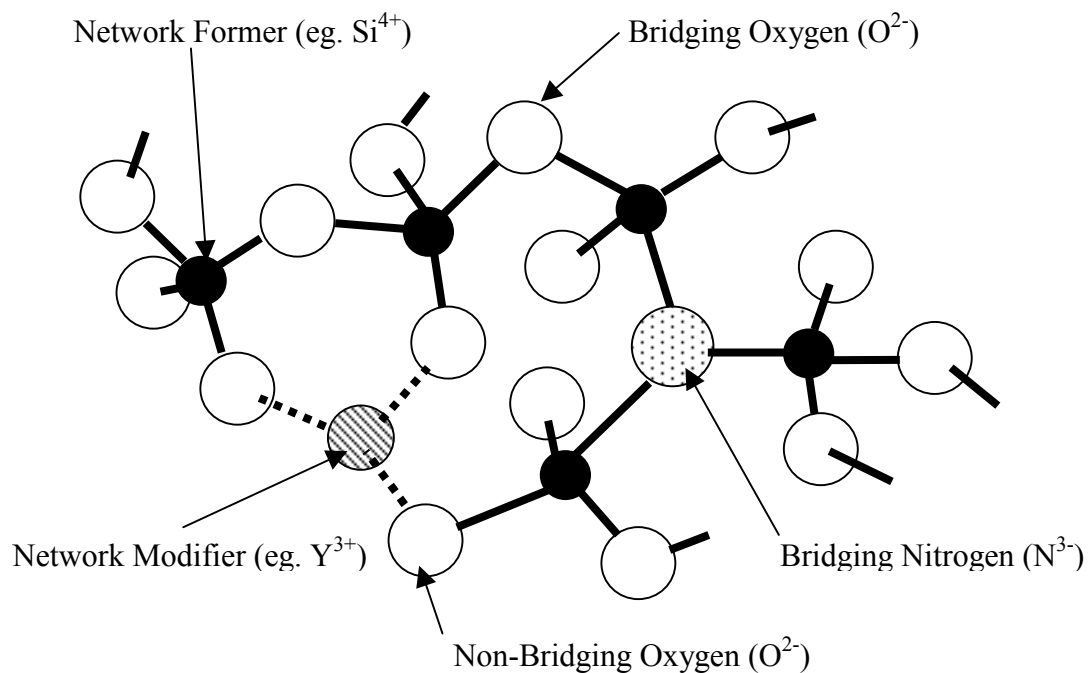


Fig. 1.2 *Schematic representation identifying the most important elements in the oxynitride glass structure.*

The structure of oxynitride glasses is similar to that of oxide glasses. It consists of two types of cations: network forming and network modifying cations [12]. In contrast to oxide glasses two types of anions are present: oxygen ( $O^{2-}$ ) and nitrogen ( $N^{3-}$ ), see figure 1.2.

Network formers are small cations with a high electronegativity, such as silicon, aluminium, boron and germanium. The oxidation state of these cations must be equal to, or larger than three. These elements are able to form covalent bonds with oxygen and nitrogen.

Network modifiers are cations with a low electronegativity. Most cations fall in this class of elements, as do the rare earth ions. Their oxidation should be equal to, or lower than three. They are coordinated by oxygen with which they form ionic bonds.

The glass network, which gives a glass its strength, consists of a framework of network forming cations, which are bound together by oxygen. Oxygen atoms, which connect two network former cations, are usually referred to as bridging oxygen. The modifier cations locally weaken the largely covalent network by introducing ionic bonds, which are less strong. These ‘flaws’ in the network give a glass its viscous nature. The oxygen atoms, which are connected to the modifier cations by ionic bonds, are called non-bridging oxygen.

If we now replace some of the oxygen by nitrogen it will have a large effect on the structure. Nitrogen will form covalent bonds with the network forming cations similar to bridging oxygen [13]. The oxidation state of nitrogen is 3- whereas that of oxygen is only 2-. Nitrogen is therefore able to bind three network-forming cations whereas oxygen can bind only two at most. This means that the bond structure of the glass network is altered and this results in a change of the glass properties.

In this study we create Si-Al-O-N glasses containing one or more rare earth ions. There is some confusion over the definition of the term rare earth (RE) element. Strictly speaking the term refers to the lanthanide series, that is those elements that have a partly-filled 4f orbital (cerium (Ce) to lutetium (Lu)). Usually lanthanum (La) is also included in the lanthanide series. However, when we view the periodic table as a grouping of elements with similar chemical characteristics then we can also count the transition metals scandium (Sc) and yttrium (Y) to the rare earths. Since this is the most widely used definition we will also use it here.

According to the Zachariasen rules [12] the rare earths can be classified as modifier cations. Compared to other modifiers like the alkaline earth and alkali ions the incorporation of the rare earths leads to a more rigid glass structure and consequently to an enhanced (mechanical) performance [14]. This explains our interest in RE-containing glasses.

### 1.3 Synthesis of oxynitride glasses

There are a number of routes available for the synthesis of oxynitride glasses. One can start by direct incorporation of the nitrogen in the raw materials or, alternatively, by nitriding an oxide glass [6]. The most widely used method is the incorporation of a nitride in the starting materials. In principle many nitrides can be used for this purpose but in practice only  $\text{Si}_3\text{N}_4$  and  $\text{AlN}$  are used since silicon and aluminium are the basic constituents of a Si-Al-O-N glass. In this study  $\text{Si}_3\text{N}_4$  is used.

The main differences between the melting of a Si-Al-O-N glass and oxide glasses are the need for higher temperatures (1600-1800 °C) and an inert atmosphere ( $\text{N}_2$ ). Therefore a furnace set-up as sketched in figure 1.3 is needed, which allows melting of the glasses at high temperatures but also offers the possibility to retract the samples from the furnace quickly in order to quench them.

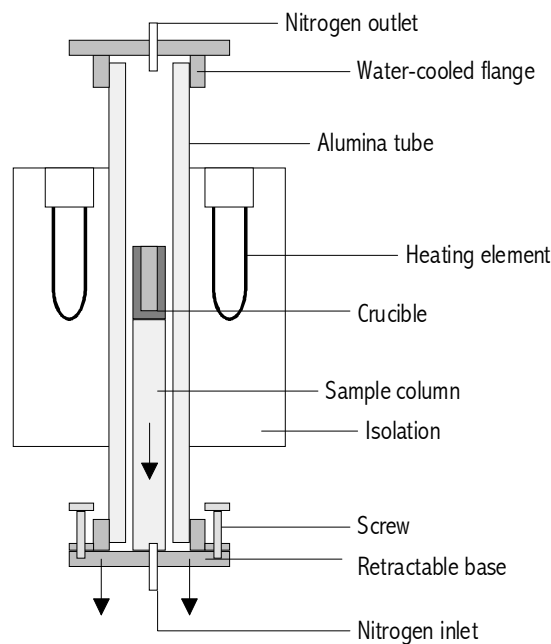


Fig. 1.3 *Vertical tube furnace designed for the preparation of Si-Al-O-N glasses.*

This rapid cooling or quenching is necessary since the vitreous state is inherently meta-stable and would crystallise when cooled too slowly. Not all the compositions in the Si-Al-O-N system can be turned into a glass. Whether or not a composition can be obtained in the amorphous state is dependent on the ease by which it crystallises, the cooling rate and the melting temperature. This so-called glass-forming region is displayed for Mg-Si-Al-O-N glasses in figure 1.4 for a melting temperature of 1700 °C and natural cooling.

This glass-forming region, which is fairly similar for most Si-Al-O-N glasses, implies that only a limited amount of nitrogen (usually <10 at%) can be incorporated in these glasses. Higher amounts are possible but require higher melting temperatures and faster cooling rates.

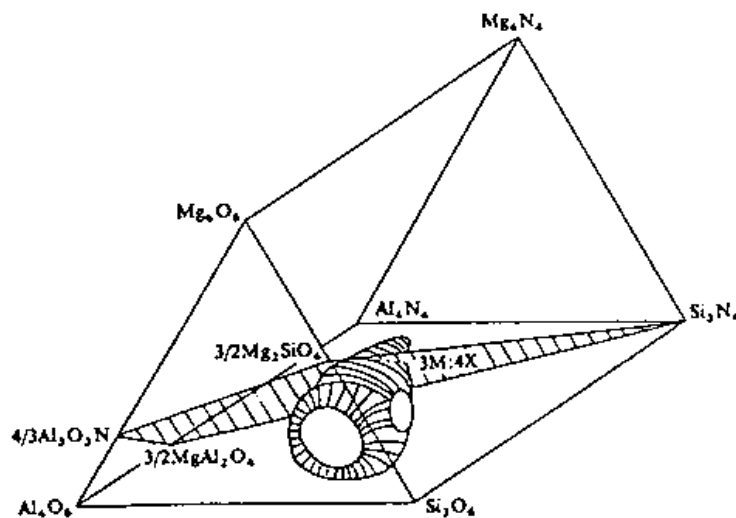


Fig. 1.4 Glass forming region (hatched volume) at 1700 °C in the Mg-Si-Al-O-N system and corresponding crystalline phases [15].



## 1.4 The rare earths and luminescence

Many of the rare earth ions display luminescence, a characteristic, which will be investigated in more detail in this thesis. A very rough definition of luminescence is: ‘the emission from an excited electronic state’.

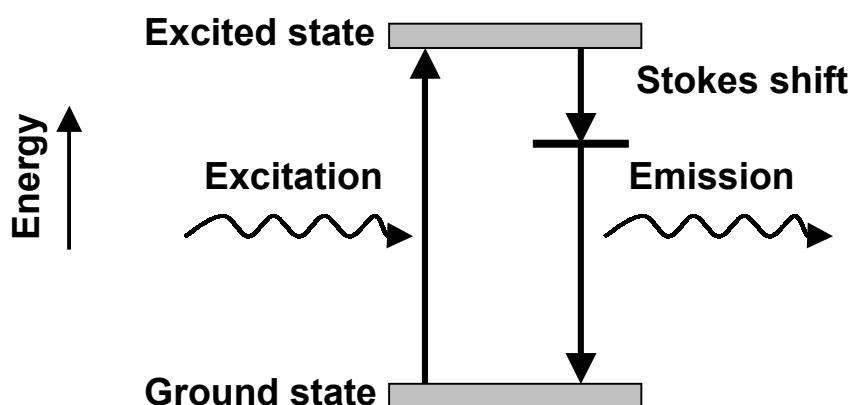


Fig 1.5 *Principle of luminescence* [16].

The basic principle of this process is sketched in figure 1.5. The luminescent ion absorbs energy (e.g. light), which causes an electron to migrate from the ground state to the excited state. This electron will fall back to the ground state. The excess energy is then released in the form of a photon. During this process some energy is lost (the Stokes shift), therefore the emission will always be at lower energy (longer wavelengths) than the excitation.

The wavelengths at which radiation is absorbed and emitted depend on the electronic structure of the ions. Therefore the luminescence characteristics of these ions are dependent on their bonding with the surrounding ions since this affects their electronic structure. For most rare earth ions these effects are negligible since the excited states are firmly locked in position, but in the case of  $\text{Eu}^{2+}$  and  $\text{Ce}^{3+}$  the luminescence can vary strongly from one host to another, due to differences in the local environment [17]. This effect we will utilise to derive information on the (local) structure of our glasses.

## 1.5 Scope and outline of this thesis

As the title implies this thesis deals with the chemistry, properties and structure of rare earth containing Si-Al-O-N glasses. The objective of this thesis is to provide an overview of the properties that can be obtained in these systems, and to serve as a basis for more application driven research. Furthermore we try to understand the properties of these glasses from a structural point of view and to study the interaction between the chemical composition, the glass structure and the properties. The work will be restricted to the RE-Si-Al-O-N systems since these glasses have been reported to have the most advantageous properties. In the course of the thesis we focus on two main issues: the effect of nitrogen and the effect of the rare-earth cation.

However, before one can start investigating a glass one should first have well characterised samples. Chapter II, III and IV of this thesis are therefore dedicated to the analysis of the chemical composition of Si-Al-O-N glasses and to changes of the oxidation state of iron and europium that take place during the synthesis of the glasses.

The second part (Chapters IV, V, VI and VII) is dedicated to the constitution and the optical properties of the glasses. When performing research on glasses (or indeed any disordered solid), one has to appreciate the tremendous complexity of these systems. The problem lies in the disorder, or rather, lack in periodicity in these systems, which complicates the description of these materials. Many of the analytical techniques such as IR-Spectroscopy and X-Ray diffraction, which have proven to be so successful in understanding crystalline systems, are severely hindered by the disorder.

In this work luminescence spectroscopy is used as an alternative tool to study the structure of these glasses. By studying the optical characteristics of the rare-earth containing glasses we derive information on the local structure (Chapter V, VI), the dispersion (Chapter VII) and the oxidation state of the rare-earth ions (Chapter V, VIII).

In the third part of this thesis (Chapters IX, X and XI) we will take a look at the mechanical and thermal properties of the glasses. The mechanical properties of these glasses initially provided a justification for the research on Si-Al-O-N glasses and the bulk of the research has been on these issues. But there are still a few areas, which are to be explored, such as the hardness (Chapter IX) and the slow crack growth resistance (Chapter X). Furthermore, virtually nothing is known about thermal conduction in these glasses although it is an important parameter for many applications. Therefore the final chapter of this thesis (Chapter XI) is dedicated to the thermal properties of these glasses.

## References

1. H.O. Mulfinger, *J. Am. Ceram. Soc.* 49 (1966) 462-467
2. T.H. Elmer and M.E. Nordberg, *Proc. 7th Congress Int. du Verres, Bruxelles, Vol I* (1965) 30 1-11
3. K.H. Jack, *J. Mater. Sci.* 11 (1976) 1135-1185
4. T. Ekström and M. Nygren, *J. Am. Ceram. Soc.* 75[2] (1992) 259-276
5. L. Bois, N. Barré, S. Guillopé, M.J. Guittet, M. Gautier-Soyer, J.P. Duraud, P. Trocellier, P. Verdier and Y. Laurent, *J. Nuc. Mater.* 227 (2000) 57-66
6. R.E. Loehmann, *Treatise on materials science and technology* (Academic Press, 1985) 119-151
7. D. Foster, L. Audoin and P. Goursat, *J. Eur. Ceram. Soc.* 21 (2001) 203-210
8. D.N. Coon, J.G. Rapp, R.C. Bradt and C.G. Pantano, *J. Non-Cryst. Sol* 56 (1983) 161-166
9. E.Y. Sun, P.F. Becher, S.-L. Hwang, S.B. Waters, G.M. Pharr and T.Y. Tsui, *J. Non-Cryst. Sol.* 208 (1996) 162-169
10. D.N. Coon, *J. Non-Cryst. Sol.* 226 (1998) 281-286
11. I.M. Peterson and T. Y. Tien *J. Am. Ceram. Soc* 78[7] (1995) 1977-1979
12. W.H. Zachariasen, *J. Am. Ceram. Soc.* 54 (1932) 3841-3851
13. R.K. Brow and C.G. Pantano, *Comm. Am. Ceram. Soc.* (1984) C-72-C74
14. J.E. Shelby and J.T. Kohli, *J. Am. Ceram. Soc.* 73[1] 29-42
15. S. Hampshire, R.A.L. Drew, and K.H. Jack, *Phys. Chem. Glass.* 26[5] (1985) 182-186
16. J. Rakovan and G. Waychunas, *The Mineralogical Record* 27 (1996) 7-19
17. L.G. van Uitert, *J. Lum* 29 (1984) 1-9

# Chapter II

---

## EPMA/WDS as a tool to analyse the local chemical composition of Si-Al-O-N glasses

*In this chapter the possibility of quantitative analysis of oxynitride glasses is explored using a Electron Probe Microanalyser (EPMA) in combination with Wavelength Dispersive Spectrometry (WDS). The goal of this work is to find an alternative (in respect to existing chemical techniques) method to measure the chemical composition of these glasses. Y-Si-Al-O-N glasses are taken as a model system. A method is developed to overcome the problems, which are associated with low-electrically conductive materials.*

## 2.1 Introduction

For a correct interpretation of the properties of a glass, knowledge about the composition of the glass is of paramount importance. For Si-Al-O-N glasses it usually suffices to take the weighed-out composition since little evaporation is expected to take place. This changes when redox reactions are expected to take place during the preparation of the glass. Changes of the oxidation state of one of the cations in the glass are usually accompanied by a change of the oxygen/nitrogen ratio in the glass. This has a pronounced influence on the properties of the glass [1]. Therefore it is important to have a method available to quantify the chemical composition and especially the oxygen and nitrogen contents in the glasses.

At the moment there are a number of methods available to determine the nitrogen and oxygen content of glasses. A disadvantage of these methods is that they can only quantify nitrogen (Kjeldall) or nitrogen and oxygen (LECO), so in order to determine the overall chemical composition one has to rely of a combination of methods. Moreover these methods require a substantial amount of material.

Electron Probe Microanalysis (EPMA) in combination with wavelength dispersive spectrometry (WDS) offers the possibility of quantifying a large number of elements including oxygen and nitrogen at the same time. This method has the advantage that it's non-destructive and that it capable of local analysis with a resolution of less than one micrometer.

Although the measurements of light elements like nitrogen with EPMA/WDS is certainly no sinecure, accurate analysis has proven to be possible for metals when proper procedures are obeyed [2]. A more fundamental problem for oxynitride glasses is posed by the low electrical conductivity of the samples [3,4], which makes the use of this technique on glasses difficult and often inaccurate [5].

The goal of this work is to solve or circumvent these problems and to develop an accurate and reliable procedure by which the chemical composition of Si-Al-O-N glasses can be determined.

## 2.2 Principles and problems for the analysis of Si-Al-O-N glasses using EPMA/WDS

In EPMA a beam of high-energy electrons is focused on the sample. By the interaction between the incident electron beam and the sample atoms, characteristic X-ray radiation is generated. This radiation can be used to identify

the different elements in the material. In order to perform this measurement quantitatively, a wavelength is selected and the monochromatic radiation is diverted to a counter. The intensity can then be translated into a concentration by accounting for the radiating volume (excitation volume) and the radiation losses during the process. By comparing the intensity of a sample of unknown composition with that of a known standard the concentration can be calculated [6].

Measurements on glasses are hampered by the low electrical conductivity of these materials. Two types of charging phenomena can be observed. When electrons are trapped near the surface of the sample we speak about surface charging. Since both the surface as the beam are negatively charged interaction between the two will cause the beam to decelerate and in the worst case to bear off. Providing an electron drain in the form of an electrically conductive coating can prevent surface charging. However, this will not prevent the occurrence of bulk charging.

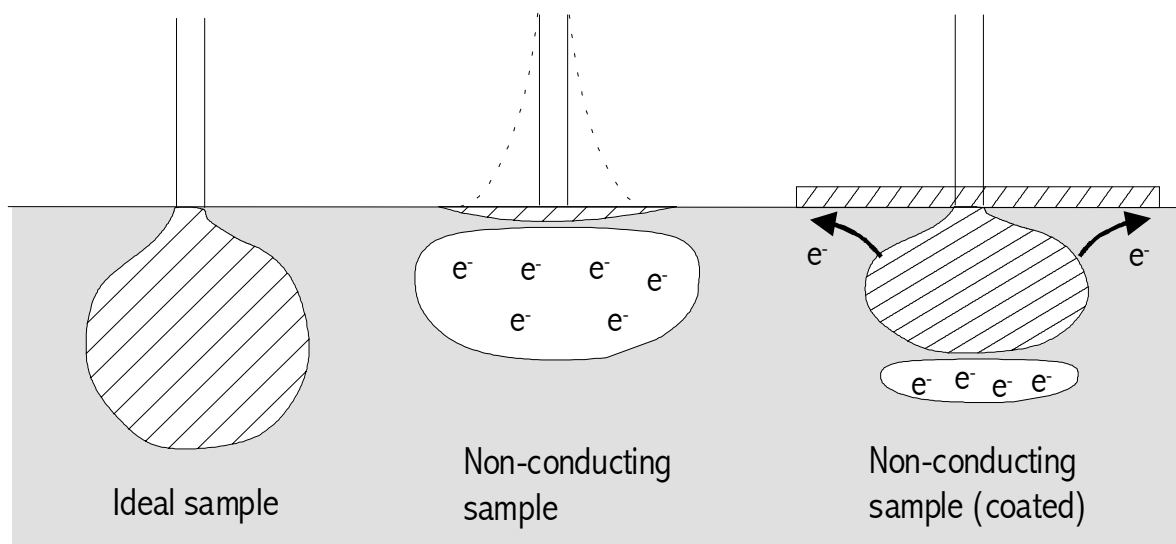


Fig 2.1 *Schematic representation of the effect of bulk- and surface charging on the penetration profile in a non-conducting sample.*

As shown in figure 2.1 the presence of sub-surface trapped electrons influences the shape of the penetration profile. This profile is of high importance for the quantification of a measurement. The emission intensity, which is registered at the detector, is dependent on a number of effects. The total amount of generated X-rays depends on the excited volume and the concentration of the element in that volume. Part of that radiation is lost by matrix absorption and other (extrinsic) effects like absorption in the detection system. The matrix absorption is dependent on the depth at which the radiation is generated (the distance radiation has to travel to escape the sample) and the absorption strength of the matrix. Other factors are matrix independent.

Even for conducting samples the correction for these matrix effects is an extremely complex mathematical procedure and relies on the fact that in most conducting materials the penetration profile can be described as ideal. This implies that the electrons collide with the sample at the ideal velocity and perform a random walk through the sample. This assumption becomes of course invalid when any form of charging occurs.

A second problem in the analysis of these glasses is the low X-Ray yield for nitrogen. Nitrogen radiation is easily absorbed by carbon, which is present in the detection system. In order to achieve a reasonable intensity one has to use relatively high beam currents, which inevitably increases the risk for charging problems. It can also lead to too high count-rates for the other elements, which have a high X-Ray yield. The photon counter can only handle one photon at a time and needs a short period to recover (dead time); if the photons enter the detector in a too rapid succession, the measured intensity falls short of the actual value.

The requirements for both the standard and the coating are summarized in table 2.1. The coating has to be electrically conductive to prevent surface charging. At the same time it should not interfere with the measurements. That means that it should not produce any emission lines in the region of the elements of interest, nor should it absorb radiation from these elements. Since the latter can never be totally avoided the coating on the standard and the sample should be of equal thickness so the amount of absorbed radiation is equal. The physical nature of the standard should approach that of the glasses. This means that it should have an equally low electrical conductivity. As with all standards it should also be homogeneous and free of pores or other flaws that could interfere with the measurements.

Table 2.1. *Requirements on coating and standards for the analysis of Si-Al-O-N glasses*

Coating	Standard
- Electrically conductive	- Low electrical conductivity
- Preferably low absorption	- Dense, single phase, flaw-free material
- No-interference with the elements which have to be measured	1
- Same thickness on sample and standard	

In this work it is tried to circumvent the boundary conditions of the correction procedure rather than to design a new correction procedure. Since the matrix correction program is used for the unknown specimen and the standard alike, it is possible to minimize the error in the measurement by taking a non-conducting standard. If the physical nature of the standard is similar to that of the specimen the deformation of the penetration profile will be the same in the standard and the specimen, leading to an overall accurate measurement [7].

### 2.3 Experimental procedure

#### *Glasses*

Nine Y-Si-Al-O-N glasses were prepared in which the concentration of the elements was varied over a broad interval. The composition of the glasses is listed in table 2.2.

As starting materials were used:  $Y_2O_3$ ,  $SiO_2$ ,  $Al_2O_3$  and  $Si_3N_4$ . The oxygen content of the  $Si_3N_4$  (0.7 wt% oxygen) was accounted for. The raw materials were mixed in a ball mill using  $Si_3N_4$  balls and isopropanol as a dispersion medium. Glasses 1-6 were molten in an induction furnace, with a melting time of 15 min after which the glasses were allowed to cool naturally. Glasses 6-9 were molten for 1 hr. in a vertical tube furnace at temperatures between 1600 °C and 1700 °C depending on the composition. The glasses were molten in a nitrogen atmosphere. In order to prolong the life of various furnace components the furnace was slowly cooled down to 1600 °C. Hereafter the furnace was opened and the samples removed.



Table 2.2 *Weighed-out compositions*

	Y	Si	Al	O	N
	[wt%]	[wt%]	[wt%]	[wt%]	[wt%]
1	39.8	18.8	6.9	29.4	5.2
2	39.4	18.7	6.9	30.5	4.5
3	44.1	13.3	8.2	34.4	0.0
4	45.0	13.6	7.7	32.8	1.0
5	45.3	13.6	7.8	31.3	2.0
6	45.5	13.8	7.9	29.2	3.5
7	44.8	9.8	12.5	31.0	2.0
8	45.7	17.2	3.5	31.6	2.0
9	50.1	12.1	6.2	29.6	1.9

### *Standards*

Two standards were selected: Single-crystalline yttrium aluminium garnet (YAG,  $Y_3Al_5O_{12}$ ) and hot-pressed  $MgSiN_2$ . The  $MgSiN_2$  sample was prepared in our own laboratory [8]. Although single crystals are usually desirable for this type of analysis,  $MgSiN_2$  was preferred above BN and AlN, due to its high degree of compaction and low levels of contamination. This approach has the additional advantage, that for the whole analysis only two standards are required.

### *Coating*

For the coating there are two materials meeting the requirements, which are explained in the previous paragraph viz. nickel and carbon. The absorption of N-K $\alpha$  radiation by these coatings can be calculated using:

$$I = I_0 \cdot e^{\left[ -\rho \cdot \left( \frac{\mu}{\rho} \right) \cdot x \right]} \quad (1)$$

with:

- $I$  Transmitted intensity
- $I_0$  Original intensity
- $\rho$  Density [ $g/cm^3$ ]
- $\mu/\rho$  Mass Absorption Coefficient (MAC) [ $cm^2/g$ ]
- $x$  Linear coating thickness [cm]

Calculation of the absorption of N-K $\alpha$  radiation by a coating of amorphous carbon (MAC = 25500,  $\rho$  = 2.0) and nickel (MAC = 9340,  $\rho$  = 8.9) shows that at equal thickness the carbon coating is preferable to nickel (Fig. 2.2). Therefore carbon was chosen despite the disadvantage of some overlap between the C-K $\alpha$  peak and the N-K $\alpha$  peak.

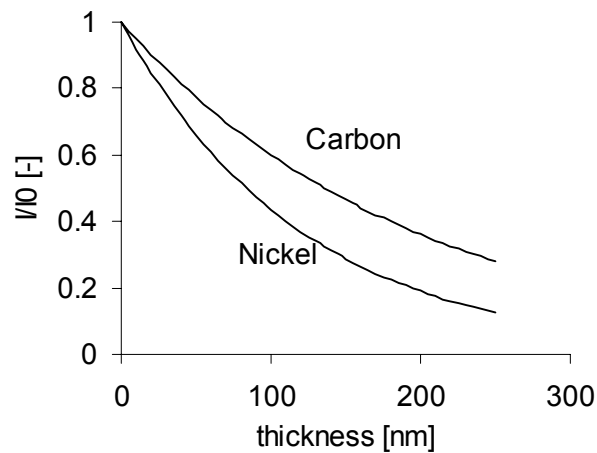


Fig. 2.2 Theoretical loss of intensity as a function of coating thickness.

Since the transmitted intensity decreases sharply with an increment of the coating thickness it is important that the coating on the specimen and the standard are of equal thickness as well as homogeneously distributed. Therefore the carbon coating was simultaneously applied on the specimen and the standards. The coating was applied using a carbon sputtering technique, which produced coatings of 15-20 nm thicknesses, with sufficient electrical conductivity.

### Measurements

The measurements were carried out on a JEOL Superprobe 8600 SX equipped with 4 wavelength-dispersive spectrometers (JEOL) and an energy dispersive system (Noran). The monochromators were fitted with Pentaerythritol (PET, 2d spacing 8.74 Å) and Thallium Acid Phthalate (TAP, 2d spacing 25.75 Å) crystals for the analysis of the heavier elements. For oxygen and nitrogen a W/Si multi-layer crystal (LDE, 2d spacing 58.9 Å) was used. PROZA was used for the matrix correction. The calibration and measurements were carried out at a beam current  $\sim$ 195 nA at an acceleration voltage of 15 kV. The measurement conditions are summarized in table 2.3.

The yield for the Si K- $\alpha_1$  radiation exceeded the dead-time limit of the detector. Therefore it is necessary to use the K- $\alpha_2$  peak of silicon. For aluminium a very high X-ray yield was measured albeit below the dead time limit. Nevertheless it was decided to perform the measurements with both the K- $\alpha_1$  and the K- $\alpha_2$  peak. At the measurement conditions the Duane-Hunt limit was determined to ensure that the coating was sufficiently conductive for the measurement. The Duane-Hunt limit or short wavelength cut-off limit is the maximum energy of the detected photons and should match the acceleration voltage. Charging effects results in energy losses and thus to a shift of the Duane Hunt limit to longer wavelengths.

Table 2.3 *Used settings for the analysis of Y-Si-Al-O-N glasses by EPMA/WDS.*

Element	Emission line	Detector	Standard	PROZA correction factor
Y	L- $\alpha$	PET	YAG	0.336246
Si	K- $\alpha_2$	TAP	MgSiN <sub>2</sub>	0.257507
Al	K- $\alpha_1$	TAP	YAG	0.187903
	K- $\alpha_2$			
O	L- $\alpha$	LDE	YAG	0.0952697
N	L- $\alpha$	LDE	MgSiN <sub>2</sub>	0.0910583

## 2.4 Results and discussion

The measurements were carried out as 20-30 point linescans. Figure 2.3 shows the results of a linescan performed on glass no 6. The step size was in this case approximately 20  $\mu\text{m}$ , which leads to a total scanned interval of 400  $\mu\text{m}$ . It is evident that over this interval the measured values are very consistent. This implies (i) that the glass is homogeneous on a microscopic level, (ii) that the coating is uniformly applied over the material and (iii) that the measurements themselves are very reproducible.

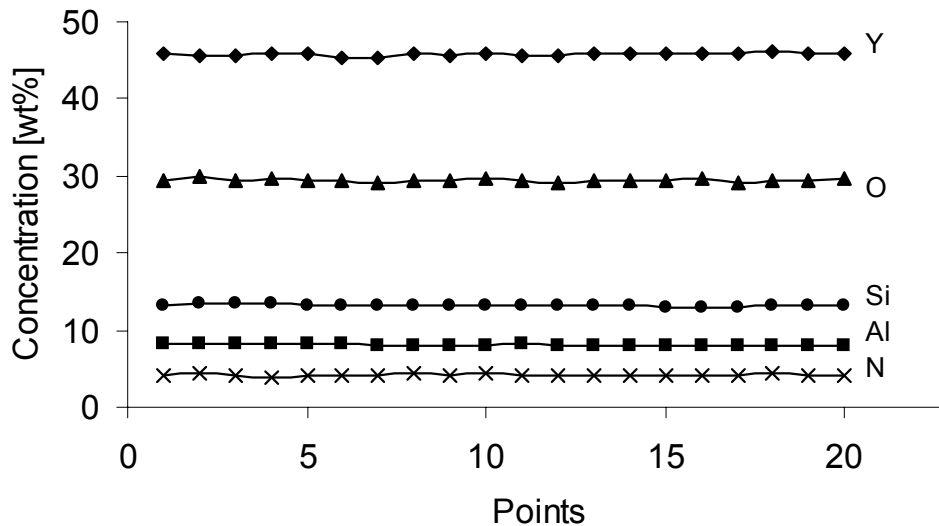


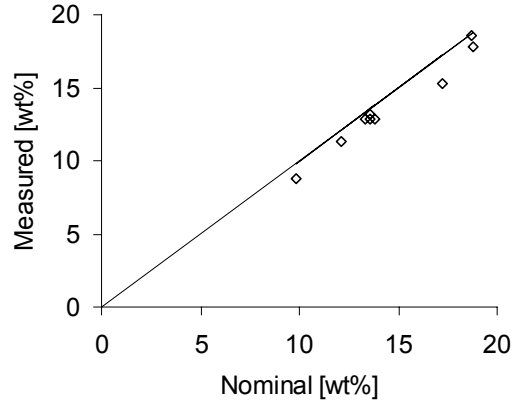
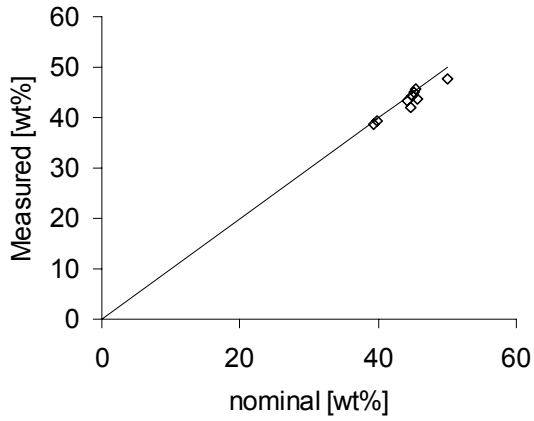
Fig. 2.3. Results of a 20 point linescan over sample 6.

Table 2.4. Averaged results of four linescans on glass no 6. The sample was polished and re-coated between the measurements.

Measurement	Y [wt%]	Si [wt%]	Al [wt%]	O [wt%]	N [wt%]	Total [wt%]
nominal	45.5	13.8	7.9	29.2	3.5	100
1 (Al K- $\alpha_1$ )	44.6	12.7	7.9	29.0	3.8	98.0
2 (Al K- $\alpha_1$ )	46.1	13.0	8.2	29.2	3.8	100.2
3 (Al K- $\alpha_1$ )	46.5	12.8	8.0	28.0	3.2	98.8
4 (Al K- $\alpha_2$ )	45.1	13.1	8.1	29.3	3.7	99.2

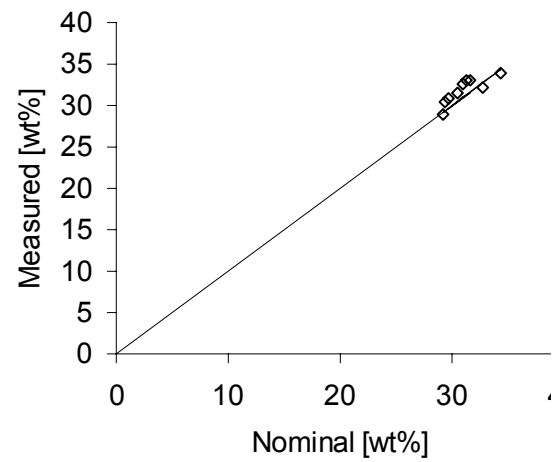
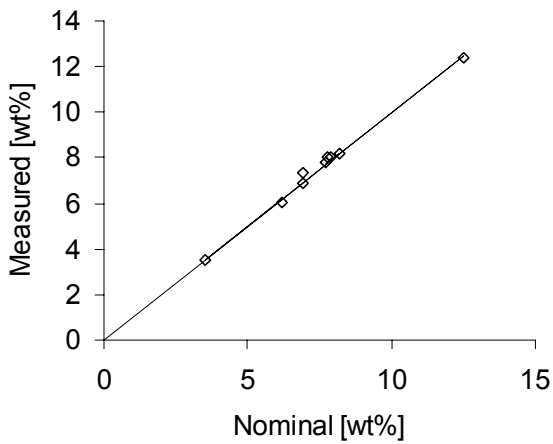
Furthermore it shows that polishing, re-coating and re-measuring had no significant effect on the measured values as can be seen in table 2.3. Switching between the Al K- $\alpha_1$  and the Al K- $\alpha_2$  peak also had no significant effect on the measured composition, which means that despite the high intensity of the Al K- $\alpha_1$  emission dead time problems are not an issue at the current measuring conditions. Use of Al K- $\alpha_1$  emission then is preferred over the Al K- $\alpha_2$  emission since, since the higher peak to background ratio increases the sensitivity of the measurement at lower Al contents.

The measured compositions are compared with the composition as weighed-out. Figure 2.4 shows this comparison for the individual elements. Each datapoint represents the averaged values of four linescans on a single glass. The measured values are mostly within 1 wt% of the weighed-out composition, which is in the same order of magnitude as the error in the measurements and therefore acceptable



Y

Si



Al

O

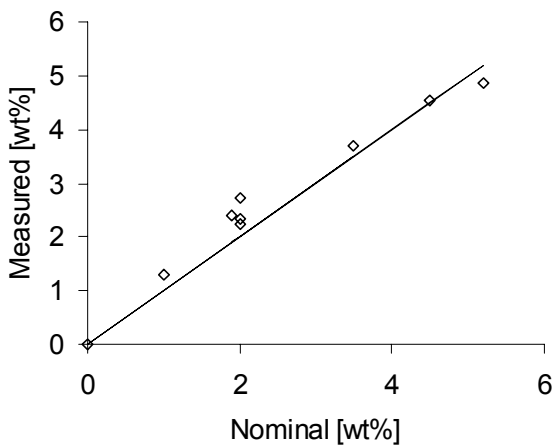


Figure 2.4  
*Nominal composition (per element) and composition as measured by EPMA/WDS for glasses 1 to 9. The line represents a 1:1 correlation.*

N

As explained in the introduction of this chapter, we are most interested in the nitrogen content of the glasses. The fact that in glass no 3, which does not contain any nitrogen, no nitrogen was detected is already reassuring. In order to estimate the sampling error at higher nitrogen contents, glass number 6 was independently analysed with LECO (Table 2.5). The difference between the two measurements is less than 10% relative, which is more than acceptable, considering the accuracy of both methods.

Table 2.5 *EPMA/WDS and LECO analysis of glass no 6 (nominal N-content = 3.5 wt%)*.

	EPMA/WDS	LECO
1	3.8	3.4
2	3.8	3.2
3	3.2	
4	3.7	
Average	3.6	3.3

There is some evidence for the occurrence of a systematic error in the determination of the silicon content. The silicon content, which is measured by the EPMA is on average 0.4 wt% lower than the weighed out silicon content. This can either be the results of the measurement procedure or the result of some silica evaporation during the synthesis of the glasses.

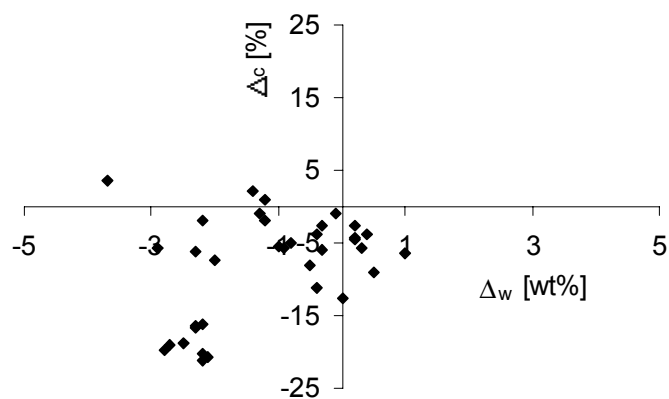


Fig 2.5 *Deviation in the measured weight total ( $\Delta_w$ ) and the charge balance ( $\Delta_c$ ) for glasses 1 to 9 (four measurements per glass).*

The former seems more likely since the measured weight total and the charge balance show a deviation. The measured weight total is in almost all cases under 100%. This difference ( $\Delta_w$ ) is plotted against the charge balance ( $\Delta_c$ ) in figure 2.5. The charge balance, which is defined as the excess charge per atom and which should be neutral, is in most cases slightly negative. The deviation of the measured weight total suggests that the deviation in the charge balance can be attributed to an underestimation of the concentration of the cations. Comparison of the measured compositions with the weighed out compositions suggests that this most likely is the result of an underestimation of the silicon content.

## 2.5 Conclusions

This work has shown that the chemical analysis of Si-Al-O-N glasses using EPMA/WDS is possible provided that the samples are well prepared and the measurements properly executed. Foremost it is eminent to prevent surface charging, but one also has to carefully select the standards to compensate for the change in the penetration profile due to bulk charging.

With the selected coating (carbon) and standards (YAG, MgSiN<sub>2</sub>) it is possible to obtain reproducible results. Moreover the measured compositions correlate well with the expected compositions. The measured weight total and the charge balance show only a small deviation and can be attributed to a slight underestimation of the silicon content

## References

1. D. de Graaf, H.T. Hintzen, S. Hampshire and G. de With, *J. Eur. Ceram. Soc.* 23 (2003) 1093-1097
2. G.F. Bastin and H.J.M. Heijligers, *Quantitative Electron Probe Microanalysis of Nitrogen*, University of Technology, Eindhoven (1981)
3. J. Cazaux, *X-Ray Spectrom.* 25 (1996) 265-280
4. J. Cazaux, In: *Microbeam analysis*, Eds. A. D. Romig, W.F. Chambers, San Francisco Press, USA (1986) 527-531
5. A. Stella and M. Verità, *Mikrochim. Acta* 114/115 (1994) 475-480
6. V.D. Scott and G. Love, *Quantitative Electron-Probe Microanalysis*, (Ellis Horwood Ltd, Great Britain 1983)
7. S. Dreer, *J. Anal. Chem.* 365 (1999) 85-95
8. R.J. Bruls, H.T. Hintzen and R. Metselaar, *J. Mater. Sci.* 34 (1999) 4519-4531

## Chapter III

---

### Redox behavior of iron in Si-Al-O-N melts; formation of iron silicides

*One of the main problems concerning the use of Si-Al-O-N glasses is their poor transparency in the visible region. It has been widely assumed that the low transparency is originating from the precipitation of small metallic particles from the glass melt. The current experiments have shown that this problem is related to the presence of iron impurities in the raw materials in combination with the low oxygen pressure during the synthesis of the glasses and that the only way to overcome this problem is the exclusion of iron and iron oxide from the raw materials.*



### 3.1 Iron and the transparency of Si-Al-O-N glasses

Although Y-Si-Al-O-N glasses are widely regarded as very interesting materials with respect to their mechanical, thermal and chemical durability their optical properties leave to be desired. Y-Si-Al-O-N glasses are usually tinted dull grey at best. At worst they can be opaque grey or completely non-transparent. A few studies have been directed towards improving the transparency of these glasses. It is generally believed that the grey colour originates from small particles present in the glass [1]. TEM studies have shown these particles to have a core-shell structure. The core consists of transition metals (like iron) and silicon and the shell of crystalline SiO<sub>2</sub> or Si [2]. The formation of these particles has been ascribed to the reaction between iron(oxide) and Si<sub>3</sub>N<sub>4</sub> [3,4] similar to reactions observed in sintered Si<sub>3</sub>N<sub>4</sub> [5,6]. Others believe the free silicon is originating from a reaction between SiO<sub>2</sub> and Si<sub>3</sub>N<sub>4</sub> [7]. In both cases N<sub>2</sub> is the evolving species. However this seems to be in conflict with the experimental observation that Y-Si-Al-O glasses prepared under the same conditions display a similar grey colour [7].

It is therefore the intention of this work to clarify the mechanism that leads to the formation of metallic particles and ultimately to the coloration of the glasses. Past efforts on this subject have been mainly focused on thermodynamic calculations. We do not favour such an approach since the atmosphere in the furnace is unknown and also that thermodynamical calculations on reactions between raw materials might not be applicable to the complex equilibrium in a multicomponent glass melt.

### 3.2 Experimental

Two types of glasses were investigated in this study: M1 (Y<sub>45.5</sub>Si<sub>13.9</sub>Al<sub>7.9</sub>O<sub>29.2</sub>N<sub>3.5</sub> [wt%]) and M2 (Y<sub>37.2</sub>Si<sub>14.5</sub>Al<sub>11.5</sub>O<sub>36.8</sub> [wt%]). In order to study the effect of iron contamination on the glasses, the iron content of the glasses was enhanced by adding 1 wt% of Fe<sub>2</sub>O<sub>3</sub> (M1Fe and M2Fe). The glasses were prepared from Y<sub>2</sub>O<sub>3</sub> (Shen Etsu), SiO<sub>2</sub> (CE Minerals), Al<sub>2</sub>O<sub>3</sub> (Taimei), Si<sub>3</sub>N<sub>4</sub> (Akzo Nobel PH95) and Fe<sub>2</sub>O<sub>3</sub> (Alfa Aesar 99.8%). These powders were mixed by wet ball-milling in isopropanol. The dried mixture was placed in a carbon crucible with hexagonal boron nitride lining. The glasses were molten in a vertical tube furnace at 1700 °C for one our under an atmosphere of flowing nitrogen atmosphere (P =1 atm). The furnace was then slowly (3°/min) cooled to 1600 °C after which glasses were rapidly retracted from the furnace and allowed to cool down in air.

### 3.3 Results and discussion

Both glasses without added  $\text{Fe}_2\text{O}_3$  (M1, M2) are tinted greyish, which hints the presence of metallic inclusions. The glasses prepared with added  $\text{Fe}_2\text{O}_3$  (M1Fe, M2Fe) are on the other hand completely transparent (Fig. 3.1). On the outside of both iron containing glasses metallic globules are visible measuring 0.5 to 1 mm in diameter (Fig. 3.2). These globules were carefully separated from the bulk glass and cross-sectioned. Both the bulk glass and the globules were analysed using SEM/EDS. Standardless EDS analysis showed that the globules in glass M1Fe and M2Fe both consists of 70 to 80 wt% iron and 20 to 30 wt% Si. No trace of iron was found in the bulk glasses so it can be assumed that all the iron has precipitated in the globules.

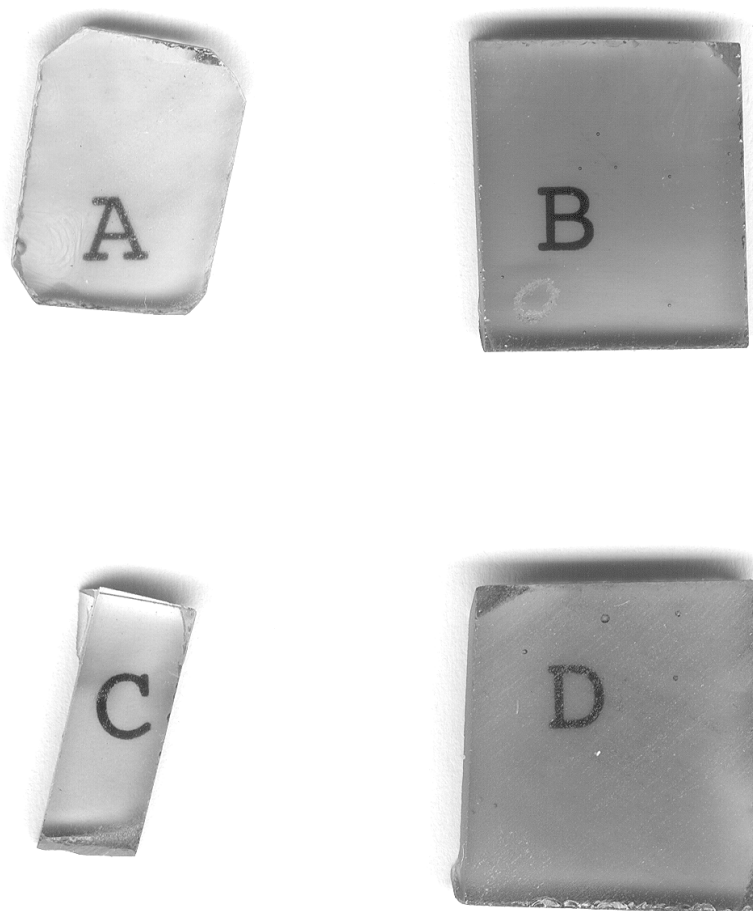


Fig. 3.1 Transparency of 2mm thick sheets of the glasses prepared in this investigation: (A) M2Fe, (B) M2, (C) M1Fe and (D) M1.

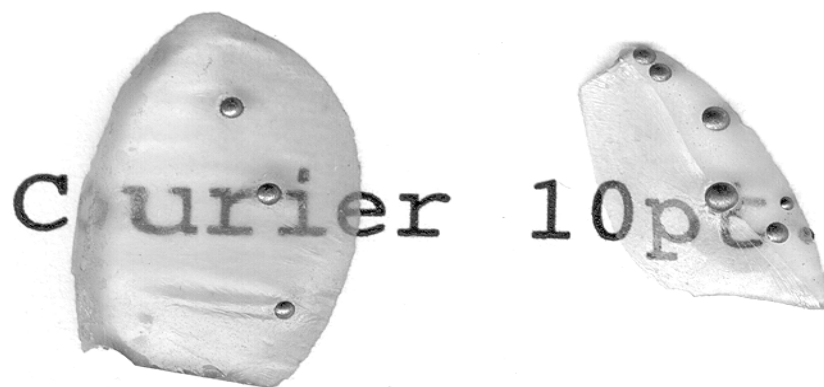


Fig. 3.2 Ironsilicide globules on the outer rim of a Y-Si-Al-O glass (right) and a Y-Si-Al-O-N glass (left.)

In order to exclude the involvement of  $\text{Si}_3\text{N}_4$  in the reduction process both M1 and M1Fe were examined using EPMA/WDS using the method which has been described in the previous chapter. The samples were coated with a 15-20 nm thick carbon coating to prevent surface charging. To compensate for the bulk charging non-conducting standards were used (hot-pressed  $\text{MgSiN}_2$  and single-crystal Yttrium Aluminium Garnet) Measurements were performed at an acceleration voltage of 15kV and a beam current of 170 nA. Linescans of 20 steps were performed on the samples and the averaged results are displayed in table 3.1.

Table 3.1 *Nominal weighed out composition and measured composition.*

	Y [wt%]	Si [wt%]	Al [wt%]	O [wt%]	N [wt%]	Total [wt%]
Nominal	45.5	13.9	7.9	29.2	3.5	100
M1	45.7	13.2	8.1	31.6	4.2	103
M1Fe	45.9	12.6	8.2	31.6	4.1	102

As can be seen in table 3.1 there is a substantial decrease of the silicon content of the glasses upon iron addition. The measured difference in silicon content of 0.6 wt% corresponds reasonably well to 20 to 30 wt% of silicon that was found in the metallic globules. The nitrogen content of the glasses remains equal suggesting that the reduction of the silicon and the iron is not accompanied by a nitrogen evolution. The measured nitrogen contents are higher than the nominal nitrogen content. This is attributed to the in accuracy of the analysis. Both the measured weight totals (>102%) and the charge balance, which is slightly negative for the measured composition, suggest that the amount of oxygen and nitrogen are slightly overestimated.

The presented results clearly show that the mechanism by which iron silicides are formed in Si-Al-O-N glasses is the same as in Si-Al-O glasses and that this process does not include a reaction with silicon nitride. We further believe that the metallic iron and silicon are originating from the dissociation of iron oxide and silicon dioxide. Since carbon and BN are used as crucible materials the oxygen partial pressure is expected to be extremely low. This causes iron to reduce readily, even before the formation of the primary melt. SiO<sub>2</sub> is thermodynamically much more stable, but the formed silicon is stabilized by incorporation in the iron silicates.

The mechanism sketched above implies that the transparency of oxynitride glasses cannot be improved by the use of different nitrides, eg. AlN instead of Si<sub>3</sub>N<sub>4</sub>, as has been suggested in other works [7]. The amount of iron silicides formed depends only on the amount of iron oxide in the raw materials. It is further shown that the formed iron silicides have a strong tendency to agglomerate, which implies that the size and distribution of these precipitates depends on the melting time and temperature. These factors in turn affect the transparency of the glasses. It has to be noted that this type of behaviour is expected to occur for a number of transition metal oxides, which reduce easily and form stable silicides like cobalt oxide.

### 3.4 Conclusions

It has been shown that iron silicide precipitations can exist in Si-Al-O and Si-Al-O-N glasses alike. The formation of these particles has been attributed to the extremely reducing conditions during melting which causes iron oxide to dissociate. The thus formed metallic iron aids the dissociation of silicon dioxide by a reaction to iron silicides. This explains how the presence of traces of iron oxide can lead to severe loss of transparency in oxynitride glasses.

### References

1. T. Rouxel and B. Piriou, *J. Appl. Phys.* 79 [12] (1996) 9074-9079
2. W.T. Young, L.K.L. Falk, H. Lemercier, V. Peltier-Baron, Y. Menke and S. Hampshire, *J. Non-Cryst. Sol.* 270 (2000) 6-19
3. P. Korgul and D.P. Thompson, *J. Mater. Sci* 28 (1993) 506-512
4. D.R. Messier, *Int. J. High Tech. Ceram.* 3 (1987) 33-41
5. A.E. Pasto, *J. Am. Ceram. Soc.* 67[9] (1984) C178-C180
6. S. Baik and R. Raj, *J. Am. Ceram. Soc.* 68[5] (1985) C124-C126
7. D.R. Messier and E.J. Deguire, *J. Am. Ceram. Soc.* 67 [9] (1984) 602-605



# Chapter IV

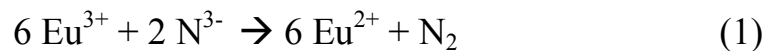
---

## Determination of the oxidation state of europium by magnetic measurements

*It has been reported that in Si-Al-O-N glasses the oxidation state of europium may be 2+ whereas it is 3+ in oxide glasses molten under normal conditions. Apparently europium, which is in the trivalent state in the raw materials, reduces to the divalent state during the preparation and processing of these glasses. In this chapter we will determine the oxidation state of europium using the specific magnetic properties of europium in the divalent state and the trivalent state. Furthermore we will focus on the underlying mechanisms.*

## 4.1 Introduction

Recent developments in the lighting and opto-electronics industry have fuelled the growth and demand for new luminescent materials. Our interest in Eu-Si-Al-O-N glasses is provoked by the work of Ramesh et al. which suggests that europium will adapt a divalent oxidation state in Si-Al-O-N glasses [1] whereas in oxide glasses the trivalent state is expected [2]. In Si-Al-O-N glasses we assume that  $\text{Eu}^{3+}$  from the raw materials is (partially) converted to  $\text{Eu}^{2+}$  during the synthesis by a reaction with the chemically incorporated nitrogen:



which is similar to reactions which have previously been observed in Ce-Si-Al-O-N glasses [3].

For phosphor applications  $\text{Eu}^{2+}$  doped materials have received special attention, not only because of the efficiency of their fluorescence but also because of the ability to control the emission and absorption wavelengths. Depending on the type of host lattice, the  $\text{Eu}^{2+}$  luminescence can also be tuned to cover a broad spectrum, which includes the whole visible region and part of the UV [4].

For most phosphor applications the often-observed coexistence of  $\text{Eu}^{3+}$  with  $\text{Eu}^{2+}$  in the materials is undesirable due to interference with the  $\text{Eu}^{2+}$  luminescence. Therefore, for a thorough characterization of the  $\text{Eu}^{2+}$  based luminescent materials, it is important to determine the relative amounts of  $\text{Eu}^{2+}$  and  $\text{Eu}^{3+}$  in a quantitative way. For this information, one often turns to Mössbauer spectroscopy [5], which is however time consuming and not readily available. In this communication, we show a relatively simple, non-destructive, yet an accurate way of determining the valence state of Eu by means of magnetization experiments.

Magnetic susceptibility is one of the most commonly used techniques to investigate and establish the number of unpaired spins in a material due to the ease in measurement and interpretation. This is particularly true for dilute systems where exchange interactions between spins can be ignored. Compounds featuring mixed-valent europium are excellent examples for demonstrating the utility of magnetic susceptibility because  $\text{Eu}^{3+}$  is a Van Vleck paramagnetic ion [6] while  $\text{Eu}^{2+}$  with a  $4f^7$  configuration has a total spin of  $J=7/2$ .

The temperature dependent magnetic susceptibility ( $\chi$ ) of  $\text{Eu}^{2+}$  (Fig 4.1) obeys the Curie law according to:

$$\frac{1}{\chi_{Eu^{2+}}} = \frac{3k_B T}{\mu_B^2 g^2 J(J+1)N_A} \quad (2)$$

where  $k_B$  is Boltzmann's constant,  $\mu_B$  the Bohr magneton,  $g$  the Landé constant and  $N_A$  Avogadro's number, yielding diamagnetic susceptibility of  $Eu^{2+}$  of  $2.6 \times 10^{-2}$  emu/mol at 300 K.

In  $Eu^{3+}$  ( $4f^6$ ) the separation between the  ${}^7F_0$  ground state and the lowest levels of the  ${}^7F_J$  multiplet is relatively small as compared to  $kT$ . Although the ground state  $J=0$  is dia-magnetic, the paramagnetic contribution of the  ${}^7F_1$  level cannot be ignored [7]. The magnetic behaviour of  $Eu^{3+}$  can be described by replacing  $N_A$  in equation 1 by  $N_J$  to account for the atoms with various different values for  $J$  and by resolving the temperature dependence of the occupation of the different  $J$  levels as has been demonstrated by van Vleck [6]. Assuming a screening constant of 34 ( $z = 365/T$ ) the temperature dependence takes the following form, which accounts for the thermal population of the different  $J$  levels:

$$\chi_{Eu^{3+}} = \frac{0.1241}{xT} \cdot \frac{24 + (13.5x - 1.5)e^{-x} + (67.5x - 2.5)e^{-3x} + (189x - 3.5)e^{-6x} + \dots}{1 + 3e^{-x} + 5e^{-3x} + 7e^{-6x} + \dots} \quad (3)$$

$Eu^{3+}$  (Figs. 4.1, 4.2) thus has a weakly temperature-dependent molar susceptibility  $\chi$  that is constant at for temperatures below 100 K and then decreases with increasing temperatures.

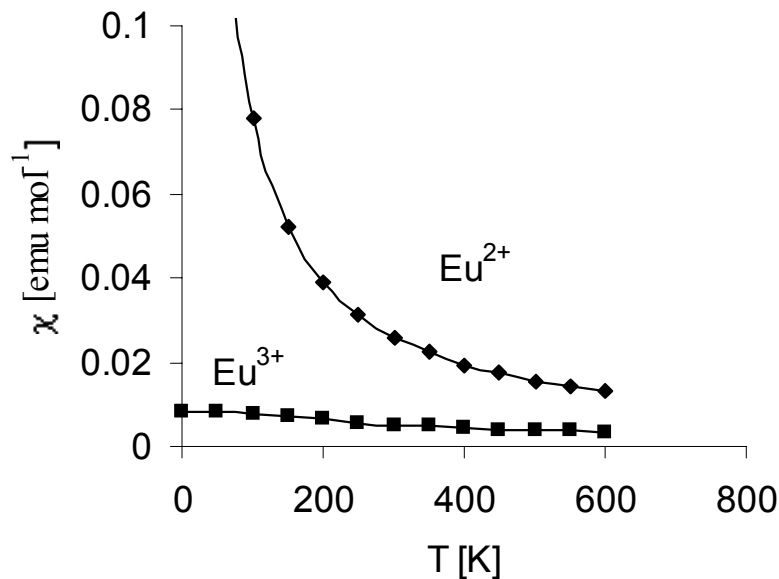


Fig. 4.1 Calculated magnetic susceptibilities of  $Eu^{2+}$  and  $Eu^{3+}$ .



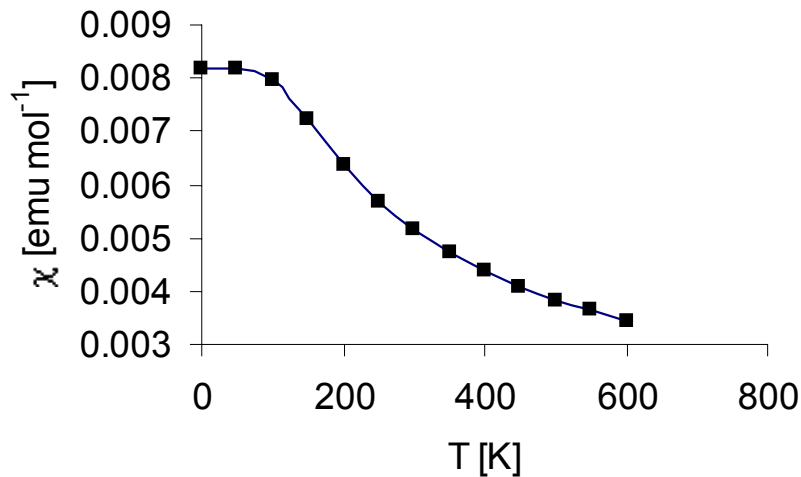


Fig. 4.2 Calculated magnetic susceptibility of  $\text{Eu}^{3+}$  (enlarged section of figure 4.1).

However, in materials, where both  $\text{Eu}^{2+}$  and  $\text{Eu}^{3+}$  are present, the magnetic susceptibility may be a complex function of temperature. Here we describe a simple method of resolving the contributions from the divalent and trivalent europium ions and demonstrate the feasibility of this method by a study on (Eu,Y)-Si-Al-O-N glasses.

## 4.2 Experimental

$\text{Eu}_x\text{Y}_{(15.2-x)}\text{Si}_{14.7}\text{Al}_{8.7}\text{O}_{54.1}\text{N}_{7.4}$  (weighed out composition) glasses were prepared from  $\text{Eu}_2\text{O}_3$ ,  $\text{Y}_2\text{O}_3$ ,  $\text{SiO}_2$ ,  $\text{Al}_2\text{O}_3$  and  $\text{Si}_3\text{N}_4$ . A homogeneous powder was obtained by ball milling the powder mixture in iso-propanol with  $\text{Si}_3\text{N}_4$  balls and subsequently drying it. The powder was isostatically compressed to a pellet. The pellet was melted in a vertical tube furnace in a nitrogen atmosphere at temperatures between 1700 and 1750 °C, depending on the glass composition. The carbon crucible was lined on the inner wall with Hex-BN powder to prevent sticking. The melt was quenched in a graphite mould, which was pre-heated at 800 °C, and subsequently annealed for two hours at this temperature in air. The glasses were determined to be X-ray amorphous.

The magnetization  $\mu$  was measured with a Quantum Design Physical Properties Measurement System for temperatures  $T$  ranging from 100 to 300 K at an applied magnetic field  $H$  of 10000 G.

The actual magnetic moment was obtained by subtracting the very weak magnetic signal from the sample holder from the measured moment. Finally,  $\chi$  was determined as

$$\chi = \frac{\mu M}{mH} \quad (4)$$

where  $M$  is the molar mass and  $m$  the sample mass. An undoped sample of Y-Si-Al-O-N glass was first measured to determine its diamagnetic molar susceptibility. The diamagnetic susceptibility of the matrix was then subtracted from the measured susceptibility of the (Eu,Y)-Si-Al-O-N samples to obtain the paramagnetic susceptibility due to the Eu spins.

### 4.3 Results and discussion

Conventionally, one plots  $1/\chi$  vs.  $T$ , the so-called Curie plot, to evaluate the Curie constants, which are used in the estimation of the effective magnetic moments (fig 4.3). In the case of a purely  $\text{Eu}^{2+}$  containing glass the slope should be 0.127 whereas the presence of  $\text{Eu}^{3+}$  leads to an increase of the slope to 0.34.

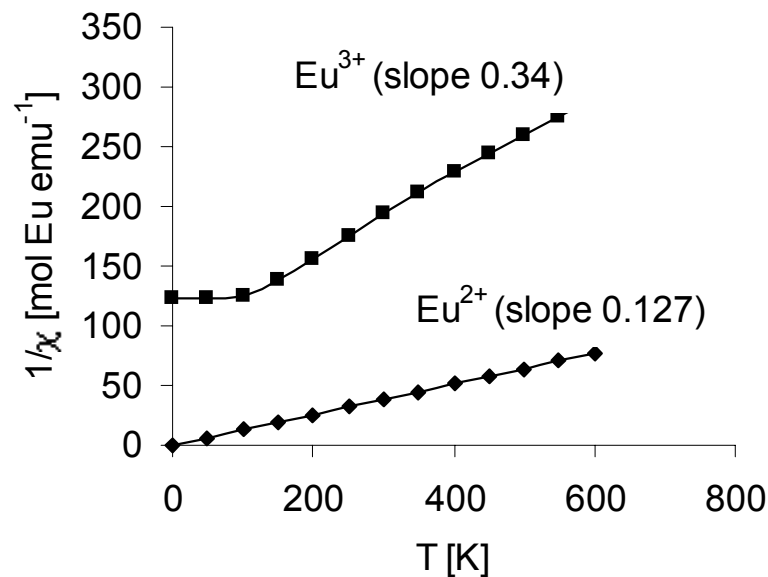


Fig 4.3 *Calculated Curie plots for a material containing europium in a single oxidation state ( $\text{Eu}^{2+}$  and  $\text{Eu}^{3+}$ ).*

For the  $x = 0.15$  sample (Fig 4.4), all the europium is in the divalent state within the accuracy of the measurement (0.119). For the  $x = 15.2$  sample the slope is higher (0.134) indicating the presence of a certain amount of  $\text{Eu}^{3+}$ . Using the compositional dependence of the magnetic susceptibility as given by equations 1 and 2, the content of  $\text{Eu}^{3+}$  and  $\text{Eu}^{2+}$  can be estimated to be 4% and 96%, respectively.

The Curie plot of this sample is still a straight line, but the  $T$ -intercept has shifted below zero. It appears that the estimate of 4%  $\text{Eu}^{3+}$  is slightly too low. Adjustment of the slope suggests that the actual amount of  $\text{Eu}^{3+}$  is 1% higher, that is 5%  $\text{Eu}^{3+}$  and 95%  $\text{Eu}^{2+}$ . In any case this deviation is not severe compared to the sensitivity of the method.

Ultimately, the overall sensitivity of this technique is controlled by the sensitivity of the magnetometer. Most magnetometers can measure  $1 \mu\text{emu}$  or better. Since  $\text{Eu}^{3+}$  has the smaller susceptibility, one should theoretically be able to detect as small as  $10^{-6}$  mol Eu at a field of 10000 G, providing the diamagnetic contributions to the magnetic moment are not too large. But for small europium concentrations, one requires larger samples. Under normal conditions, one can generally not expect better than 2% accuracy with most magnetometers.

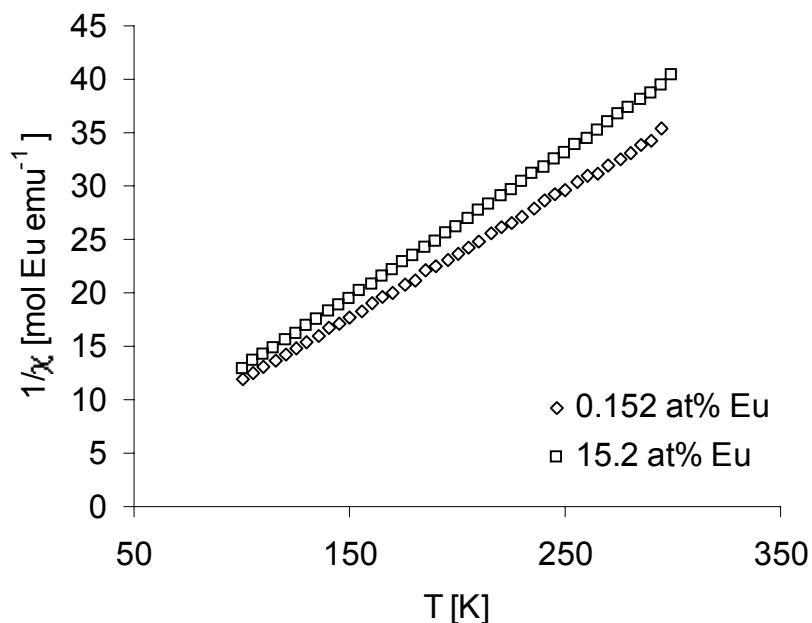


Fig. 4.4 Measured Curie plots of the  $\text{Eu}_{0.152}\text{Y}_{15.0}\text{Si}_{14.7}\text{Al}_{8.7}\text{O}_{54.1}\text{N}_{7.4}$  glass and the  $\text{Eu}_{15.2}\text{Si}_{14.7}\text{Al}_{8.7}\text{O}_{54.1}\text{N}_{7.4}$  glass.

Since nitrogen is consumed by this reaction the nitrogen content in the glasses should be lower than expected from the weighed-out composition. In order to validate this assumption the nitrogen content of several glasses with varying nitrogen content was measured with LECO O/N analysis. The results are plotted in figure 4.5. It is clearly visible that with an increasing europium content of the glasses the difference between the weighed out nitrogen content and the measured nitrogen content increases. Moreover the measured nitrogen content is in accordance (within the error margin) with the nitrogen content, which has been calculated assuming a full conversion of europium according to reaction 1. Based on these results and the foregoing we can conclude that a reduction according to reaction 1 indeed occurs and can be considered to be (nearly) complete.

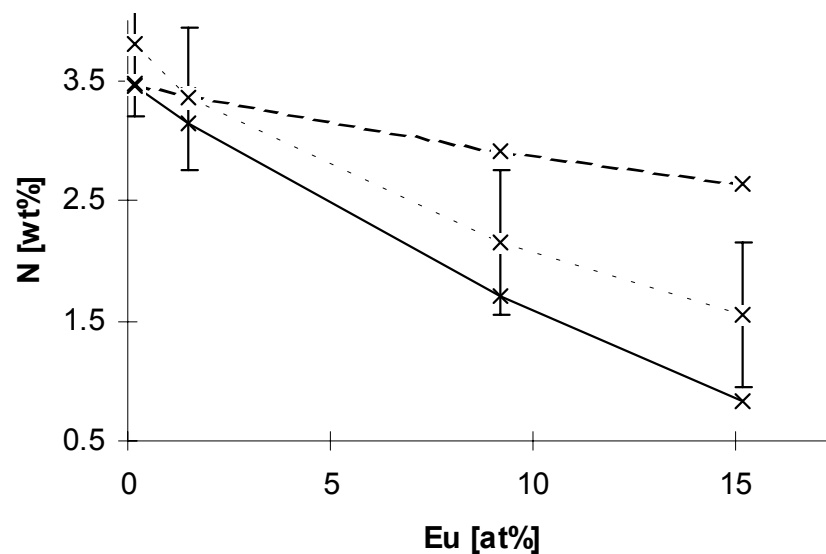


Fig. 4.5 Nitrogen content as weighed out (— —), as measured by LECO (— —) and as expected from full europium conversion (-----).

#### 4.4 Conclusions

The magnetic measurements confirm that in Si-Al-O-N glasses europium will adopt a divalent state instead of the trivalent. It is shown that at low concentrations all the europium is expected to be in the divalent state whereas some remnants of  $\text{Eu}^{3+}$  from the starting materials could be detected at higher concentrations. Magnetic susceptibility measurements thus show to be a promising alternative for the quantification of mixed-valent europium containing systems.

---

**References**

1. R. Ramesh, E. Nestor, M.J. Pomeroy and S. Hampshire, *J. Eur. Ceram. Soc.* 17 (1999) 1933-1939
2. J.E. Shelby and J.T. Kohli, *J. Am. Ceram. Soc.* 73[1] (1990) 39-42
3. A. Diaz, S. Guillope, P. Verdier, Y. Laurent, A. Lopez, J. Sambeth, A. Paul and J.A. Ordriozola, *Mater. Sci. Forum* 325-326 (2000) 283.
4. G. Blasse, B.C. Grabmaier, *Luminescent Materials*, Springer, Berlin (1994)
5. H.T. Hintzen and H.M. van Noort, *J. Phys. Chem. Sol.* 49 [8] (1988) 873-881
6. A.J.H. van Vleck, *The theory of electric and magnetic susceptibilities* (Oxford University Press, London, 1932)
7. G.F. Goya, R.C. Mercader, M.T. Causa and M. Tovar, *J. Phys. Condens. Matter* 8 (1996) 8607-8612

# Chapter V

---

## Eu<sup>2+</sup> luminescence in Si-Al-O-N glasses

*This chapter describes a study on the optical properties of (Y,Eu)-Si-Al-O-N glasses. Luminescence spectroscopy confirms the presence of Eu<sup>2+</sup> in the samples in agreement with the magnetic measurements described in the previous chapter. The optical properties of these glasses further show that the emission characteristics of Eu<sup>2+</sup> are strongly dependent on the overall composition. As a function of the europium content the emission can shift from 500 nm to as far as 650 nm, which is exceptional for europium-bearing materials. The emission shift is attributed to the existence of different europium sites and energy transfer between them.*

## 5.1 Introduction

Recent investigations have shown that the incorporation of europium in nitrogen containing crystal lattices can lead to very interesting luminescence properties [1]. The direct coordination of  $\text{Eu}^{2+}$  by nitrogen leads to luminescence characteristics, which are significantly different from those that can be found in oxide environments. Examples are  $\text{Eu}^{2+}$  doped  $\text{M}_2\text{Si}_5\text{N}_8$  and  $\text{MSi}_7\text{N}_{10}$  ( $\text{M} = \text{Ce}, \text{Sr}, \text{Ba}$ ), which display very long-wavelength emission for  $\text{Eu}^{2+}$  ( $>600 \text{ nm}$ ) [1]. In  $\text{Ca-}\alpha\text{-sialon}$  the  $\text{Eu}^{2+}$  emission can also be found at much longer wavelengths than usual (560-590 nm instead of 350-450 nm) [2], while the excitation band is also located at relatively low energies.

The luminescence properties, in combination with their environmental stability and low toxicity, make these materials interesting for application in the phosphor and pigment industry. Therefore it was decided to also turn our attention to the optical properties of oxynitride glasses, a field, which is relatively unexplored.

In the previous chapter europium was suggested to be present in the divalent form in Eu-doped Y-Si-Al-O-N glasses. In the present study the oxidation state of europium will be investigated as well as the optical properties of the materials.

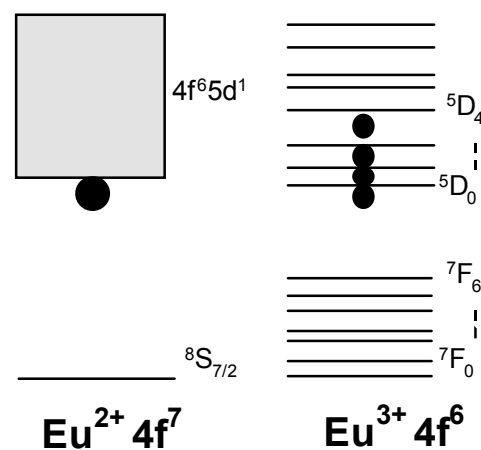


Fig 5.1 *Electronic structure of  $\text{Eu}^{2+}$  and  $\text{Eu}^{3+}$  (•: emitting levels).*

The electronic structures of  $\text{Eu}^{3+}$  and  $\text{Eu}^{2+}$  are sketched in figure 5.1. The excited states of  $\text{Eu}^{2+}$  are characterised by the broad  $4f^65d^1$  level, while for  $\text{Eu}^{3+}$  a distinct number of 4f lines are visible. The reason for this difference is the shielding of the 4f levels. Because this shielding is absent for the 5d levels of  $\text{Eu}^{2+}$ , the  $4f^65d^1$  level is spread out over an energy interval. This lack of shielding also makes the  $4f^65d^1$  level susceptible to coordination effects.

Depending on the distance, location and the covalence of the surrounding ions the position (in energy) of the  $4f^65d^1$  band can vary. Three effects can be distinguished. The nephelauxetic effect can shift the  $4f^65d^1$  band as a whole to lower energies. It is related to the covalence of the site. A more covalent surrounding lowers the position of the  $4f^65d^1$  band. A second effect is the Stokes Shift. The Stokes shift can be described as the energy loss during the excitation and relaxation of the ion. It is related to the size of the europium site. The smaller the size the larger the Stokes shift. The third effect is the crystal field splitting. As a result of the site symmetry and the orbital overlap between europium and the neighbouring ions the  $4f^65d^1$  band can be split up in separate levels. Since emission is occurring from the lowest levels this process lowers the emission energy. For the  $4f \rightarrow 4f$  luminescence of  $\text{Eu}^{3+}$  these considerations are absent, since the positions of the  $4f$  levels are only marginally affected by the nature of the site. Therefore  $\text{Eu}^{3+}$  emission is characterised by a number of emission lines at well-defined wavelengths, whereas  $\text{Eu}^{2+}$  leads to a broadband emission, spread out over a large wavelength interval.

## 5.2 Experimental

### *Preparation of the glasses*

In most M-sialon systems, such as the Y-Si-Al-O-N system, a considerable glass-forming region can be found at low nitrogen to oxygen ratio. The composition  $\text{Y}_{35}\text{Si}_{45}\text{Al}_{20}\text{O}_{83}\text{N}_{17}$  [eq%] has been chosen as a central point since this composition has been reported to yield the B-phase upon crystallisation [3, 4,5]. In this composition a variable amount of yttrium was replaced by europium to act as an activator cation. The composition was further varied along the three axes which are defined by the: (Eu,Y)/Al, Si/Al and O/N ratio. The compositions of the starting mixtures that have been weighed-out in this investigation are listed in table 5.1.  $\text{Eu}_2\text{O}_3$  (99.9% Rare-earth Products Ltd.),  $\text{Y}_2\text{O}_3$  (99.9% Rare-earth Products Ltd),  $\text{SiO}_2$  (Fluka Chemicals Ltd.),  $\text{Al}_2\text{O}_3$  (BDH laboratory supplies) and  $\text{Si}_3\text{N}_4$  (Starck) were taken as raw materials. All oxides were calcined at 900 °C to remove any volatiles and/or chemically absorbed water. A homogeneous powder was obtained by ball-milling the powder mixture overnight in iso-propanol with  $\text{Si}_3\text{N}_4$  balls and subsequently drying it. The powder was iso-statically compressed (dry-bag, 150 MPa) to a pellet of 50 gram. The pellet was melted in a vertical tube furnace at temperatures between 1700 and 1750 °C, depending on the glass composition.



Melting was performed in a nitrogen atmosphere. The carbon crucible was lined on the inner wall with Hex-BN powder to prevent sticking. The melt was quenched by pouring it into a graphite mould, which was pre-heated at 800 °C and subsequently annealed for two hours at this temperature in air. The glasses were determined to be X-ray amorphous.

UV-Vis transmission spectra were taken of these samples in the range of 200-900 nm, using a Shimadzu PC-2401 Spectrophotometer equipped with an integrating sphere assembly. The glasses were cut and polished into sheets of 500 µm thickness. Luminescence measurements were performed on bulk samples using a Perkin-Elmer LS-50B spectrofluorometer equipped with a Xenon flashlamp.

Table 5.1: *Weighed-out compositions of the investigated glasses.*

Code	Eu [at%]	Y [at%]	Si [at%]	Al [at%]	O [at%]	N [at%]
S1G1	0.15	15.0	14.7	8.7	54.1	7.4
G1	1.5	13.7	14.7	8.7	54.1	7.4
S1G2	9.1	6.1	14.7	8.7	54.1	7.4
S1G3	15.2	0	14.7	8.7	54.1	7.4
S2G1	1.8	16.0	14.7	6.1	54.1	7.4
G1	1.5	13.7	14.7	8.7	54.1	7.4
S2G2	1.0	8.8	14.6	14.3	54.0	7.4
S3G1	1.5	13.8	18.5	4.0	54.7	7.4
S3G2	1.5	13.8	16.7	6.1	54.4	7.4
G1	1.5	13.7	14.7	8.7	54.1	7.4
S3G3	1.5	13.4	10.6	14.1	53.1	7.3
S4G1	1.5	13.3	14.3	8.5	60.3	2.1
S4G2	1.5	13.5	14.4	8.6	57.8	4.3
G1	1.5	13.7	14.7	8.7	54.1	7.4

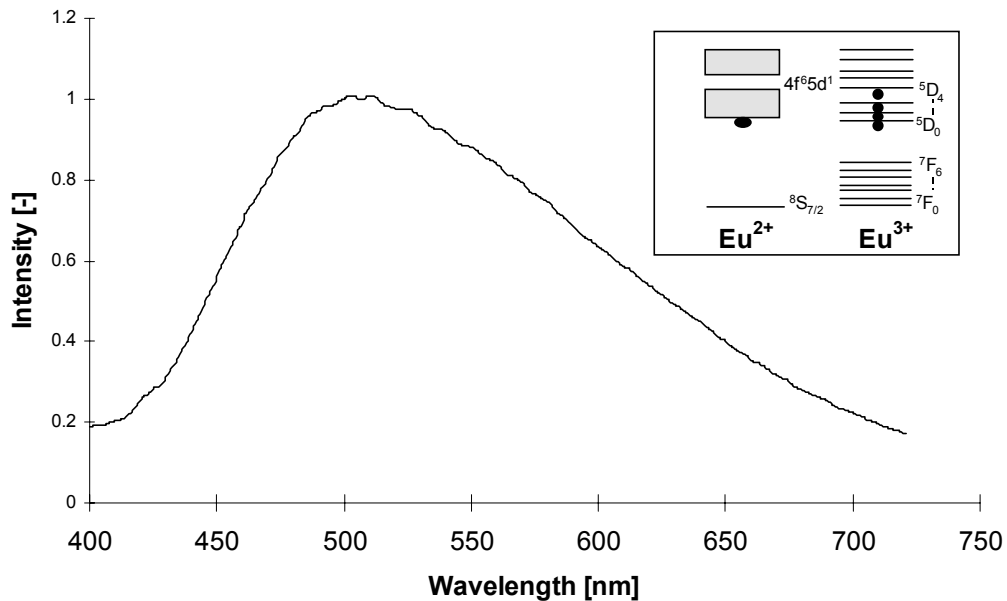


Fig. 5.2 Emission spectrum of glass SIG1 and energy level diagram of  $\text{Eu}^{2+}$  and  $\text{Eu}^{3+}$  (inset).

### 5.3 The oxidation state of europium

The emission spectra of the glasses are characterised by a single broad band (Fig 5.2). This is strong evidence for the presence of europium in the divalent state, since  $\text{Eu}^{2+}$  gives broadband emission while the presence of  $\text{Eu}^{3+}$  should result in a number of sharp lines around 610 nm. The absence of these lines leads us to conclude that the major part of  $\text{Eu}^{3+}$  in the starting mixture has reduced to  $\text{Eu}^{2+}$  in the glasses. Although the emission of  $\text{Eu}^{3+}$  is relatively strong at low concentrations, it can (in theory) be quenched by energy transfer to defects or to the present  $\text{Eu}^{2+}$ .

### 5.4 Optical properties of (Eu,Y)-Si-Al-O-N glasses

#### *Transmittance/absorbtion*

Undoped Y-Si-Al-O-N glasses are reported to be colourless [4,6], in contrast to the Eu-doped ones. Depending on the europium content of the glasses the colour can range from green (low Eu-content) to amber (high Eu-content). This is reflected by the UV-Vis spectra (Fig. 5.3), which show an increase of the absorption with increasing Eu content. The absorption edge is shifted into the visible region. From the spectra it becomes apparent that the Eu 5d band is located just below the bandgap of the Si-Al-O-N glass matrix.

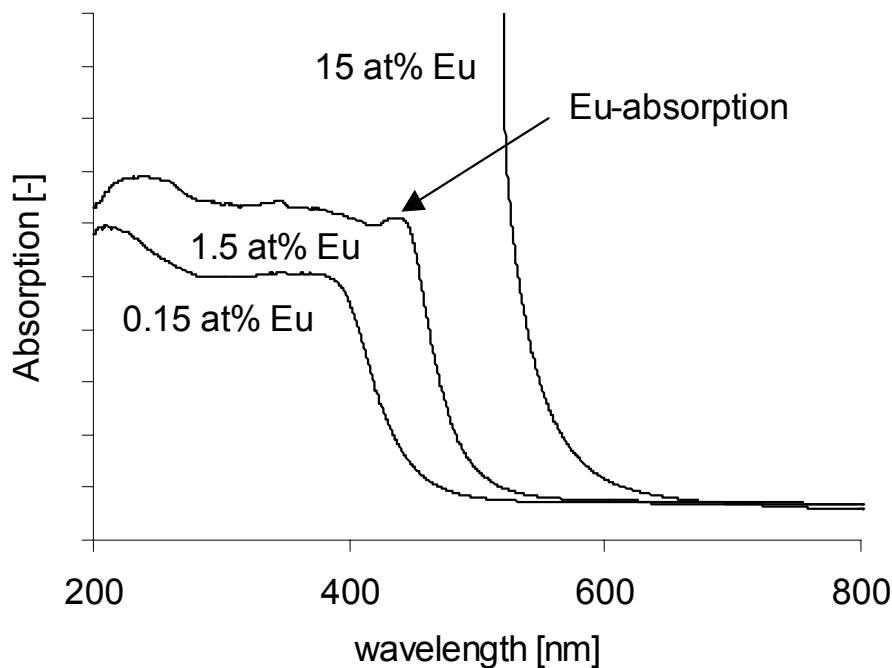


Fig 5.3 *UV-Vis transmission spectra of glasses SIG1, G1 and SIG3. The arrow denotes a region of enhanced absorption presumably caused by europium.*

A change of other parameters, e.g. the Si/Al ratio has no effect on the transmittance of the glasses in the ultraviolet and visible region. An enhanced absorption in the visible region upon nitrogen addition has not been observed although this has been reported for Y-Si-Al-O-N glasses. From these results it seems more likely reported absorption in the visible region is more likely correlated to impurities in the silicon nitride (see chapter 2) than a decrease of the bandgap.

### *Excitation/Emission*

Both the series with a varying Si/Al ratio and a varying O/N ratio show no significant change of the position of the emission and excitation band, which are located at approximately 430 nm and 600 nm, respectively. This indicates that nitrogen for this overall composition is not directly coordinated with europium. This is in accordance with claims that nitrogen in M-Si-Al-O-N glasses of similar composition only performs a bridging function between three silicon atoms [7], which need not to be necessarily true for other compositions, which lie outside the compositional range measured in this study, since a significant

amount of non-bridging nitrogen ( $=N^-$  and  $-N^{2-}$ ) has been found in Na-Si-O-N glasses [8,9]. For the investigated compositions it can be concluded that charge compensation is predominantly delivered by non-bridging oxygen ( $-O^-$ ) and/or aluminium.

Strong changes of the luminescence characteristics were found by changing the Eu/Y ratio. With increasing Eu-content the low-energy edge of the excitation band is extended towards longer wavelengths (Fig. 5.4), which corresponds with the shift of the absorption edge in the UV-Vis spectra. The emission also undergoes a shift to longer wavelengths with increasing Eu-contents (Fig. 5.5). For the concentration range, which has been used in this investigation (0.15-9.2 at% Eu) the emission shifts from 500 to 640 nm.

A similar effect occurs when altering the (Eu,Y)/Al ratio (series 2). In this series the wavelength of the  $Eu^{2+}$  emission increases with increasing (Eu,Y)/Al ratio. In Figure 5.6 the energy of the emission maximum is plotted against the Eu-content for the glasses of series 1 and 2. The position of the emission band appears to be primarily dependent on the concentration of europium, while there is a minor influence of yttrium.

Energy transfer, where a  $Eu^{2+}$  site is excited and subsequently donates its energy to a neighbouring  $Eu^{2+}$  site, can explain the strong shift of the emission to longer wavelengths and its dependence on the  $Eu^{2+}$  concentration. Of course this can only occur if the excited state of the receiving  $Eu^{2+}$  ion is located at lower energies than that of the donating ion. This is the case in glasses where a distribution of  $Eu^{2+}$  sites is present rather than one well-defined site. The probability of energy transfer between two ions increases as the distance between the donor and the acceptor ion decreases, which is in accordance with the observed dependence of the emission energy on the europium concentration (Fig. 5.6).

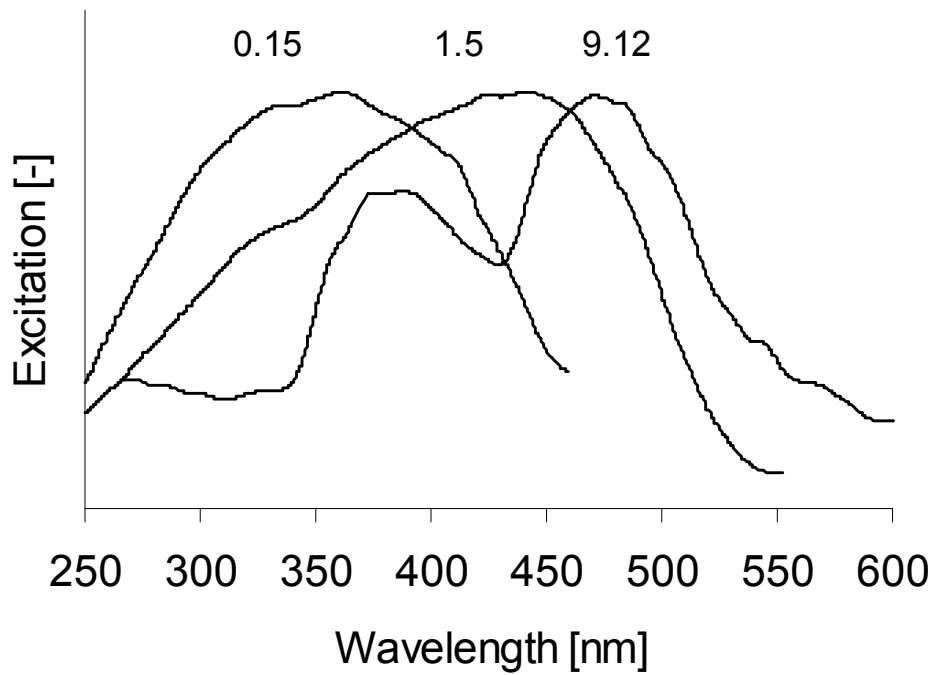


Fig 5.4 *Excitation characteristics of glasses SIG1, G1 and SIG2 (0.15, 1.5 and 9.12 at% Eu);  $\lambda_{Mon}$  510 nm (0.15), 600 nm (1.5), 640 nm (9.12).*

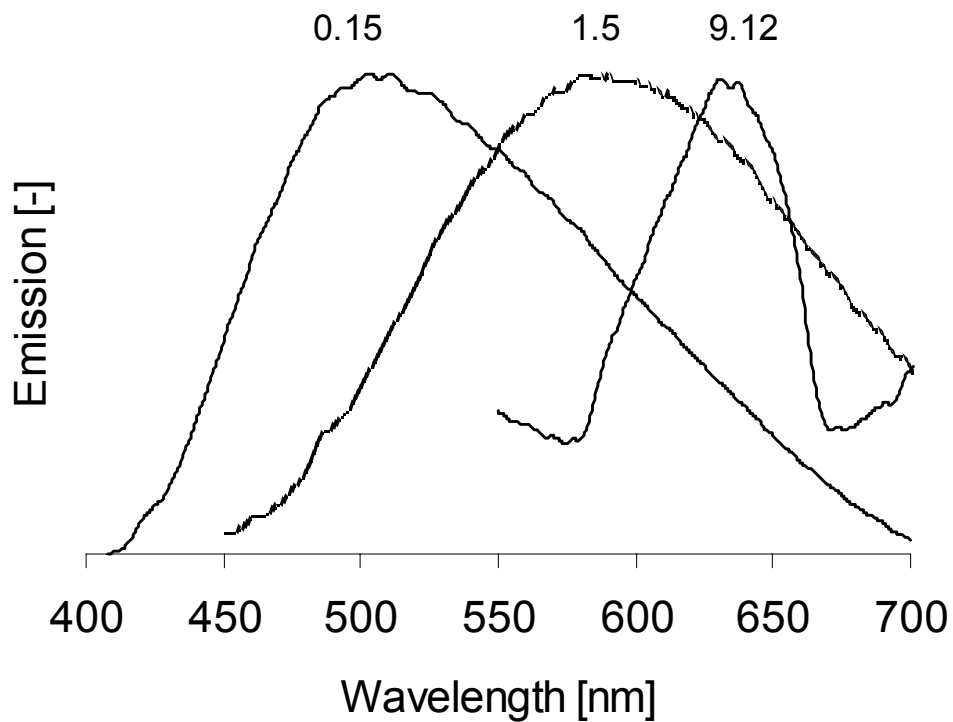


Fig 5.5 *Emission characteristics of glasses SIG1, G1 and SIG2 (0.15, 1.5 and 9.12 at% Eu);  $\lambda_{Exc}$  350 nm (0.15), 400 nm (1.5), 450 nm (9.12).*

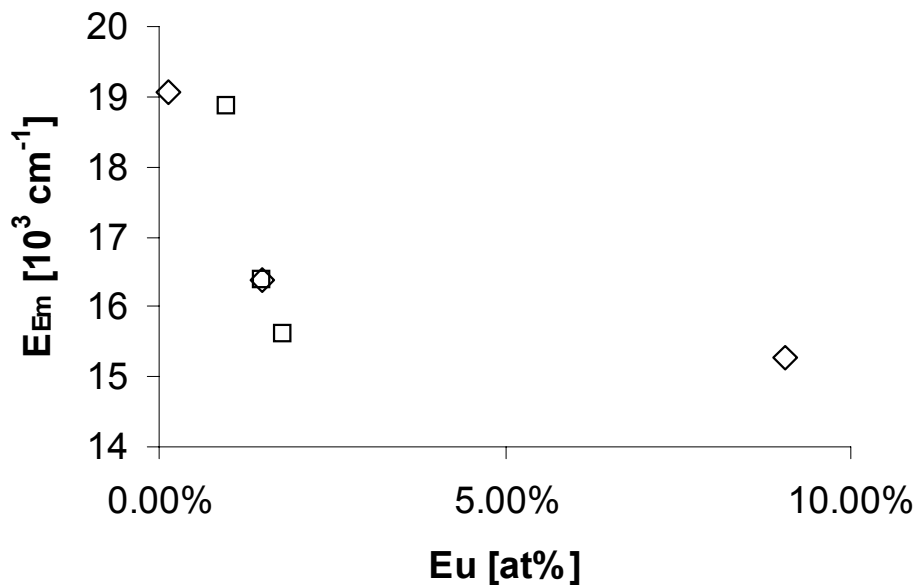


Fig. 5.6 *Emission energy as a function of the absolute europium content* (◇ series 1, □ series 3).

Apart from the fact that energy transfer is a logical explanation for the emission shift, the existence of the low-energy emitting sites indicates a very special  $\text{Eu}^{2+}$  coordination. The fact that it is not possible to produce long-wavelength emission at low  $\text{Eu}^{2+}$  contents, suggests that these sites are only formed at higher  $\text{Eu}^{2+}$  contents. Evidently, at high  $\text{Eu}^{2+}$  contents, part of the  $\text{Eu}^{2+}$  ions experience a large nephelauxetic effect and a large ligand field due to incorporation on a small covalent site [10], the nature of which is a point for further research.

## 5.5 Conclusions

$\text{Eu}^{3+}$  in the starting materials of (Eu,Y)-Si-Al-O-N glasses is reduced to its divalent form by a reaction with the chemically incorporated nitrogen. The luminescence characteristics of these glasses appear to be only marginally dependent on the network forming cations and anions, but strongly on the concentration and type of network modifying cations (Eu,Y). By a variation of the cationic composition the emission can be shifted over a large interval 500-650 nm, while the excitation also shifts to long wavelengths. The concentration dependence of the emission and excitation wavelengths can be explained by assuming a changing site distribution and energy transfer between the different sites.

## References

1. J.W.H. van Krevel, "On new rare-earth doped M-Si-Al-O-N materials, Luminescence properties and oxidation resistance", Ph.D. thesis, Eindhoven University of Technology (2000)
2. J.W.H. van Krevel, J.H.T. van Rutten, H.T. Hintzen, R. Metselaar and H. Mandal, *J. Solid State Chem.* 165[1] (2002) 19-24
3. H. Lemercier, R. Ramesh, J-L. Besson, K. Liddell, D. P. Thompson and S. Hampshire, *Key Engineering Materials Vols. 132-136* (1997) 814-817
4. S. Hampshire, E. Nestor, R. Flynn, J-L. Besson, T. Rouxel, H. Lemercier, P. Goursat, M. Sebai, D. P. Thompson and K. Liddell, *J. Eur. Ceram. Soc.* 14 (1994) 261-273
5. M.F. Gonon, J-C. Descamps, F. Cambier, D.P. Thompson, *Ceram. Int.* 26 (2000) 105-111
6. R.E. Loehman, *J. Am. Ceram. Soc.* 62(10) (1979) 491-494
7. M. Schneider, V.A. Gasparov, W. Richter, M. Deckwerth and C. Russel, *J. Non-Cryst. Sol.* 215 (1997) 201-207
8. S. Kohn, W. Hoffbauer, M. Jansen, R. Franke and S. Bender, *J. Non-Cryst. Sol.* 224 (1998) 232-243
9. J. Jin, T. Yoko, F. Miyaji, S. Sakka, T. Fukunaga and M. Misawa, *J. Am. Ceram. Soc.* 76 [3] (1993) 630-634
10. G. Blasse and A. Bril, *Philips Technical Review* 31[10] (1970) 304-334

# Chapter VI

---

## Ce<sup>3+</sup> Luminescence in Si-Al-O-N glasses

*In this chapter the effect of the chemical composition on 5d→4f emission is further explored using Ce<sup>3+</sup>-doped Ln-Si-Al-O-N (Ln = Sc, Y, La, Gd) glasses as a model system. It is shown that in this system the Ce<sup>3+</sup> emission shows a similar dependence on the chemical composition as europium in the previous chapter. As a function of the cerium content the emission shifts from ~340 nm to ~500 nm. This behaviour can be understood by assuming a changing site population and energy transfer between different cerium sites, which are both affected by the overall chemical composition.*



## 6.1 Introduction

It was shown in the previous chapter that the luminescence properties of  $\text{Eu}^{2+}$  in Y-Si-Al-O-N glasses are strongly affected by the chemical composition. In this chapter we try to focus on the underlying mechanisms causing the emission shift. However instead of  $\text{Eu}^{2+}$ ,  $\text{Ce}^{3+}$  is selected as a luminescent centre. The reason for this choice is quite simple. The oxidation state of  $\text{Ce}^{3+}$  makes it a better match with  $\text{Y}^{3+}$ , which makes it possible to prepare (Ce,Y)-Si-Al-O-N glasses whilst maintaining a constant O/N ratio. From a chemical point of view  $\text{Ce}^{3+}$  also bears more resemblance to the other trivalent lanthanide ions, which means that it will occupy similar sites.

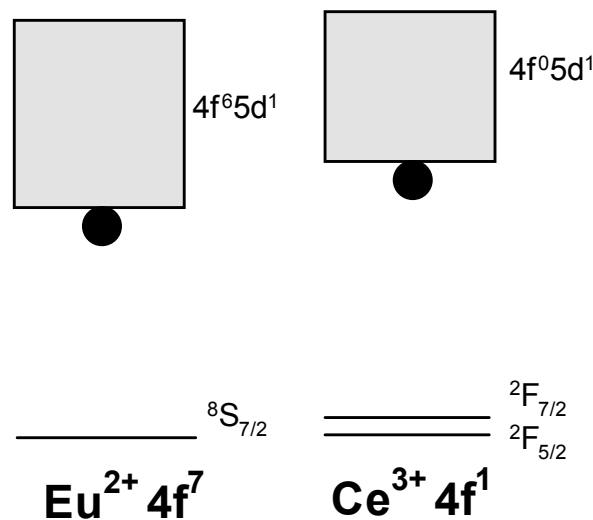


Fig. 6.1 *Schematic representation of the energy levels of  $\text{Eu}^{2+}$  and  $\text{Ce}^{3+}$ .*

The energy level diagrams of  $\text{Ce}^{3+}$  ( $4f^1$ ) and  $\text{Eu}^{2+}$  ( $4f^7$ ) are very similar (Fig 6.1). Therefore these ions share common luminescence characteristics. In both cases the emission spectrum is dominated by broadband  $5d \rightarrow 4f$  emission. For europium the emission is usually located at shorter wavelengths than that of  $\text{Ce}^{3+}$  due to the lower position (in energy) of the  $4f^6 5d^1$  band of  $\text{Eu}^{2+}$ . The energy difference between the split  ${}^2F_J$  levels of  $\text{Ce}^{3+}$  is in practice so small that both emission peaks can usually not be separated so we will treat them indiscriminately.

## 6.2 Experimental

Starting from a central composition  $\text{Ce}_{15.2}\text{Si}_{14.7}\text{Al}_{8.7}\text{O}_{54.1}\text{N}_{7.4}$  the composition is altered by the (partial) replacement of  $\text{Ce}^{3+}$  with other lanthanide ions ( $\text{Sc}^{3+}$ ,  $\text{Y}^{3+}$ ,  $\text{La}^{3+}$ ,  $\text{Gd}^{3+}$ ). The weighed-out compositions are listed in table 6.1.

Table 6.1 *Weighed-out compositions, measured density and emission wavelength of the (Ce,Ln)-Si-Al-O-N (Ln = Sc, Y, La, Gd) glasses prepared in this investigation.*

Compositions [at%]							$\rho$ [g/cm <sup>3</sup> ]	$\lambda_{\text{em}}$ [nm]	Compositions [at%]							$\rho$ [g/cm <sup>3</sup> ]	$\lambda_{\text{em}}$ [nm]											
<b>Ce</b>	<b>Y</b>	<b>Si</b>	<b>Al</b>	<b>O</b>	<b>N</b>				<b>Ce</b>	<b>La</b>	<b>Si</b>	<b>Al</b>	<b>O</b>	<b>N</b>				<b>Ce</b>	<b>Gd</b>	<b>Si</b>	<b>Al</b>	<b>O</b>	<b>N</b>					
15.2	0	14.7	8.7	54.1	7.4	4.7	<b>500</b>		6.0	9.2	14.7	8.7	54.1	7.4	4.5	<b>490</b>		6.0	9.2	14.7	8.7	54.1	7.4	4.9	<b>485</b>			
6.0	9.2	14.7	8.7	54.1	7.4	4.3	<b>485</b>		3.0	12.2	14.7	8.7	54.1	7.4	4.5	<b>480</b>		3.0	12.2	14.7	8.7	54.1	7.4	5.0	<b>465</b>			
3.0	12.2	14.7	8.7	54.1	7.4	4.1	<b>470</b>		1.5	13.7	14.7	8.7	54.1	7.4	4.5	<b>465</b>		1.5	13.7	14.7	8.7	54.1	7.4	5.1	<b>450</b>			
1.5	13.7	14.7	8.7	54.1	7.4	4.0	<b>450</b>		0.2	15.	14.7	8.7	54.1	7.4	4.5	<b>420</b>		0.2	15.	14.7	8.7	54.1	7.4	5.1	<b>405</b>			
0.2	15.	14.7	8.7	54.1	7.4	4.0	<b>405</b>		0.04	15.2	14.7	8.7	54.1	7.4	4.5	<b>400</b>		0.04	15.2	14.7	8.7	54.1	7.4	5.1	<b>395</b>			
0.04	15.2	14.7	8.7	54.1	7.4	4.0	<b>395</b>																					
9.7	0	14.7	14.1	54.1	7.4	4.1	<b>470</b>		<b>Ce</b>	<b>Gd</b>	<b>Si</b>	<b>Al</b>	<b>O</b>	<b>N</b>				<b>Ce</b>	<b>Sc</b>	<b>Si</b>	<b>Al</b>	<b>O</b>	<b>N</b>					
7.7	1.9	14.7	14.1	54.1	7.4	3.9	<b>455</b>		6.0	9.2	14.7	8.7	54.1	7.4	4.9	<b>485</b>		8.4	6.8	14.7	8.7	54.1	7.4	4.2	<b>480</b>			
4.4	5.3	14.7	14.1	54.1	7.4	3.8	<b>445</b>		3.0	12.2	14.7	8.7	54.1	7.4	5.0	<b>465</b>		3.7	11.5	14.7	8.7	54.1	7.4	3.8	<b>460</b>			
2.1	7.6	14.7	14.1	54.1	7.4	3.6	<b>430</b>		1.5	13.7	14.7	8.7	54.1	7.4	5.1	<b>450</b>		1.1	14.1	14.7	8.7	54.1	7.4	3.4	<b>430</b>			
0.8	8.8	14.7	14.1	54.1	7.4	3.6	<b>415</b>		0.2	15.	14.7	8.7	54.1	7.4	5.1	<b>405</b>												
0.1	9.6	14.7	14.1	54.1	7.4	3.5	<b>385</b>		0.04	15.2	14.7	8.7	54.1	7.4	5.1	<b>395</b>												
17.8	0	14.7	6	54.1	7.4	<b>4.9</b>	<b>510</b>		<b>Ce</b>	<b>Sc</b>	<b>Si</b>	<b>Al</b>	<b>O</b>	<b>N</b>														
3.5	14.3	14.7	6	54.1	7.4	<b>4.3</b>	<b>480</b>		8.4	6.8	14.7	8.7	54.1	7.4	<b>4.2</b>	<b>480</b>												
0.8	17	14.7	6	54.1	7.4	<b>4.2</b>	<b>460</b>		3.7	11.5	14.7	8.7	54.1	7.4	<b>3.8</b>	<b>460</b>												
0.04	17.8	14.7	6	54.1	7.4	<b>4.1</b>	<b>420</b>		1.1	14.1	14.7	8.7	54.1	7.4	<b>3.4</b>	<b>430</b>												

*Compositions are corrected for the reduction of  $\text{Ce}^{4+}$  by  $\text{N}^{3-}$ . Excitation was performed at wavelengths between 340 and 385 nm depending on the highest emission yield.*

The following starting materials were used (purity > 99.9%): CeO<sub>2</sub> (Rhône Poulenc), La<sub>2</sub>O<sub>3</sub> (Rhône Poulenc), Sc<sub>2</sub>O<sub>3</sub> (Aldrich), Y<sub>2</sub>O<sub>3</sub> (Shin Etsu Y-474), Gd<sub>2</sub>O<sub>3</sub> (Reade), Al<sub>2</sub>O<sub>3</sub> (Taimei), SiO<sub>2</sub> (Aerosil OX50) and Si<sub>3</sub>N<sub>4</sub> (Akzo Nobel P95H). Although added as CeO<sub>2</sub>, cerium is assumed to be fully converted to the trivalent state in the glasses as a result of reaction with the added Si<sub>3</sub>N<sub>4</sub>:



This mechanism is well established for Si<sub>3</sub>N<sub>4</sub>-CeO<sub>2</sub> reaction systems [1] and is in accordance with thermodynamic calculations for Ce-Si-Al-O-N glass [2]. The change of the overall composition due to this reaction is accounted for by adapting the Si<sub>3</sub>N<sub>4</sub>/SiO<sub>2</sub> ratio in the starting mixture accordingly.

The powder mixtures were wet mixed in a ball mill, dried and uni-axially pressed into pellets of ca. 2 g. The pellets were fired in an induction furnace at temperatures of approximately 1650-1750 °C. A molybdenum crucible was used which was lined with hexagonal-BN to prevent sticking. Melting and cooling was performed under nitrogen. The melting times and current (temperature) were adjusted per sample to obtain thoroughly melted, X-Ray amorphous glass droplets. The density of the samples was determined using the Archimedes technique. The samples were crushed into powders prior to spectroscopy. Excitation and emission spectra were measured using a Perkin-Elmer LS-50B spectrofluorometer equipped with a Xe flashlamp. The spectra were corrected for lamp characteristics, detector characteristics and system transmission.

### 6.3 Results and discussion

Figure 6.2 shows the results of the emission measurements for several Ce<sub>x</sub>Y<sub>1-x</sub>-Si-Al-O-N glasses. Over the whole cerium concentration range a strong emission was observed which suggest that these glasses are less susceptible to concentration quenching than the (Eu,Y)-Si-Al-O-N glasses studied in Chapter V. The curves show a systematic increase of the emission wavelength with the cerium content and for high cerium contents the emission shifts to over 500 nm (<20\*10<sup>3</sup> cm<sup>-1</sup>) similar to the europium doped glasses.

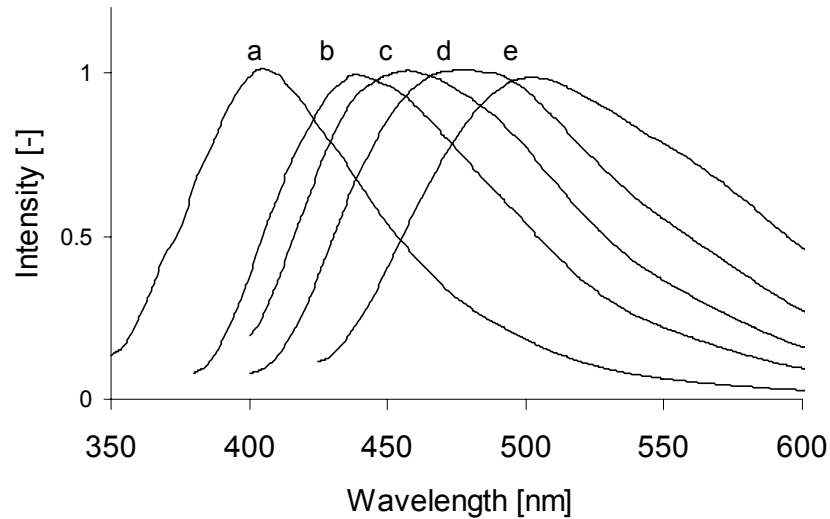


Fig. 6.2 Normalised emission spectra of  $Ce_{(x)}Y_{(15.2-x)}Si_{14.7}Al_{8.7}O_{54.1}N_{7.4}$  glasses as a function of the cerium content ( $x= 0.2$  (a),  $1.5$  (b),  $3.0$  (c),  $6.0$  (d),  $15.2$  (e)).

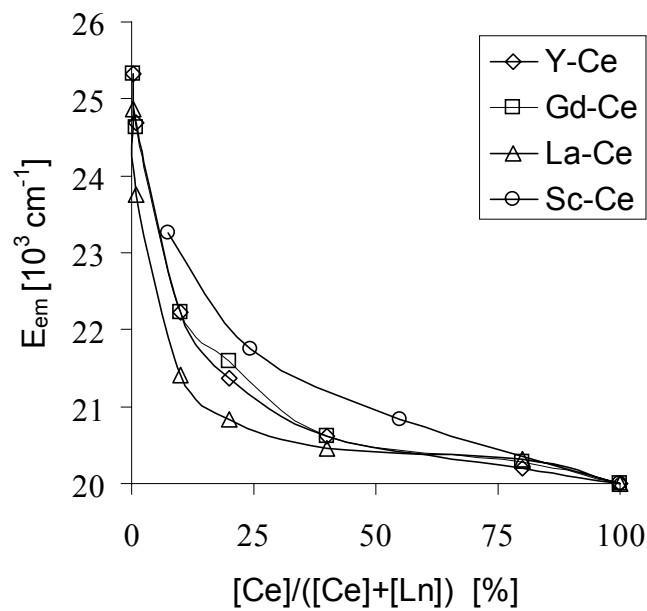


Fig. 6.3 Changes of the emission energy ( $E_{em}$ ) induced by the replacement of Ln by Ce ( $Ce_{(x)}Ln_{(15.2-x)}Si_{14.7}Al_{8.7}O_{54.1}N_{7.4}$ , Ln = Sc, Y, Gd, La). Lines are drawn as a guide for the eye only.

Using scandium, gadolinium and lanthanum instead of yttrium leads to similar results (Fig. 6.3), with only a minor difference between the curves. At low cerium concentrations the excitation and emission bands are positioned at  $\sim 340$  and  $\sim 400$  nm, respectively (Fig. 6.4) and the emission shows only a minor dependence on the excitation wavelength, which is consistent with a single site population in the glass matrix. At higher concentrations of cerium excitation at 340 nm leads to a longer emission wavelength ( $\sim 500$  nm). Moreover, in the excitation spectrum two distinct bands can now be distinguished, one corresponding to the original site population and one at longer wavelengths (lower energies), belonging to a second site population (Fig. 6.4). Excitation in either of the excitation bands leads to a similar emission signature. This strongly suggests that the energy of the first site population is transferred to the second one, effectively quenching the emission of the first one.

The dependence of the emission spectrum on the cerium concentration is thus ascribed to a changing occupancy of mainly two different cerium sites (S and A) and energy transfer between them.

The probability of energy transfer between two luminescent centres is strongly dependent on the distance between the luminescent centres [3,4]. The average distance between the luminescent centres ( $\bar{d}_{ce}$ ) was calculated from the average volume that one Ce atom occupies in the glass assuming an ideal dispersion ( $\bar{V}_{ce}$ ). The molar volume ( $V_m$ ) was calculated from the weighed out composition and the measured density and was used to determine  $\bar{V}_{ce}$ .

$$\bar{d}_{ce} \approx 2 * \left( \frac{\bar{V}_{ce}}{\frac{4}{3}\pi} \right)^{\frac{1}{3}} = 2 * \left( \frac{1}{N_{av}} \cdot \frac{V_m}{x_{ce}} \right)^{\frac{1}{3}} \quad (2)$$

Theory predicts that for two well-defined centres, which are homogeneously distributed, the energy transfer processes will become negligible at sufficiently large distances. In this case high-energy S emission will exclusively be present. The emission energy of our Si-Al-O-N glasses shows the expected dependence on  $\bar{d}_{ce}$  with a stronger dependence for smaller Ce-Ce distances (Fig. 6.5). The emission energy appears to be dependent on the type of lanthanide used and increases in the order La < Gd, Y < Sc, which corresponds with the ionic radii. Figure 6.6 shows that the high-energy emission is also enhanced when the Al concentration of the glass is increased.

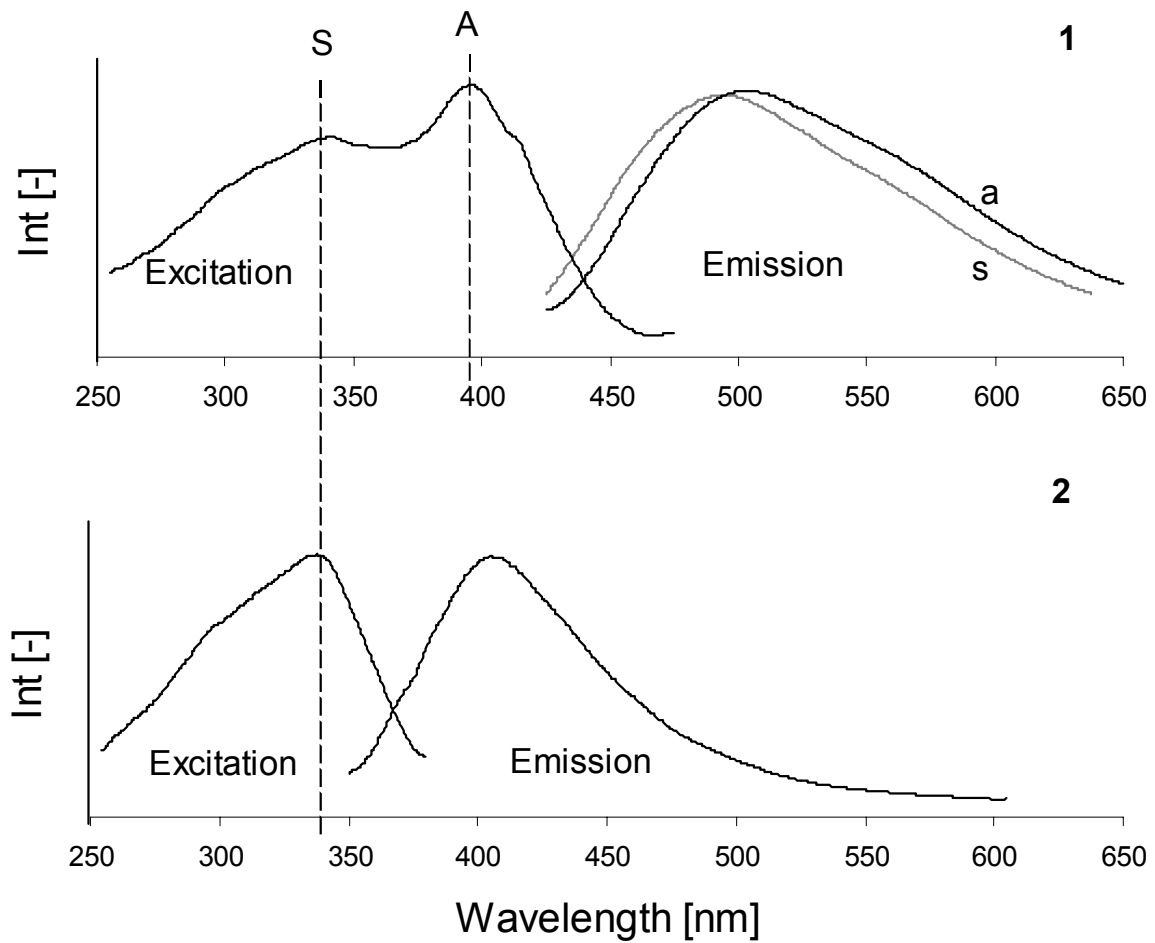


Fig. 6.4 Normalised excitation and emission spectra of (1)  $Ce_{15.2}Si_{14.7}Al_{8.7}O_{54.1}N_{7.4}$  glass and (2)  $Ce_{0.2}Y_{15.0}Si_{14.7}Al_{8.7}O_{54.1}N_{7.4}$  glass. The overlap between the excitation band of site A and the emission band of site S is clearly visible ( $\lambda_{mon} = 485$  (1), 405 (2),  $\lambda_{exc} = 395$  (1a), 340 (1s), and 340 nm (2)).

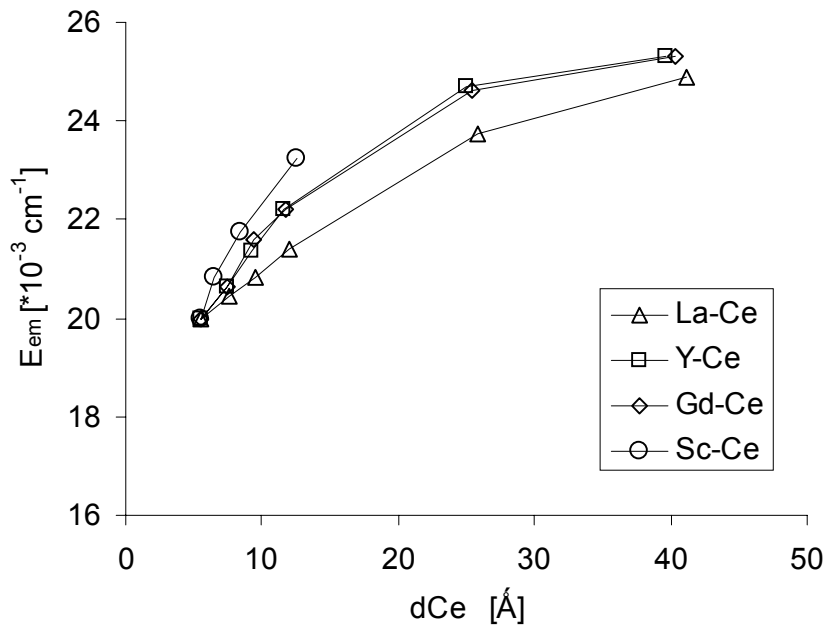


Fig. 6.5 Emission energy ( $E_{em}$ ) as a function of the calculated average Ce-Ce distance ( $\bar{d}_{ce}$ ) for the different chemical compositions ( $Ce_{(x)}Ln_{(15.2-x)}Si_{14.7}Al_{8.7}O_{54.1}N_{7.4}$ ,  $Ln = Sc, Y, Gd, La$ ). Lines are drawn as a guide for the eye only.

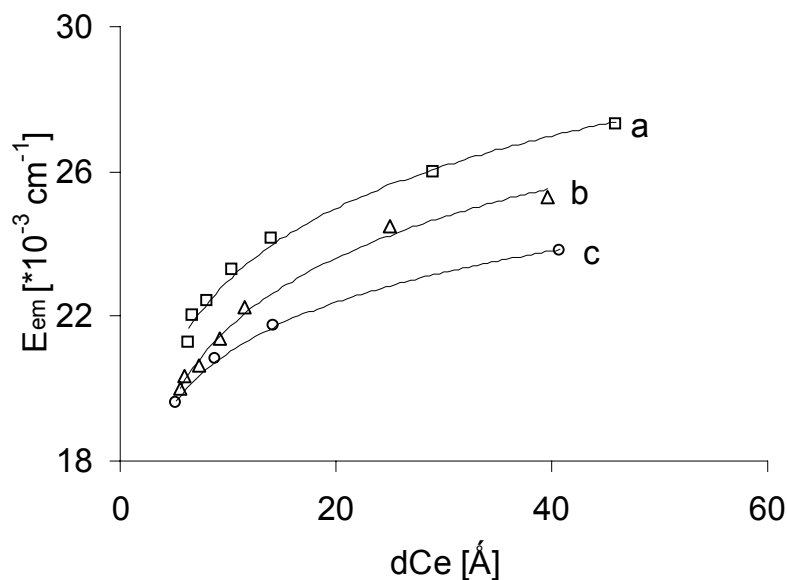


Fig. 6.6 Emission energy ( $E_{em}$ ) as a function of the calculated average Ce-Ce distance ( $\bar{d}_{ce}$ ) for the (Ce,Y)-Si-AL-O-N glasses with different Al to (Ce,Y) ratios ( $[Al/(Ce,Y)] = [14.1/9.7]$  (a),  $[8.7/15.2]$  (b),  $[6/17.8]$  (c) at%). Lines are drawn as a guide for the eye only.

Thus far we have established that the emission is originating from two different sites. The long-wavelength emitting sites are expected to be relatively small and covalent in nature, whereas the short-wavelength emitting sites are expected to be larger and more ionic in nature [10,5,6]. At small Ce concentrations the Ce ion mainly occupies the largest ionic site (near to Al on a Si site), resulting in short wavelength emission.  $\text{Al}^{3+}$  incorporated on a  $\text{Si}^{4+}$  site can provide charge compensation for the lanthanide modifier cations, which results in a more ionic surrounding of the  $\text{Ce}^{3+}$  ion than in the case with charge compensation by non-bridging oxygen.

With increasing Ce concentration the Ce-ion starts ousting the other lanthanides (Sc, Y, Gd, La) from the smaller, more covalent, sites (near non-bridging oxygen). This gives the origin of the long-wavelength emission. Meanwhile the short-wavelength emission is gradually suppressed due to more efficient energy transfer between the Ce-ions (Fig. 6.7). The process can be enhanced by the (partial) removal of Al. Aluminium is known to aid the dispersion of the modifier cations in a glass matrix [7]. With a decrease of the Al content the Ce-Ce distances decrease, resulting in a more efficient energy transfer.

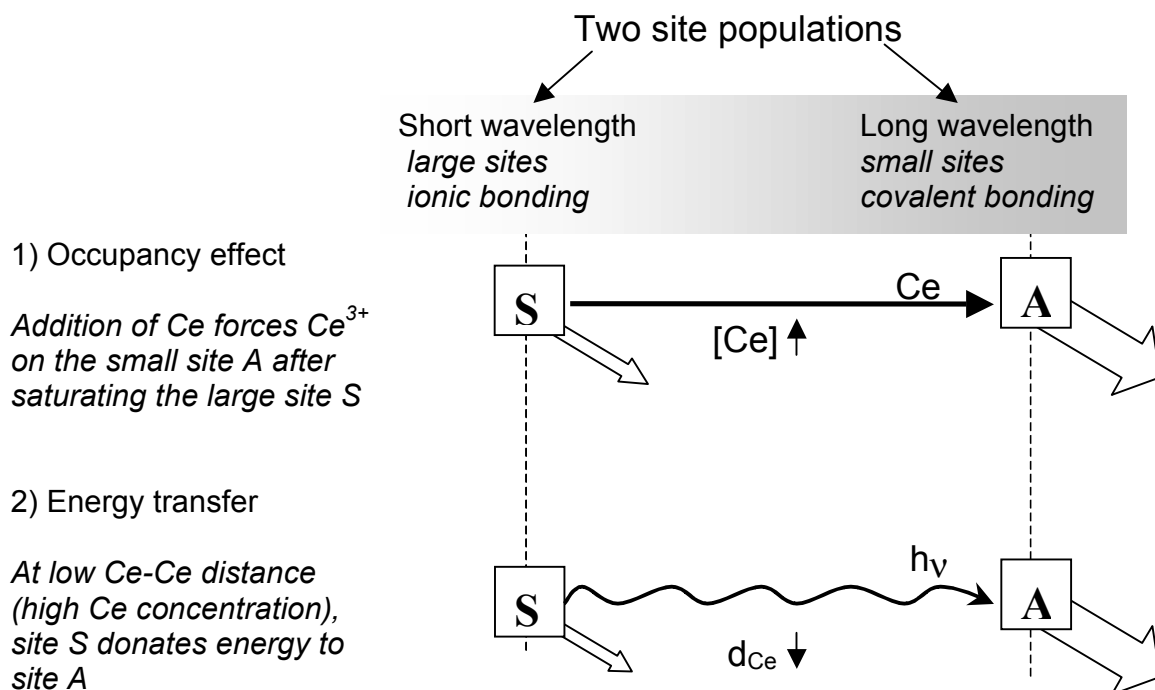


Fig. 6.7 Schematic representation of the various parameters determining the emission wavelength of cerium in Ln-Si-Al-O-N glasses.



Two different Ce site populations with varying site occupancies, and energy transfer between them, explain the effect of Ln (for the smallest Sc ion the intensity of the long-wavelength emission is lower) and the effect of Al (for larger Al contents the intensity of the long-wavelength emission is lower due to more ionic sites and less energy transfer due to a more homogeneous distribution of Ce ions).

## 6.4 Conclusions

The emission of Ce doped Ln-Si-Al-O-N glasses can be varied over a large spectral interval (380-500 nm). The source of this variation lies in the presence of at least two groups of Ce sites in the investigated glasses with different excitation and emission wavelengths. The occupancy of these sites is governed by a competition between Ce and the other lanthanides depending on their relative sizes. At low Ce concentrations, Ce will occupy the short-wavelength emitting site (ionic, large), while at high concentrations it will also occupy the long-wavelength emitting sites (covalent, small). In the latter situation, energy transfer will suppress the short-wavelength emission.

## References

1. R.J. Meyer, E.H.E. Pietsch, A. Kotowski and M. Becke-Goehring, "Gmelin handbook of inorganic and organometallic chemistry", Si Suppl. B5d1, (Springer-Verlag 1995) 219-224
2. A. Diaz, S. Guillope, P. Verdier, Y. Laurent, A. Lopez, J. Sambeth, A. Paul and J.A. Ordriozola, Mater. Sci. Forum 325-326 (2000) 283-288
3. G. Blasse and A. Bril, Philips Technical Review 31[10] (1970) 304-335
4. L.G. van Uitert and L.F. Johnson, J. Chem. Phys. 44[9] (1966) 3514-3522
5. G. Blasse, Phys. Stat. Sol. (b) 55, (1978) K131-K134
6. L.G. van Uitert, J. Lum. 29 (1984) 1-9
7. H. Zhong, W. Cai and L. Zhang, Mater. Res. Bull. 34[2] (1999) 233-238

# Chapter VII

---

## Tb<sup>3+</sup> distribution and luminescence

*In this chapter the luminescence of Tb<sup>3+</sup> is used in order to study the distribution of lanthanides in Si-Al-O-N glasses. The emission color of terbium is known to vary with the distance between the terbium ions. For this purpose different amounts of terbium were incorporated in the glasses and their emission studied. On comparison with other terbium-activated materials these glasses show typical behavior. That is the distance, which can be estimated from the emission, corresponds to the terbium-terbium distance, as can be expected on basis of the composition and the density. Therefore it can be concluded that the dispersion of the terbium ions can be considered to be ideal.*

## 7.1 Introduction

From the foregoing it is clear that the behavior of lanthanides in Si-Al-O-N glasses is by no means straightforward. It is likely that many of the lanthanides in analogy to europium and cerium can occupy different sites in the glasses. Understanding of this behavior is important since it is expected not only to affect the luminescence properties of the glasses, but also to have an influence on the mechanical properties. Using tools such as XPS [1] and  $^{27}\text{Al} / ^{28}\text{Si}$  NMR [2,3] a clearer picture has been produced of the network structure and the location and role of nitrogen in that structure. There is, however, little detailed information available on how the modifier cations are incorporated in the glass matrix. Since it has been shown in a number of investigations that the properties of these glasses are at least as much dependent on the modifier cation as on the incorporated nitrogen [4,5], it is clear that in order to be able to understand the properties of the glasses we have to increase our knowledge on the modifiers.

In the previous chapters it has been shown that (in the case of cerium and europium) an increase of the modifier content leads to the occupation of new sites. One of the plausible explanations of this behavior is phase separation or clustering. This means that we could be saturating our system with the lanthanides so that an increase of the lanthanide content causes the lanthanide to be incorporated in a separate (clustered) phase. Such behavior has often been suggested for lanthanides. Experimentally it is, however, very hard to verify. Most methods, which are used to characterize glasses, only give information on the glass network. Although clustering and phase separation theoretically lead to a change in density, the difference is in practice minimal and can easily be subject to misinterpretation.

The luminescence characteristics of  $\text{Tb}^{3+}$  can provide an elegant solution for this problem. It is possible to evaluate lanthanide clustering in these glasses by studying the luminescence properties of  $\text{Tb}^{3+}$  [6, 7]. In figure 7.1 the energy levels of  $\text{Tb}^{3+}$  are shown. The emission is occurring from the  $^5\text{D}_3$  (blue emission) and the  $^5\text{D}_4$  (green emission) levels. Cross-relaxation refers to the process where excitation from the  $^7\text{F}_6$  to the  $^7\text{F}_0$  level promotes the non-radiative drain from the  $^5\text{D}_3$  to the  $^5\text{D}_4$  level of a neighbouring ion. The probability of this process is strongly dependent on the distance between the two activators [8, 9]. In an ideal dispersion an increase of the terbium concentration will lead to a gradual shift from blue to green emission, whereas predominantly green emission will be observed at much lower terbium contents in a phase-separated or otherwise clustered situation.

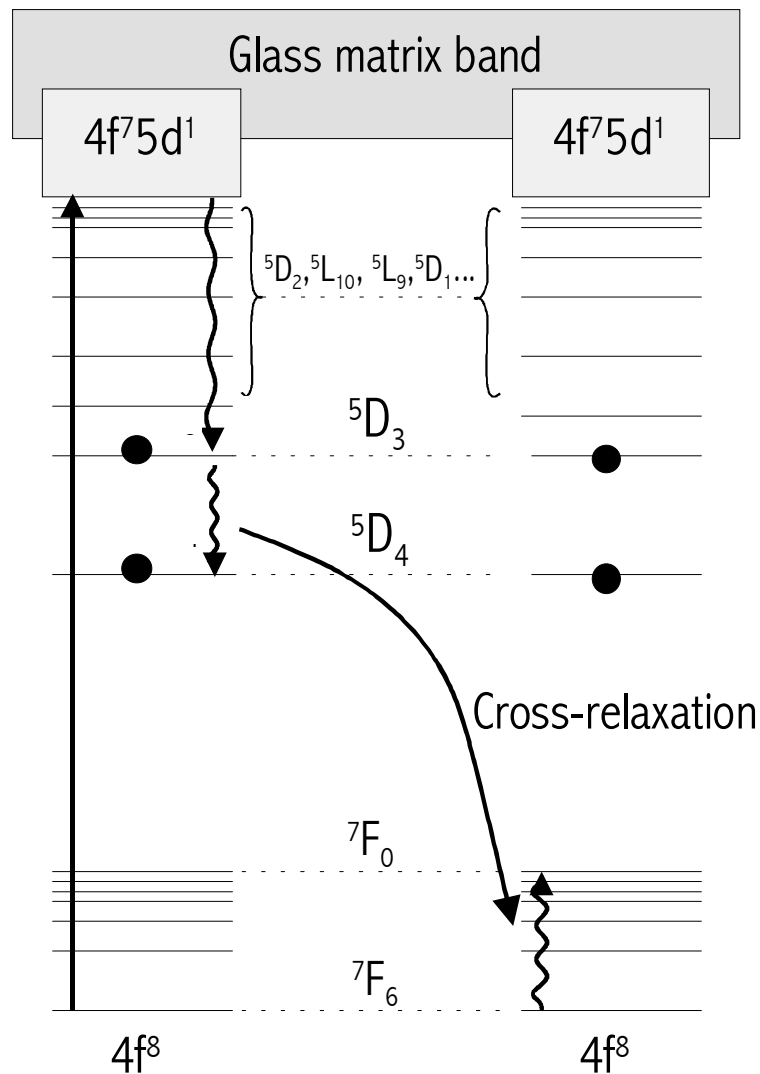


Fig. 7.1 Schematic energy level diagram of two neighboring  $Tb^{3+}$  ions and the cross-relaxation mechanism. (● emitting levels).

## 7.2 Experimental

A number of Si-Al-O-N glasses have been prepared based on the composition of the B-Phase:  $Y_{15.2-x}Tb_xSi_{14.2}Al_{8.7}O_{54.2}N_{7.38}$  [5] (Table 7.1). Adjustment of the  $x$ -value allows for change of the average Tb-Tb distance. The glasses were prepared from  $Tb_4O_7$  (99.9%, Rhodia),  $Y_2O_3$  (99.999%, Rhone Poulenc),  $SiO_2$  (99.7%, fused silica, C-E Minerals),  $Al_2O_3$  (99.99%, Taimei) and  $Si_3N_4$  (Akzo Nobel P95H).  $Tb^{4+}$ , which is present in the raw materials, is expected to thermally reduce to  $Tb^{3+}$  due to the high temperatures and low oxygen-partial pressure used in the synthesis.

Table 7.1. Prepared glasses, (composition  $Y_{15.2-x}Tb_xSi_{14.2}Al_{8.7}O_{54.1}N_{7.38}$ ), measured density ( $\rho_{glass}$ ), calculated number of Tb ions per unit volume ( $1/V_{Tb}$ ) and ratio between summed  ${}^5D_3$  and  ${}^5D_4$  emission intensities ( $\Sigma^5D_4/\Sigma^5D_3$ ).

Glass no	x	$\rho_{glass}$ [g cm <sup>-3</sup> ]	$1/V_{Tb}$ [Å <sup>-3</sup> ]	$\Sigma^5D_4/\Sigma^5D_3$ [-]
1	0.025	3.9	$2.0 * 10^{-5}$	0.13
2	0.05	3.9	$3.9 * 10^{-5}$	0.11
3	0.12	4.0	$9.8 * 10^{-5}$	0.14
4	0.50	4.0	$4.0 * 10^{-4}$	0.56
5	1.5	4.1	$1.2 * 10^{-3}$	3.7
6	3.0	4.2	$2.4 * 10^{-3}$	24
7	15.2	4.9	$1.1 * 10^{-2}$	>300*

\* No  ${}^5D_3$  emission was observed. This estimate is based on the  ${}^5D_3$  detection limit.

The powders were dispersed in isopropanol and mixed overnight in a ball mill using agate balls. The resulting mixture (10 g) was dried and placed in a graphite crucible powder-lined with Hex-BN to prevent sticking. The crucible with contents was fired in a vertical tube furnace during one hour at temperatures of 1700 °C in a nitrogen atmosphere. Afterwards the furnace was cooled down slowly to 1600 °C at which temperature the crucible was rapidly extracted from the furnace. The glass was then allowed to cool down to room temperature in air.

The oxide scale, which had formed during cooling, was removed by grinding the surface. The density of the glasses was measured using the Archimedes method in distilled water. From the density the average volume per Tb ion ( $V_{Tb}$ ) and the number of Tb ions per unit volume ( $1/V_{Tb}$ ) can be calculated using equation 1.

$$V_{Tb} = \frac{1}{N_{Av} \cdot x_{Tb}} \cdot \frac{M_{glass}}{\rho_{glass}} \quad (1)$$

wherein

$N_{Av}$  = number of Avogadro [ $6.023 * 10^{23}$ ]

$x_{Tb}$  = molar fraction of Tb [-]

$M_{glass}$  = molar weight of the glass [g/mol]

$\rho_{glass}$  = measured density of the glass [g/cm<sup>3</sup>]

The glass was crushed to a fine powder prior to the spectroscopic analysis. The luminescence characteristics of the glasses were measured using a fluorophotospectrometer equipped with a Xe-flashlamp. The glasses were measured in reflection, excitation and emission mode. For reflection the spectra were corrected for lamp and detector characteristics and system transmission using the known spectra of BaSO<sub>4</sub> and black felt as standards. The emission spectrum was calibrated using a tungsten lamp as standard. For calibration of the excitation spectra rhodamine was used as a standard in combination with a second photomultiplier.

### 7.3 Results

The measured density increases with the Tb content (Fig. 7.2), which can be expected from the significantly larger atomic mass of Tb as compared to Y.

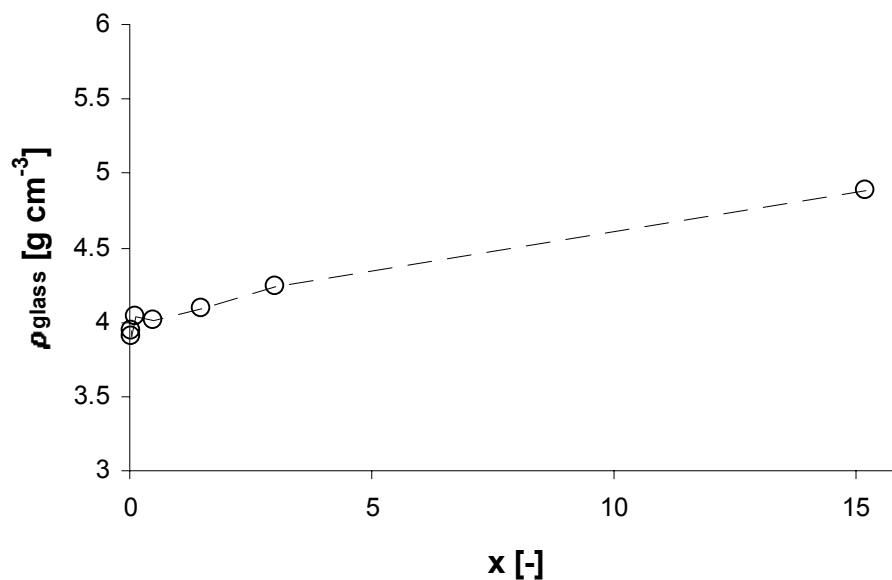


Fig. 7.2 Density of  $Y_{15.2-x}Tb_xSi_{14.2}Al_{8.7}O_{54.2}N_{7.38}$  glasses as a function of the Tb content ( $x$ ).

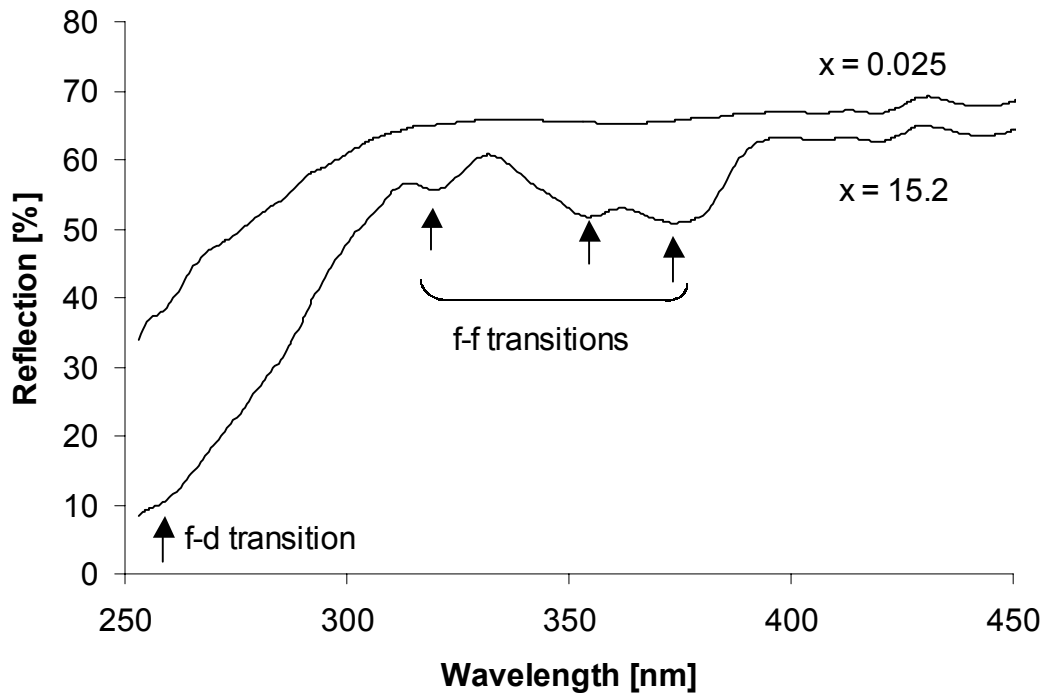


Fig. 7.3 Reflection spectra of  $Y_{15.2-x}Tb_xSi_{14.2}Al_{8.7}O_{54.2}N_{7.38}$  glasses ( $x = 0.025$  and  $x = 15.2$ ). Arrows denote terbium absorption.

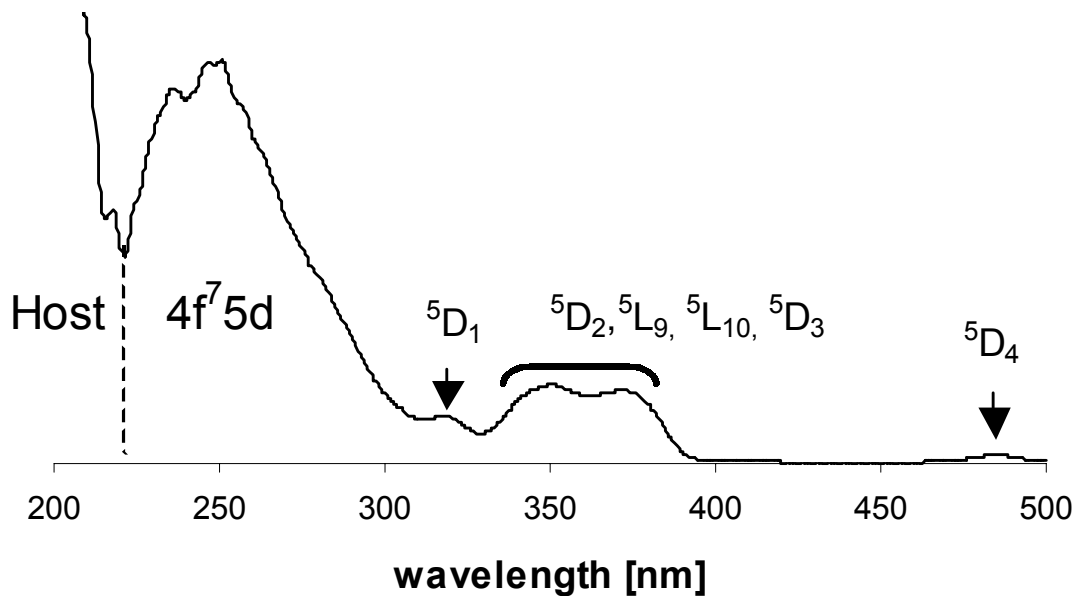


Fig. 7.4 Excitation spectrum of  $Tb_{15.2}Si_{14.2}Al_{8.7}O_{54.2}N_{7.38}$  glass ( $\lambda_{mon} = 545$  nm,  ${}^5D_4 \rightarrow {}^7F_5$ ).

The reflection measurements for low Tb contents (Fig. 7.3) show a strong absorption at low wavelengths, which can be attributed to the glass matrix absorption. With an increasing Tb concentration additional regions of enhanced absorption can be discriminated. These Tb<sup>3+</sup> absorption bands also show up in the excitation spectrum (Fig. 7.4) and can be attributed to the various transitions from the <sup>7</sup>F<sub>6</sub> ground state to higher states (f→d and f→f transitions). In this spectrum it can be clearly seen that the glass matrix excitation of the host lattice is located at relatively high energies and is not expected to interfere with the terbium emission. From these spectra it can be concluded that the optimum Tb<sup>3+</sup> excitation wavelength for this material is ~250 nm.

Excitation for low concentrations of Tb ( $\lambda_{\text{ex}} = 254 \text{ nm}$ ) leads to predominant blue (<sup>5</sup>D<sub>3</sub>) emission (Fig. 7.5). With increasing Tb content an increase of the <sup>5</sup>D<sub>4</sub> emission over the <sup>5</sup>D<sub>3</sub> emission can be observed as expected from the cross-relaxation mechanism.

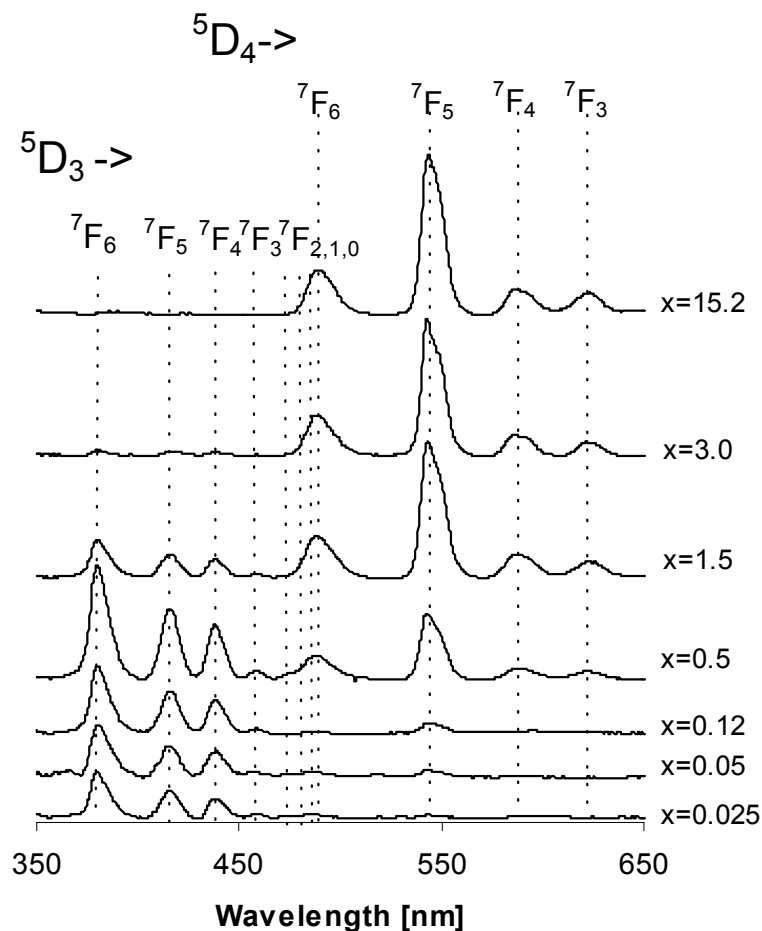


Fig. 7.5 Emission of  $Y_{15.2-x}Tb_xSi_{14.2}Al_{8.7}O_{54.2}N_{7.38}$  glasses as a function the Tb content (x) ( $\lambda_{\text{ex}} = 254 \text{ nm}$ ).



## 7.4 Discussion

The ratio between the integrated intensity of the  ${}^5D_3 \rightarrow {}^7F_{0-6}$  emission ( $\Sigma^5D_3$ ) and that of the  ${}^5D_4 \rightarrow {}^7F_{0-6}$  emission ( $\Sigma^5D_4$ ) was calculated from the experimental data. The overlap between the  ${}^5D_4 \rightarrow {}^7F_6$  transitions at  $\sim 490$  nm and the  ${}^5D_3 \rightarrow {}^7F_{0,1,2}$  transitions at 475-485 nm was resolved by analysing the concentration dependence of both bands. The  $\Sigma^5D_4/\Sigma^5D_3$  ratio varies with three orders of magnitude over the Tb concentration range (Fig. 7.6). The error bars in this figure reflect the accuracy in the procedures, which were used for the determination of the peak height and the baseline subtraction.

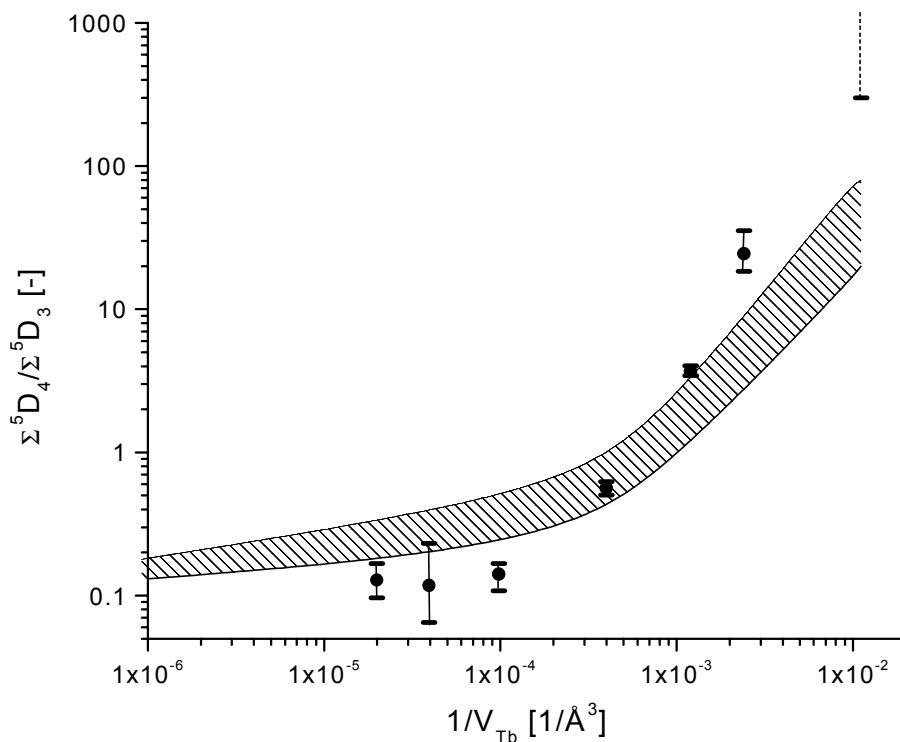


Fig. 7.6 Ratio between integrated  ${}^5D_4$  and  ${}^5D_3$  emission intensities versus the terbium content ( $x$ ) of  $Y_{15.2-x}Tb_xSi_{14.2}Al_{8.7}O_{54.2}N_{7.38}$  glasses. The hatched area represents the YAG:Tb standard curve [9].

From this figure it is clear that the emission behaviour of  $Tb^{3+}$  in Y-Si-Al-O-N glasses is similar to that of  $Y_3Al_5O_{12}:Tb^{3+}$  (YAG:Tb $^{3+}$ ), i.e. a constant value at low Tb concentrations and a steep increase at high Tb contents. At infinite Tb-Tb distance (low Tb contents) the remaining  ${}^5D_4$  emission occurs due to direct feeding from the  $4f^75d$  band. The ratio between this spontaneous  ${}^5D_3$  and  ${}^5D_4$  emission is referred to as the feeding ratio ( $f_{5D_4}/f_{5D_3}$ ), which can be assumed to

be only marginally matrix dependent. This ratio is extrapolated from the graph, assuming a 2<sup>nd</sup> order dependence, yielding a value of 0.11 (+/- 0.02), which is in good agreement with the range of 0.12-0.18 as reported in refs. 11 and 9 for other Tb-activated materials. This value can be divided in the individual contribution of the  $^5D_3$  level ( $f_{5D3} \approx 0.9$ ) and that of the  $^5D_4$  level ( $f_{5D4} \approx 0.1$ ). Calculation of the interaction distance, i.e. the Tb-Tb distance at which the  $^5D_3$  emission and  $^5D_3$  cross-relaxation rates equal ( $1/2f_{5D3}/(f_{5D4}+1/2f_{5D3})$ ), yields a value of 1.43 nm, which is roughly the same as the values reported for YAG:Tb<sup>3+</sup> (1.15 [9], 1.34 [10]). Both the feeding ratio and the interaction distance correspond to an ideal dispersion of Tb<sup>3+</sup> in the glass. It is apparent that over the whole measured range the behaviour of the (Tb,Y)-Si-Al-O-N glass is somewhat different from that of YAG:Tb, i.e. lower values at low Tb concentrations and higher values at high Tb concentrations. It must however be noted that this effect is relatively insignificant to that caused by cluster or pair formation, which enhances the green emission by a few orders of magnitude over the whole Tb-concentration range [6]. These effects are clearly absent, showing that the distribution of the terbium ions is normal.

This raises the question whether these observations can be extended to predict the distribution of other lanthanides in Si-Al-O-N glasses. For the small trivalent lanthanides (high-z) this seems likely because of the chemical similarity between these ions. However, for the large ions (low-z) it is recommended to be determined independently.

## 7.5 Conclusions

The strong increase of the Tb<sup>3+</sup>  $^5D_3$  emission over the  $^5D_4$  emission in Y-Si-Al-O-N:Tb glasses when lowering the Tb concentration has shown beyond doubt that Tb<sup>3+</sup> pair formation, clustering, and phase separation are absent in these glasses. Both the interaction distance for  $^5D_4/^5D_3$  cross relaxation as well as the feeding ratio ( $^5D_4/^5D_3$ ) correspond to an ideal Tb<sup>3+</sup> dispersion.

**References**

1. T. Hanada, N. Ueda and N. Soga, *J. Ceram. Soc. Jpn. Inter. Ed.* 96 (1988) 281-289
2. S. Sakka, *J. Non-Cryst. Sol* 181 (1995) 215-224
3. A. Nordmann, Y.-B. Cheng and M.E. Smith, *Chem. Mater.* 8 (1996) 2516-2522
4. R. Ramesh, E. Nestor, M.J. Pomeroy and S. Hampshire, *J. Eur. Ceram. Soc.* 17 (1997) 1933-1939
5. Y. Menke, V. Peltier-Baron and S. Hampshire, *Brit. Ceram. Soc.* 60 [1] (1999) 361-362
6. A.M.A. van Dongen, *J. Non-Cryst. Sol.* 139 (1992) 271-273
7. C. Armellini, M. Ferrari, M. Montagna, G. Pucker, C. Bernard and A. Monteil, *J. Non-Cryst. Sol.* 245 (1999) 115-121
8. L.G. van Uitert and L.F. Johnson, *J. Chem. Phys.* 44[9] (1966) 3514-3522
9. W.F. van der Weg, Th.J.A. Popma and A.T. Vink, *J. App. Phys.* 57 [12] (1985) 5450-5456
10. D.J. Robbins, B. Cockayne, B. Lent and J.L. Glasper, *Sol. Stat. Comm.* 20 (1976) 673-676

# Chapter VIII

---

## Mixed oxidation states of Yb and Sm

*In previous chapters (IV, V) it has been established that europium can be reduced to the divalent state during the preparation of sialon glasses. In this chapter we will focus on two other ions with similar characteristics as europium, samarium and ytterbium. These elements are well known to be stable both in the divalent state as the trivalent state. Therefore it is possible that these elements will undergo a similar reduction during the preparation and there are some indications that this indeed is the case. In this chapter all the properties (optical and mechanical), which can be related to the oxidation state are examined.*

## 8.1 Introduction

Several studies have been dedicated to the effect of the lanthanide ions on the (mechanical) properties of Re-Si-Al-O-N glasses [1,2,3,4]. These studies show that, like in aluminosilicate glasses [5], the main parameters influencing the glass properties are the size and valence of the cation. In oxide glasses most lanthanide ions adopt a trivalent state. In oxynitride glasses the valence could be lower since the introduction of nitrogen alters the reductive potential of the glasses [6,7].

Such a reduction has already been observed in the case of europium (Chapter IV,V). The mechanical performance of Eu-Si-Al-O-N glass suggested a divalent state for europium [1] whereas it is trivalent in oxide glasses. Detailed optical, magnetic and chemical analyses showed that europium had been reduced from the trivalent state in the raw materials to the divalent state in the glasses by a chemical reaction between  $\text{Eu}^{3+}$  and the chemically incorporated nitrogen ( $\text{N}^{3-}$ ) [7]. Similar effects can play a role in the case of ytterbium and samarium, which are known to be stable in the divalent as well as the trivalent state. In previous investigations of the mechanical properties of these glasses both ions were assumed to be in the trivalent state in the glass [1,2]. However, the data provided show a small discrepancy with the data on other trivalent lanthanides.

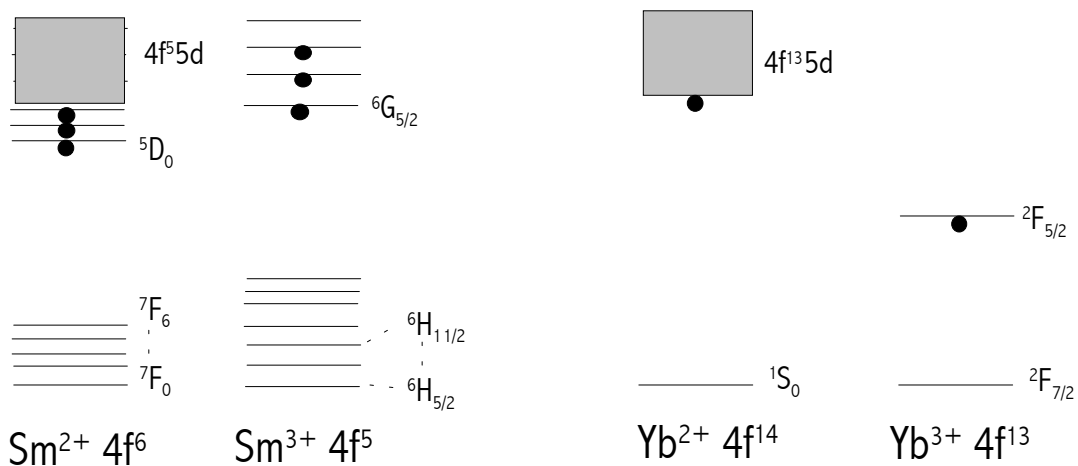


Fig. 8.1 *Energy level diagrams of Sm and Yb (for reasons of clarity not all levels have been displayed).*

The main objective of this work is to evaluate important data, which could be related to the oxidation state of these ions. Except for glass characteristics such as the density and mechanical properties such as the Young's modulus, the luminescence characteristics of the glasses are also studied. Samarium and

ytterbium are both luminescent ions, showing different luminescence characteristics for the divalent as compared to the trivalent state (Fig 8.1). Characteristic  $\text{Sm}^{3+}$  ( $4f^5$ ) and  $\text{Sm}^{2+}$  ( $4f^6$ ) transitions can be found in the red part of the visible spectrum (550 - 750 nm). Since the positions of the 4f levels are well known,  $\text{Sm}^{3+}$  and  $\text{Sm}^{2+}$  4f $\rightarrow$ 4f emission lines can be easily discriminated [8,9,10].  $\text{Yb}^{2+}$  ( $4f^{14}$ ) and  $\text{Yb}^{3+}$  ( $4f^{13}$ ) also have very different emission characteristics. The  $\text{Yb}^{2+}$  emission is characterized by broadband 5d $\rightarrow$ 4f emission, which can usually be found in the blue/green part of the spectrum [11,12], while  $\text{Yb}^{3+}$  produces 4f $\rightarrow$ 4f line emission at approximately 900 nm [13,14].

Table 8.1 *Observed transitions in Sm doped Y-Si-Al-O-N glass.*

	Excitation	[nm]	Emission	[nm]
$\text{Sm}^{2+}$ ( $4f^6$ )	${}^7F_0 \rightarrow$ $4f^5 5d$	340-400	${}^5D_0 \rightarrow {}^7F_0$	683
			${}^5D_0 \rightarrow {}^7F_1$	700
			${}^5D_0 \rightarrow {}^7F_2$	725
$\text{Sm}^{3+}$ ( $4f^5$ )	${}^6H_{5/2} \rightarrow$ ${}^4K_{11/2}$	404	${}^4G_{5/2} \rightarrow {}^6H_{5/2}$	565
			${}^4G_{5/2} \rightarrow {}^6H_{7/2}$	600
			${}^4G_{5/2} \rightarrow {}^6H_{9/2}$	650
			${}^4G_{5/2} \rightarrow {}^6H_{11/2}$	710

## 8.2 Experimental

Two series of Y-Si-Al-O-N glasses were made in which yttrium was partially replaced by either samarium or by ytterbium. The overall weighed-out composition was  $\text{Ln}_x\text{Y}_{(15.2-x)}\text{Si}_{14.7}\text{Al}_{8.7}\text{O}_{54}\text{N}_{7.4}$  (Ln = Sm, Yb) and was varied by taking x: 0.03, 0.3, 3, 6.1, 9.1, 12.2 and 15.2. As raw materials  $\text{Sm}_2\text{O}_3$  (REacton),  $\text{Yb}_2\text{O}_3$  (REacton),  $\text{Y}_2\text{O}_3$  (Sheng-Etsu),  $\text{SiO}_2$  (CE-Minerals),  $\text{Al}_2\text{O}_3$  (Taimei) and  $\text{Si}_3\text{N}_4$  (Akzo Nobel, Permascand) were used. The powders were mixed in a ball mill (isopropanol, agate balls). Hereafter the mixture was dried and placed in a Hex-BN powder lined graphite crucible. The starting mixtures were heated under a nitrogen atmosphere in a vertical tube furnace at a rate of 3 °C/min to 1700 °C. After a dwell time of 1 hour the glasses were quenched by rapidly extracting them from the furnace and placing them in an annealing furnace operating at 800 °C. The glasses were annealed for 1 hour at this temperature in air.

The thin oxide scale, which had formed on the glass and the adhering BN were removed by grinding the surface. The glass was then cut to prepare specimens for further testing. The density of the glasses was measured using the Archimedes method in water. The Young's modulus was measured using the ultrasonic pulse echo method on plane-parallel specimens of 2 millimeters thickness.

Room temperature optical measurements were performed on powdered samples using a Perkin-Elmer LS-50B photofluorospectrometer. Reflection, emission and excitations spectra were taken of the samples. The reflection measurements were done using black felt and Ba(SO<sub>4</sub>) as standards.

### 8.3 Results

#### *Density and Young's modulus*

The density measurements show a clear increase of the density for higher samarium and ytterbium contents. In the case of ytterbium the molar volume of the glass remains equal ( $\rho_Y = \rho_{Yb} = 7.47 \text{ mol/cm}^3$ ) while the addition of samarium leads to a significant increase of the molar volume ( $\rho_{Sm} = 8.74 \text{ mol/cm}^3$ ). The molar volume calculations are based on the weighed-out composition assuming a trivalent oxidation state for the lanthanides. In figure 8.2 the molar volume of several Ln(III)-Si-Al-O-N glasses is plotted versus the ionic radius [15] of the lanthanide ion. The glasses are all prepared and measured in our own laboratory except for the Er-Si-Al-O-N glass, for which the values were derived from ref. 2. The molar volume of the glass is a function of the ionic radius of the lanthanide ion used. However, both for ytterbium as for samarium the molar volume is much larger than expected from the radius of the trivalent ions. This deviation suggests the presence of both the divalent and the trivalent state of these ions.

A similar relationship was found for the Young's modulus. (Fig. 8.3). While the other trivalent lanthanides show a systematic correlation between the Young's modulus and the ionic radius, Sm- and Yb-Si-Al-O-N glass show a deviating behaviour when assuming the trivalent state and this again indicates mixed oxidation states.

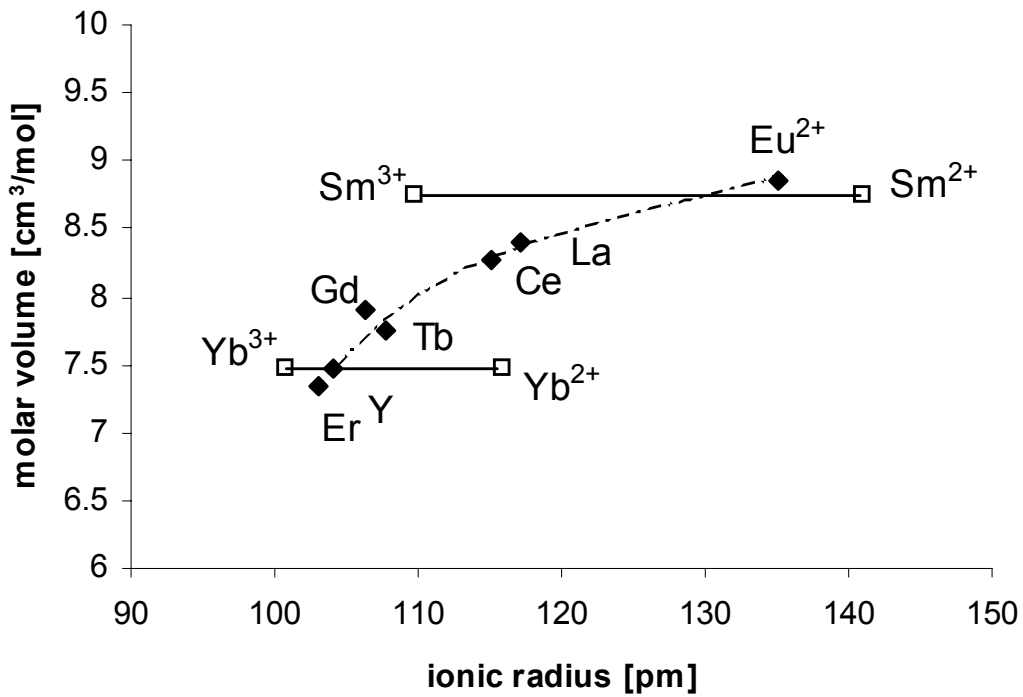


Fig. 8.2 Molar volume of Ln-Si-Al-O-N glasses as a function of the ionic radius of the Ln ion.

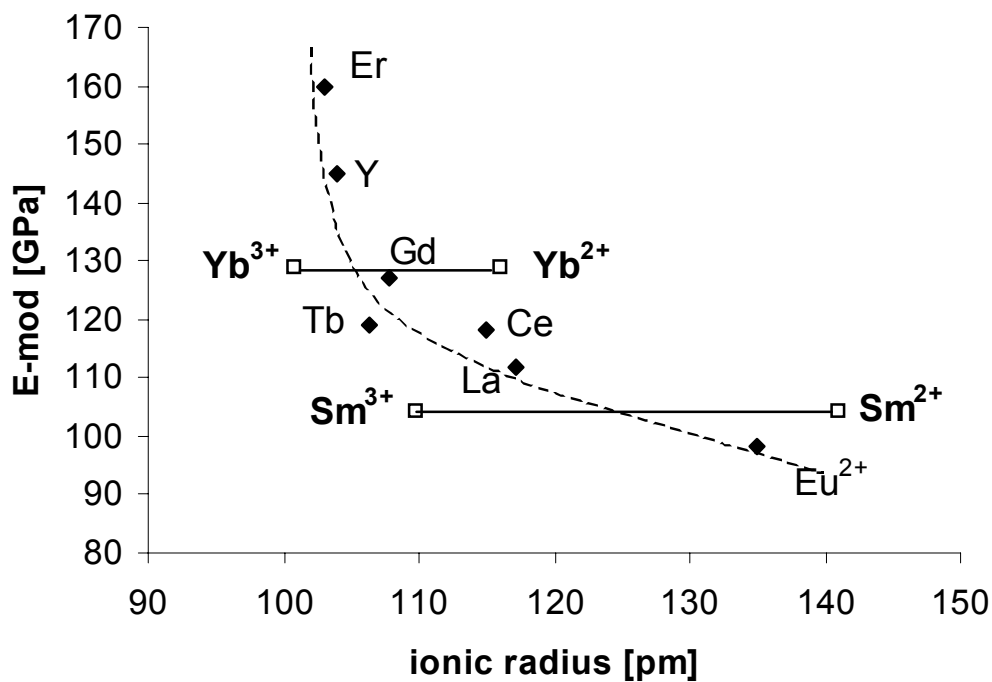


Fig. 8.3 E-modulus of Ln-Si-Al-O-N glasses as a function of the ionic radius of the Ln ion.



### Optical properties of the Sm-glasses

The reflection spectra (Fig. 8.4) show that the addition of samarium leads to a strong absorption over a large spectral region covering the UV and the visible part of the spectrum. The main absorption takes place in the region between 350-450 nm and around 550 nm, which causes the glasses to turn black upon samarium addition.

The emission spectra (Fig. 8.5) clearly show the presence of both  $\text{Sm}^{2+}$  and  $\text{Sm}^{3+}$  emission lines. The excitation spectra (Fig. 8.6) show a number of bands and lines, which correlate to the observed absorption maximum in the reflection spectra. The main excitation signals can be attributed to the  ${}^6\text{H}_{5/2} \rightarrow {}^4\text{K}_{11/2}$  transition of  $\text{Sm}^{3+}$  and the  $4f^6 \rightarrow 4f^5 5d$  transitions of  $\text{Sm}^{2+}$  (Table 8.1). The large excitation band at short wavelengths corresponds to the matrix absorption (Fig. 8.4) and can be attributed to host matrix sensitisation. Because of the overlap of the excitation bands complete separation of the emission spectra is not possible. Excitation in the glass matrix leads to predominant  $\text{Sm}^{3+}$  emission whilst excitation at longer wavelengths leads to predominant  $\text{Sm}^{2+}$  emission.

Although the samarium emission is reasonably strong at low concentrations, the emission intensity drops sharply with the concentration and no emission whatsoever can be observed at  $x > 3$ . This is not surprising since  $\text{Sm}^{3+}$  is very susceptible to self-quenching [16] at interatomic distances below 15-20 Å, which corresponds to  $\text{Sm}^{3+}$  contents higher than 0.1 at%.

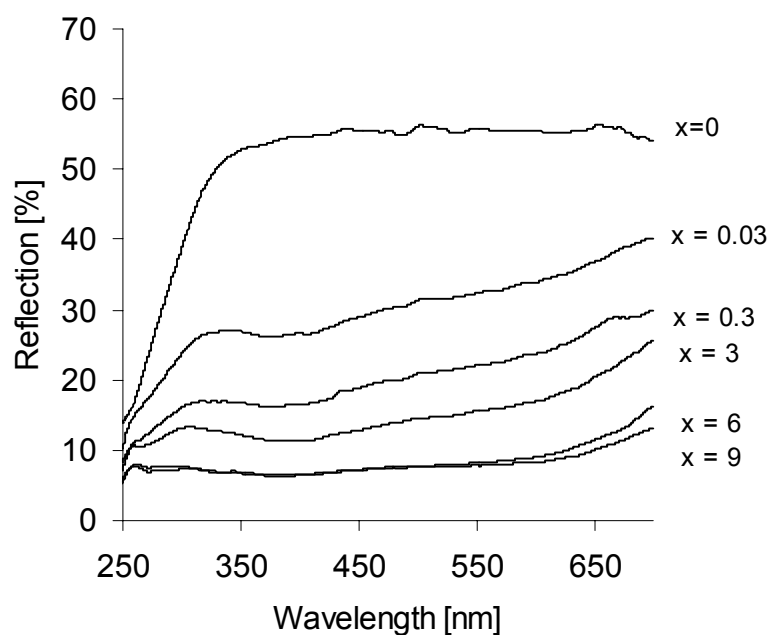


Fig. 8.4 Reflection spectra of powdered  $\text{Sm}_x \text{Y}_{(15.2-x)} \text{Si}_{14.7} \text{Al}_{8.7} \text{O}_{54.1} \text{N}_{7.4}$  glasses as a function of the Sm content ( $x$ ).

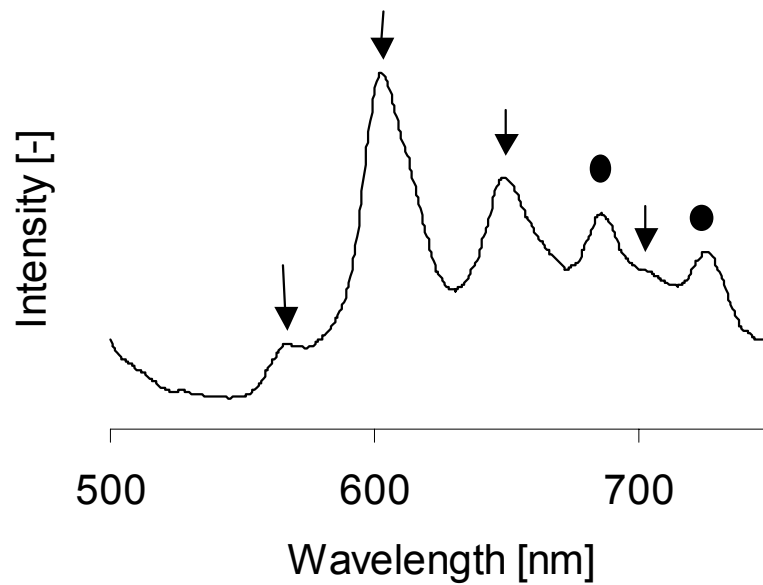


Fig. 8.5 Emission spectrum of a powdered  $Sm_{0.3}Y_{14.9}Si_{14.7}Al_{8.7}O_{54.1}N_{7.4}$  glass ( $\lambda_{ex}=404$  nm).  $\downarrow$ :  $Sm^{3+}$  transitions,  $\bullet$ :  $Sm^{2+}$  transitions.

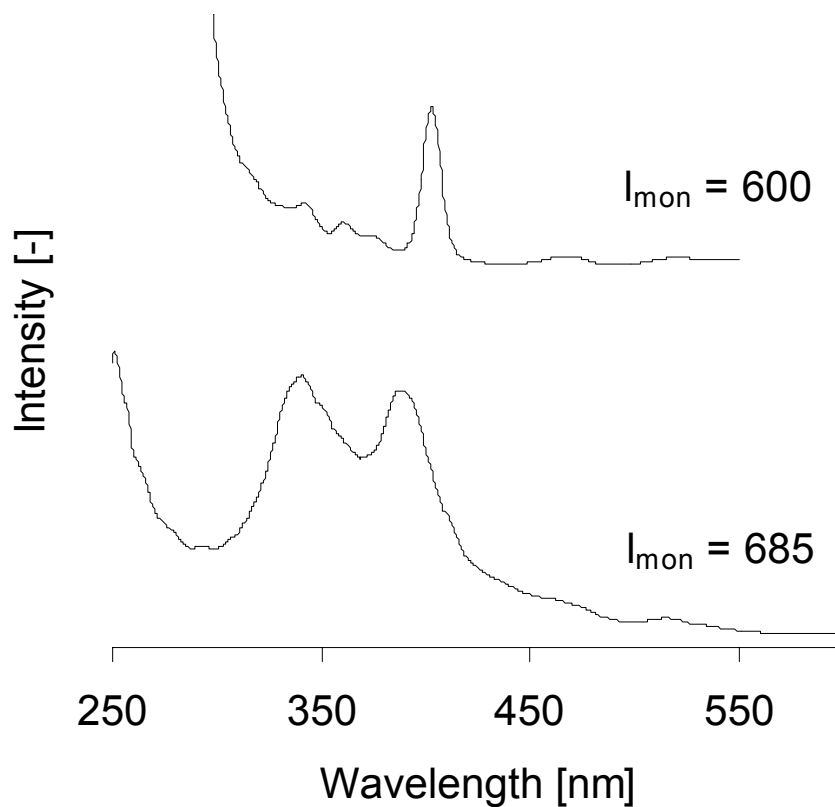


Fig. 8.6 Excitation spectra of  $Sm_{0.3}Y_{14.9}Si_{14.7}Al_{8.7}O_{54.1}N_{7.4}$  glass at two different monitor wavelengths. The upper graph corresponds to the  ${}^4G_{5/2} \rightarrow {}^6H_{7/2}$  transition of  $Sm^{3+}$  (600 nm). The lower spectrum has been taken while monitoring the  ${}^5D_0 \rightarrow {}^7F_0$  transition of  $Sm^{2+}$  (683 nm).

### Optical properties of the Yb-glasses

The reflection spectra of the ytterbium doped glasses (Fig. 8.7) show a pronounced absorption band at  $\sim 360$  nm with a sideband at  $\sim 260$  nm. The color of these glasses turns from yellow to amber-brown upon ytterbium addition due to this absorption.

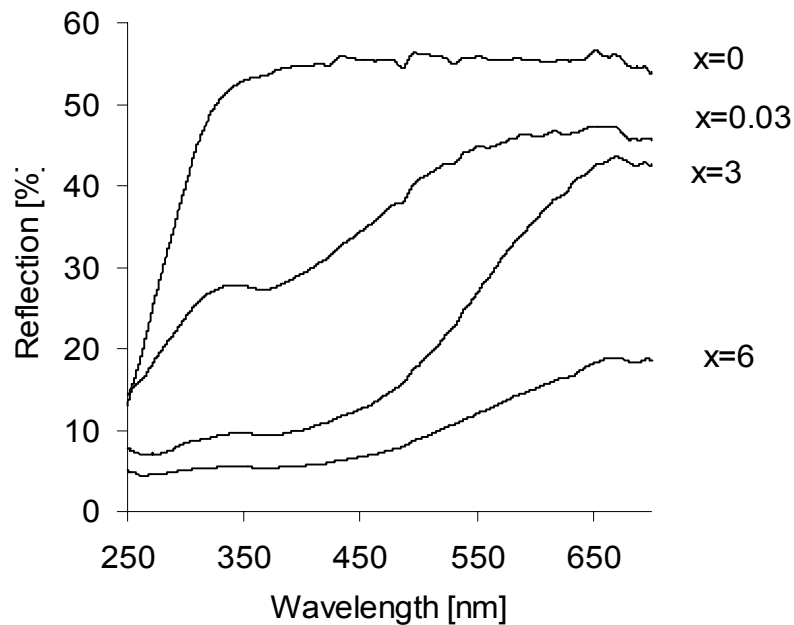


Fig. 8.7 Reflection spectra of  $Yb_x Y_{(15.2-x)} Si_{14.7} Al_{8.7} O_{54.1} N_{7.4}$  glasses as a function of the Yb content ( $x$ ).

The characteristic  $4f \rightarrow 4f$  transitions of  $Yb^{3+}$  are located above 900 nm [17] and therefore cannot lead to the coloration of the glasses. Estimation of the position of the  $4f^{13} \rightarrow 4f^{12}5d$  bands of  $Yb^{3+}$  with the method of Dorenbos [18] using the excitation spectra of Ce(III)-Si-Al-O-N glass [19] leads to the conclusion that these bands are too far up the UV ( $E_{fd}(Yb^{3+}) > 70 \cdot 10^3 \text{ cm}^{-1}$ ) to cause the observed absorption. The  $4f^{13} \rightarrow 4f^{14}O^{-1}$  charge-transfer band of  $Yb^{3+}$  is also expected at higher energies ( $\sim 50 \cdot 10^3 \text{ cm}^{-1}$ ) and can therefore not cause the main absorption at 360 nm ( $28 \cdot 10^3 \text{ cm}^{-1}$ ) [20].

Since the observed absorption cannot be originating from  $Yb^{3+}$  it suggests the presence of  $Yb^{2+}$ . The absorption bands at  $\sim 260$  and  $\sim 360$  nm are thus tentatively ascribed to the  $4f^{14} \rightarrow 4f^{13}5d$  transitions of  $Yb^{2+}$ . The position for the  $4f^{13}5d$  band of  $Yb^{2+}$  can be estimated from the position of the  $4f^65d$  band of  $Eu^{2+}$ , which should be by approximation equal when incorporated in the same host lattice [21]. The  $4f^65d$  band of  $Eu^{2+}$  in  $Eu_x Y_{15.2-x} Si_{14.7} Al_{8.7} O_{54.1} N_{7.4}$  glass ( $x = 0.15$ ) has been determined at 350 nm, which is equal to the observed absorption maximum in the Yb-doped glass at low concentrations ( $x = 0.03-0.3$ )

[7]. At higher concentrations of  $\text{Eu}^{2+}$  the  $4f^65d$  excitation band is shifting to longer wavelengths. This could be the reason for the strong decrease of the reflection at longer wavelengths with increasing ytterbium content. Although the reflection spectra suggest the presence of a substantial amount of  $\text{Yb}^{2+}$ , no  $\text{Yb}^{2+}$  could be generated by excitation in the observed bands. The lack of  $\text{Yb}^{2+}$  emission is possibly the result of strong temperature quenching which is a common problem in Yb-doped materials [14].

#### 8.4 Discussion

From the presented results it becomes clear that both samarium and ytterbium partially reduce from the trivalent to the divalent state during the synthesis of oxynitride glasses. The reduction of  $\text{Yb}^{3+}$  and  $\text{Sm}^{3+}$  to the divalent state is less likely than that of for instance europium therefore a full reduction of these ions has only been achieved in a few compounds [22,23]. However, the reduction potential of oxynitride glasses is far greater than that of oxide glasses. It has been shown in a number of studies that chemically incorporated nitrogen reacts with the lanthanides according to the following general mechanism [7]



The nitrogen gas produced by this reaction then evolves from the melt, resulting in a glass with lower content of incorporated nitrogen than expected from the weighed-out composition. For europium-containing glasses this mechanism has been validated [7] and we therefore attribute this mechanism also to the observed reactions of in Yb- and Sm-Si-Al-O-N glasses.

In previous cases a complete conversion of the lanthanide ion was observed whereas presently only a partial reduction has occurred. To look at the evolution of the  $\text{Ln}^{2+}/\text{Ln}^{3+}$  ratio with time, the glasses  $\text{Sm}_{0.3}\text{Y}_{14.9}\text{Si}_{14.7}\text{Al}_{8.7}\text{O}_{54.1}\text{N}_{7.4}$  and  $\text{Yb}_{15.2}\text{Si}_{14.7}\text{Al}_{8.7}\text{O}_{54.1}\text{N}_{7.4}$  were heated at shorter times ( $\frac{1}{2}$  hr at  $1700^\circ\text{C}$ ). Since the sensitivity of the reflection spectra is considered to be too low to monitor compositional variations, the  $\text{Yb}^{2+}/\text{Yb}^{3+}$  ratio is to be estimated from the mechanical properties, whereas luminescence was the ideal tool in the case of samarium. In the emission spectrum presented in figure 8.8, it can be seen that less  $\text{Sm}^{2+}$  emission is present in this sample heated for  $\frac{1}{2}$  hour, as compared to the glass, which was molten for 1 hour. Similarly the Young's modulus of the Yb-Si-Al-O-N glass decreases with heating time while the molar volume increases (Fig. 8.9) suggesting that the conversion of  $\text{Yb}^{3+}$  to  $\text{Yb}^{2+}$  is proceeding with time.

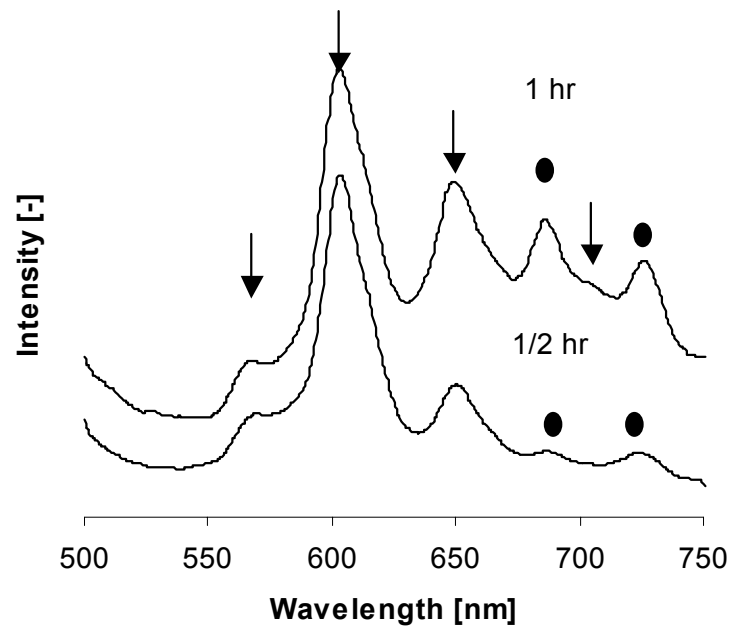


Fig. 8.8 Emission spectrum of a  $Sm_{0.3}Y_{14.9}Si_{14.7}Al_{8.7}O_{54.1}N_{7.4}$  glass as a function of the melting time ( $\lambda_{ex}=404$  nm).  $\downarrow$ :  $Sm^{3+}$  transitions,  $\bullet$ :  $Sm^{2+}$  transitions.

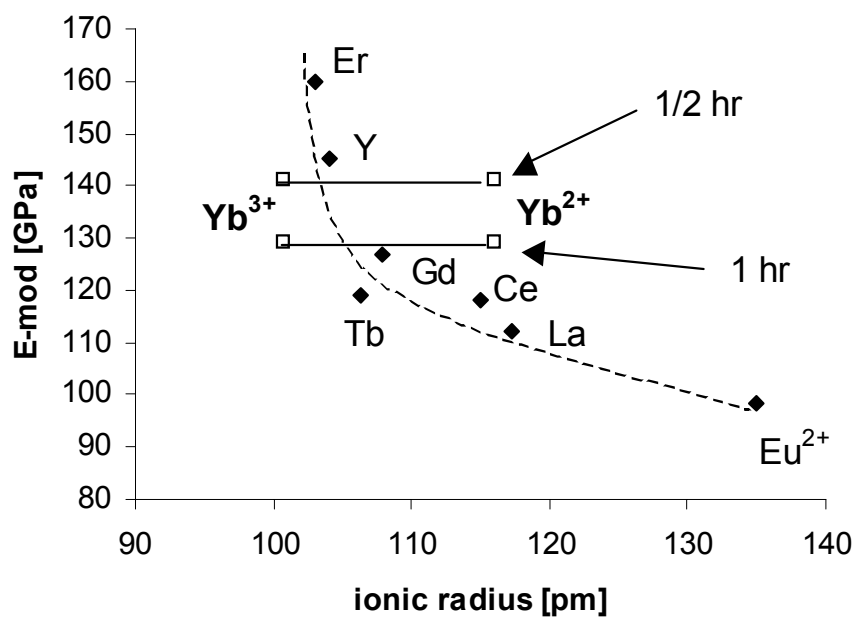


Fig. 8.9 E-modulus as a function of the ionic radius of selected glasses with a weighed-out composition of  $Ln_{15.2}Si_{14.7}Al_{8.7}O_{54.1}N_{7.4}$  (line serves as a guide for the eye only). For Yb-Si-Al-O-N glasses the data points represent the Young's modulus after  $\frac{1}{2}$  hr and 1 hr melting time.

These changes can be attributed to the replacement of  $\text{Yb}^{3+}$  by the larger  $\text{Yb}^{2+}$  and (in a lesser extend) to the decrease of the nitrogen content of the glass due to this reduction. Experiments with longer melting times were also attempted, but they led to catastrophic failure of the BN-lining and consequently to glass sticking so these experiments were abandoned.

It goes beyond the scope of this study to provide a detailed analysis of the reaction kinetics, but these results clearly show, that the reduction process takes place during the hottest stages of the melting process, and that the reduction itself is very slow.

## 8.5 Conclusions

Samarium and ytterbium partially reduce from the trivalent to the divalent oxidation state during the synthesis of Ln-Si-Al-O-N glasses (Ln = Sm, Yb). In the case of samarium this reduction has been confirmed by the presence of both  $\text{Sm}^{3+}$  as well as  $\text{Sm}^{2+}$  transitions in the emission spectrum of Sm-doped Y-Si-Al-O-N glasses and is further supported by the values of the density and Young's modulus.

For the ytterbium containing Si-Al-O-N glasses a strong  $\text{Yb}^{2+}$  absorption band was observed in the reflection spectra. Measurements on the density and Young's modulus also suggest the presence of a substantial amount of unconverted  $\text{Yb}^{3+}$ , indicating that the reduction in this case is also partial.

The reductions from  $\text{Ln}^{3+}$  to  $\text{Ln}^{2+}$  are attributed to the presence of  $\text{N}^{3-}$  in the glass melt. Increasing the melting time resulted in a variation of properties in accordance with an increasing  $\text{Ln}^{2+}$  content. This means that at this temperature, which is typical for Si-Al-O-N glass synthesis, these systems may need several hours to reach equilibrium. This dependence on the thermal history can well be the reason for the scatter in results, which are reported in literature for Sm- and Yb-Si-Al-O-N glasses.

## References

1. R. Ramesh, E. Nestor, M.J. Pomeroy and S. Hampshire, *J. Eur. Ceram. Soc.* 17 (1997) 1933-1939
2. Y. Menke, V. Peltier-Baron and S. Hampshire, *J. Non-Cryst. Sol.* 276 (2000) 145-150
3. P.F. Becher, S.B. Waters, C. G. Westmoreland and L. Riester, *J. Am. Ceram. Soc.* 85[4] (2002) 897-902
4. Y. Murakami and H. Yamamoto, *J. Ceram. Soc. Jpn. Int. Ed.* 102 (1994) 234-237
5. J.E. Shelby and J.T. Kohli, *J. Am. Ceram. Soc.* 73[1] (1990) 39-42
6. A. Le Sauze, E. Gueguen and R. Marchand, *J. Non-Cryst. Sol.* 217 (1997) 83-91
7. D. de Graaf, H.T. Hintzen, S. Hampshire and G. de With, *J. Eur. Ceram. Soc.* 23[7] (2003) 1093-1097
8. A.G. Souza Filho, J. Mendes Filho, F.E.A. Melo, M.C.C. Custódio, L. Lebullenger and A.C. Hernandez, *J. Phys. Chem. Sol.* 61 (2000) 1525-1542
9. A. Gros, F. Gaume and J.C. Gacon, *J. Sol. State. Chem.* 36 (1981) 324-330
10. A. Patra, R. Reisfeld and H. Minti, *Mater. Lett.* 37 (1998) 325-329
11. S. Lizzo, A. Meijerink, G.J. Dirksen and G. Blasse, *J. Lum.* 63 (1995) 223-234
12. Q. Zeng, Z. Pei, Z. Wang, Q. Su and S. Lu, *Mat. Res. Bull.* 34[12/13] (1999) 1837-1844
13. X. Zou and H. Toratani, *Phys. Rev. B* 52[22] (1995) 15889-15897
14. S. Lizzo, E.P. Klein Nagelvoort, R. Erens, A. Meijerink and G. Blasse, *J. Phys. Chem. Sol.* 58[6] (1997) 963-968
15. R.D. Shannon, *Acta Cryst.* A32 (1976) 751-767
16. L.G. van Uitert and L.F. Johnson, *J. Chem. Phys.* 44[9] (1966) 3514-3522
17. J. Dong, P. Deng and J. Xu, *Opt. Mat.* 14 (2000) 109-113
18. P. Dorenbos, *J. Lum.* 91(2000) 91-106
19. D. de Graaf, H.T. Hintzen and G. de With, *J. Lum.* 104 (2003) 131-136
20. E. Nakazawa, *J. Lum.* 100 (2002) 89-96
21. J.W.M. Verwey and G. Blasse, *J. Phys. Chem. Sol.* 53[9] (1992) 1157-1162
22. G. von Brauer, H. Bärninghausen and N. Schultz, *Zeit. für Anorg. und Allgem. Chem.* (in German) 356 (1967) 46-54
23. G.J. McCarty and W.B. White, *J. of Less-Common Metals* 22 (1970) 409-417

# Chapter IX

---

## Hardness and indentation size effect in Ln-Si-Al-O-N glasses

*In this chapter the hardness of Ln-Si-Al-O-N glasses is determined using the standard Vickers indentation technique. Special attention is provided for the contribution of elastic phenomena to the measured hardness. These phenomena, which are referred to as the indentation size effect are discarded by applying the theorem of Bull et al.*



## 9.1 Introduction

For many applications the hardness is an important parameter since it reflects the amount of permanent deformation sustained, when a material is subjected to a mechanical force. Therefore it gives an indication of the scratch and abrasion performance of the material. The Vickers indentation technique is widely applied to determine the hardness of brittle materials such as glasses. In this technique an imprint is made by pressing a diamond with a certain force (load) against the surface of the material. The size of the imprint is then dependent on the used load and the hardness of the material.

In the literature, a few Vickers hardness values have been reported for Y-Si-Al-O-N glasses. These values indicate that the hardness can be as high as 10-13 GPa [1,2,3], which is more than twice as high as for vitreous silica and soda-lime glass. Despite these encouraging results, the authors feel that two matters have to be resolved in order to estimate their performance in real applications. Firstly, the effect of the overall composition of the glass on the hardness is not clear yet and secondly, the hardness measurements have so far been performed at a single (low) load (1-3 N). In order to make a good comparison between two materials the effect of the load on the measured hardness has also to be taken into account [4].

An impression is made on a glass surface with a diamond of pyramidal geometry by applying a certain force (Fig. 9.1). The size of the resulting impression is a function of the applied load and the hardness of the material. For a Vickers indentation the microhardness ( $H_v$ ) is defined as the ratio between the applied load ( $P$ ) and the squared length of indentation diagonal ( $d_i$ ) multiplied by a geometrical factor:

$$H_v = \frac{1.854P}{d_i^2} \quad (1)$$

This relation does not account for elastic recovery, which implies that the measured hardness is still a function of the load. When the indenter is removed from the surface, the material will partially elastically recover. Due to this process the indentation size will decrease somewhat. This results in an apparent indentation diagonal ( $d_m$ ). Substitution of  $d_m$  for  $d_i$  in equation 1 leads to the apparent hardness ( $H_v^{\text{app}}$ ). Since  $d_m < d_i$  the apparent hardness will be always higher than the load-independent hardness ( $H_v^0$ ). This effect is referred to as the indentation size effect (ISE) [5,6]. There are a number of ways to describe the indentation size effect, e.g. the model of Bull, the Proportional Specimen

Resistance (PSR) model, or Meyer's Law [7]. Of these methods the approach of Bull et al. is chosen because, for most materials it fits the effect very well and gives an output in the form of a load independent hardness which can be used to directly compare different materials. The authors are aware that in some cases Bull's equation can lead to a slight underestimation of the load-independent hardness due a transition from load-dependent to load-independent behaviour at high loads [8]. The error introduced by such a transition would be very small for these materials as compared to the obtained load-dependence and load-independent hardness.

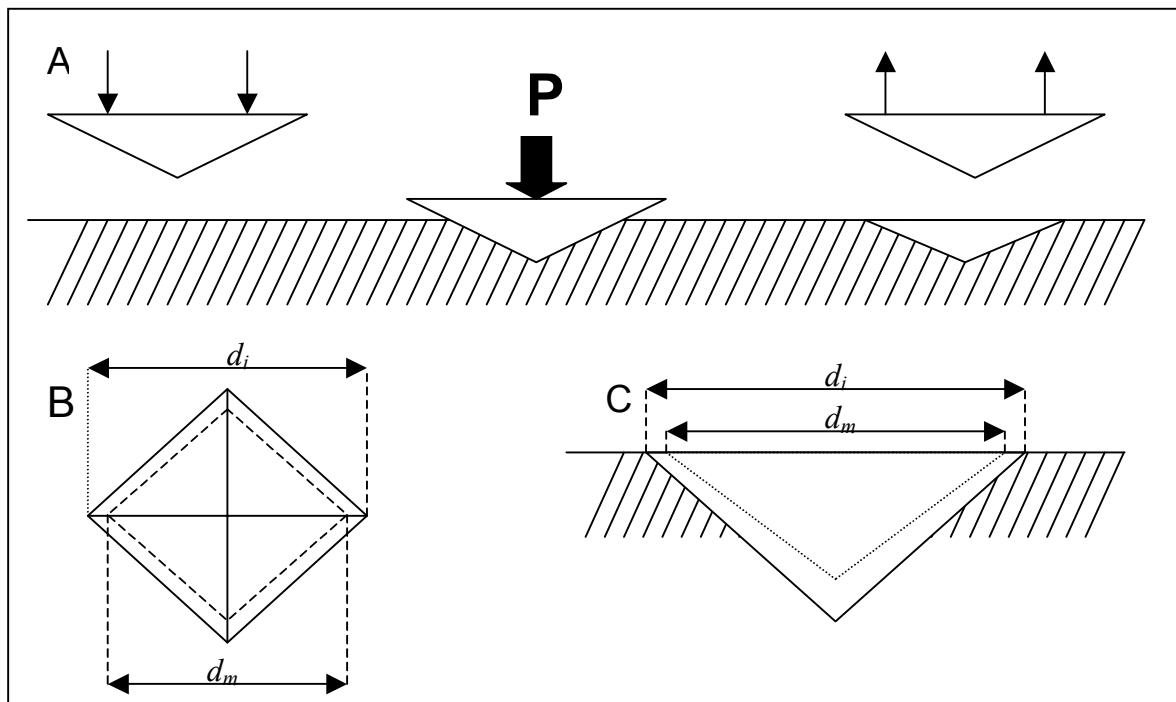


Fig. 9.1 Principle of Vickers indentation (A). Top view (B) and cross-section (C) of the indentation, before ( $d_i$ ) and after relaxation ( $d_m$ ).

The method of Bull et al. separates the apparent hardness into a load dependent and a load independent part, described by:

$$H_v^{\text{app}} = \frac{1.854P}{d_m^2} = H_v^0 \left( 1 + \frac{d_i - d_m}{d_m} \right)^2 = H_v^0 \left( 1 + \frac{\delta}{d_m} \right)^2 \quad (2)$$

The elastic recovery parameter ( $\delta$  [ $\mu\text{m}$ ]) is used to describe the susceptibility of the material to ISE. It is defined as the difference between the length of the indentation diagonal before and after relaxation. In this description  $\delta$  is assumed to be independent of the load and is considered to be material specific. Since  $\delta$  for most materials is 1-2  $\mu\text{m}$  the difference between the apparent and load-independent hardness will be substantial for small indents while the apparent

hardness will approach the load-independent hardness with increasing indent size [4]. This means one has to be especially careful when measuring harder materials since smaller indents are generated.

In order to make a well-defined comparison between the hardness of different materials one has to correct for the ISE by determining the load-independent hardness from load dependent measurements or by minimizing the ISE by taking a sufficiently high load. The goal of this investigation is to obtain load-independent hardness data for Y-Si-Al-O-N glasses and to study the load-dependence of the hardness. Moreover the effect of the chemical composition of the glass on the hardness is studied. This kind of data is needed to evaluate and optimise the performance of these materials in different types of applications.

## 9.2 Experimental

The size and position of the Y-Si-Al-O-N glass-forming region was estimated from available data in the literature and a matrix of compositions was drawn up to cover a large part of this region [3]. Weighed-out compositions are listed in Table 9.1. Starting materials were:  $Y_2O_3$  (Shin Etsu Y-474),  $SiO_2$  (aerosil OX50),  $Al_2O_3$  (Taimei >99.99% pure) and  $Si_3N_4$  (Akzo Nobel P95H). The starting powders were dispersed in isopropanol and mixed in a ball mill using  $Si_3N_4$  balls. The resulting mixture was dried and pressed into pellets of 1-2 gram. These pellets were fired in an induction furnace for a short period (8-15 min) under flowing nitrogen. Rapid cooling was achieved by switching-off the power supply to the coil, whilst maintaining a nitrogen atmosphere in the furnace. The crucible consisted of a molybdenum melting pot and lid, which was powder-lined on the inside with hexagonal-BN powder to prevent sticking. Melting temperatures and time were adjusted per sample in order to obtain thoroughly molten, transparent, X-ray amorphous, glass droplets. The microhardness tests were carried out on polished (10  $\mu m$  diamond polishing wheel) glass samples using a Leitz Miniload 2 microhardness tester with a Vickers diamond. Since tip blunting has a pronounced effect on the measured hardness [9] a new diamond was used. The quality and top angles of the diamond were checked with confocal microscopy (Nanofocus  $\mu Surf$ ). The samples were cleaned with ethanol and dried prior to measuring. Loads from 1 to 20 N were applied to the samples for 30 seconds. Both indentation diagonals were measured and averaged. Per load a total of six indents were made.

Table 9.1 *Weighed-out compositions of the investigated Y-Si-Al-O-N glasses, load-independent hardness ( $H_v^0$ ) and elastic recovery parameter ( $\delta$ ) as calculated from experimental data.*

Sample	Equivalent percent [eq%]					Molar percent [mol%]				Hardness	
	Y	Si	Al	O	N	Y <sub>2</sub> O <sub>3</sub>	SiO <sub>2</sub>	Al <sub>2</sub> O <sub>3</sub>	Si <sub>3</sub> N <sub>4</sub>	$H_v^0$ [GPa]	$\delta$ [ $\mu\text{m}$ ]
K1	35	45	20	83	17	33.2	39.8	19.0	8.1	9.3	1.5
K2	35	45	20	90	10	31.1	46.7	17.8	4.4	8.7	1.0
K3	35	45	20	95	5	29.8	51.1	17.0	2.1	8.3	1.0
K4	35	32.5	32.5	83	17	35.3	23.4	32.7	8.6	9.3	1.2
K5	35	32.5	32.5	90	10	32.9	31.8	30.6	4.7	9.2	1.5
K6	35	32.5	32.5	95	5	31.5	37.1	29.2	2.2	--	--
K7	35	56	9	83	17	31.5	52.7	8.1	7.7	9.0	1.3
K8	35	56	9	90	10	29.7	58.5	7.6	4.2	8.5	1.2
K9	35	56	9	95	5	28.5	62.2	7.3	2.0	8.2	1.6
K10	41	42	17	83	17	39.4	36.1	16.3	8.2	9.3	1.7
K11	41	42	17	90	10	36.9	43.2	15.3	4.5	8.9	1.7
K12	41	42	17	95	5	35.3	47.8	14.7	2.2	8.8	1.4
K13	25	52	23	83	17	22.9	48.2	21.1	7.8	8.9	1.5
K14	25	52	23	90	10	21.6	54.3	19.8	4.3	8.5	1.1
K15	25	52	23	95	5	20.7	58.3	19.0	2.1	7.7	1.4

### 9.3. Results and discussion

Except for composition K6, homogeneous glasses were obtained. Composition K6 repetitively formed a milk-white translucent material, which was excluded from further investigation. The other glasses were completely transparent. They were smoke-grey of colour as has been reported by other authors [1,10]. With increasing nitrogen content they became darker in appearance.

#### *Determination of the load-independent hardness ( $H_v^0$ )*

The measurements show a substantial decrease of the apparent hardness with increasing load (Fig. 9.2). At higher loads these curves are expected to level off, although this does not occur in the measured range. Over the whole load range these curves show that the loads, which have been used in literature (0.1 to 0.3 kg) lead to a severe overestimation of the load-independent hardness of the glasses, which can lead to an error of up to 25%. The hardness values, which have been reported in literature, have to be interpreted with this effect in mind.

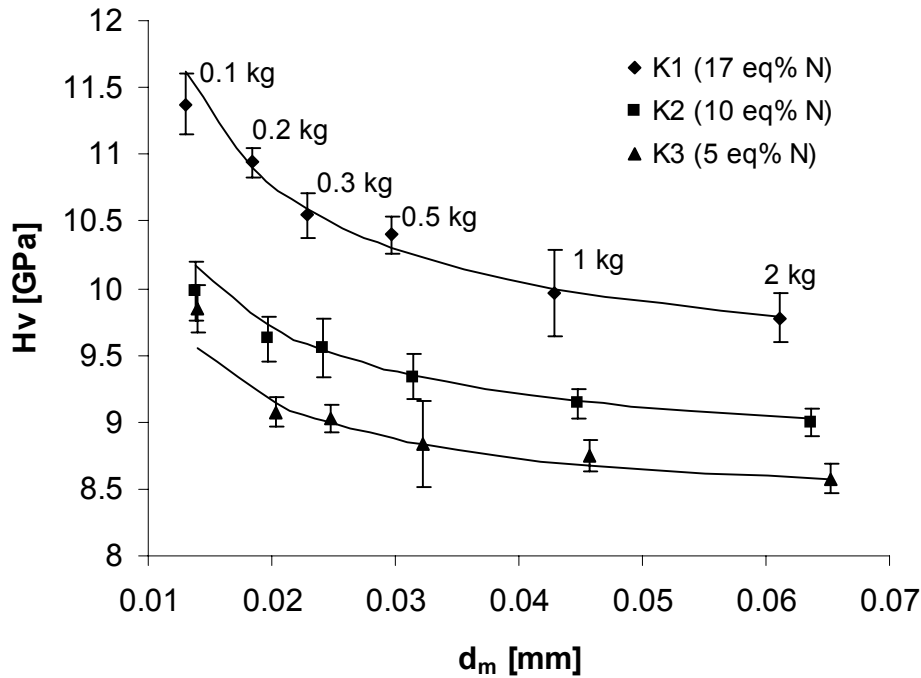


Fig. 9.2 Apparent hardness ( $H_v^{app}$ ) versus the measured indentation diagonal ( $d_m$ ) for glasses K1, K2 and K3. Error bars represent the 95% confidence interval. The measurements are fitted to the Bull's equation (eq. 2).

In order to obtain the load-independent hardness ( $H_v^0$ ) from the measured indentation size ( $d_m$ ) equation 2 is rearranged to the linear equation [7]

$$d_m = \left( \frac{1.854}{H_v^0} \right)^{\frac{1}{2}} P^{\frac{1}{2}} - \delta \quad (3)$$

Thus a plot of  $d_m$  versus  $P^{1/2}$  should yield a straight line with intercept  $-\delta$  and slope  $(1.854/H_v^0)^{1/2}$ . Applying this method to the raw data results in a good fit (Fig. 9.3). This indicates that Bull's equation is adequate to describe hardness-load curves for these systems. The parameters  $H_v^0$  and  $\delta$  as derived from the slope and the intercept of the fit are listed in Table 9.1. The load-independent hardness ( $H_v^0$ ) ranges from 7.7 to 9.3 GPa, which is significantly lower (~30%) than apparent hardness values thus far reported for Y-Si-Al-O-N glasses [1,2,3] but is still higher than values known for conventional glass systems (e.g. vitreous silica = 5.3 GPa [7]).

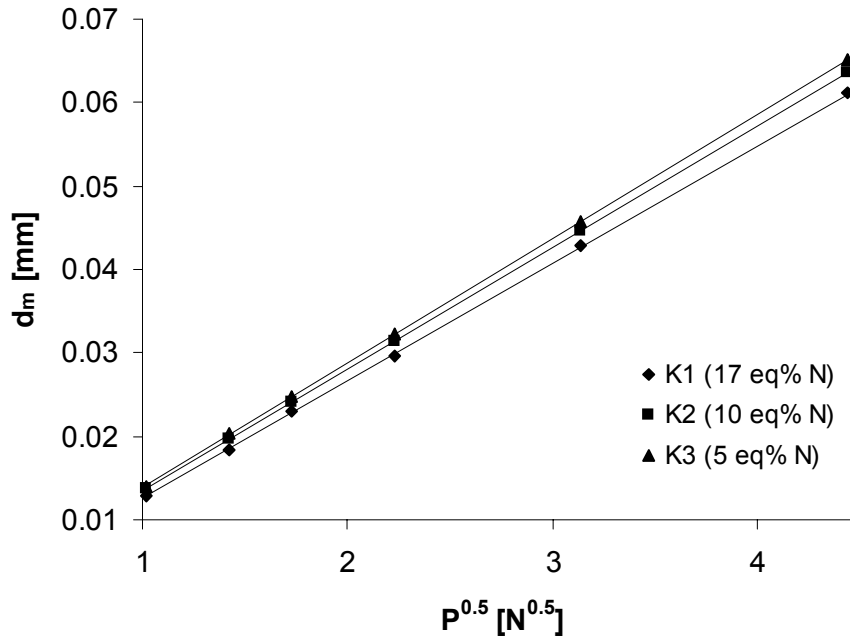


Fig. 9.3 Plot of the measured indentation diagonal ( $d_m$ ) versus the square root of the load ( $P^{0.5}$ ). Lines represent the linear least-squares estimate (glasses K1, K2 and K3).

*The dependence of the load-independent hardness ( $H_v^0$ ) on the chemical composition*

There are no correlations readily available to link the hardness of this complex system directly to the chemical composition. A great complication is the presence of both four- and higher coordinated aluminium which prevents accurate estimation of the amount of the non-bridging oxygen (NBO) in the glasses. Furthermore, most theories, which are designed for relatively simple oxide glasses fail to describe the influence of nitrogen in the glass network.

A simple solution would be to assume that the load-independent hardness is linearly dependent on the composition. An additive type equation can then be written down:

$$H_v^{0,calc} = \sum_{i=1}^n a_i x_i \quad (4)$$

This means that the load-independent hardness ( $H_v^0$ ) can be expressed as the sum of the molar fractions ( $x_i$ ) of its individual components (i) times a ‘partial hardness’ ( $a_i$ ). The values for  $a_i$  have been calculated for  $H_v^0$  and are given in

Table 9.2. Comparison of all the measured hardness values with the calculated ones shows that this crude model provides a fair description of the influence on the individual components on the load-independent hardness.

Table 9.2. *Additive parameters ( $a_i$ ) of  $Y_2O_3$ ,  $Al_2O_3$ ,  $SiO_2$ , and  $Si_3N_4$ .*

i	$a_i$ [GPa]
$Y_2O_3$	10.7
$SiO_2$	6.8
$Al_2O_3$	7.9
$Si_3N_4$	17.9

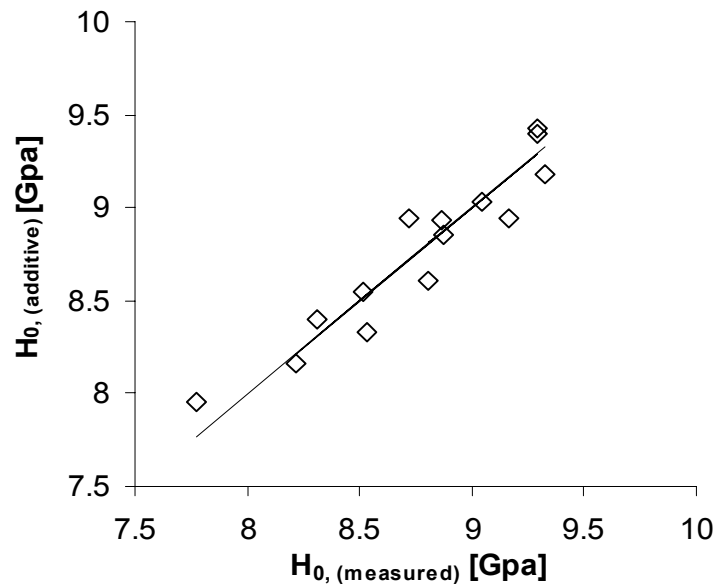


Fig. 9.4 *Correspondence between the measured  $H_0$  and  $H_0$  derived from the additive rule.*

It shows that the addition of silicon nitride clearly enhances the hardness of the glasses, which can be attributed to the formation of  $NSi_3$  links in the glass network. From a structural point of view we can understand these changes. The Si-N bond is not much stronger than the Si-O bond, but the bending resistance of the  $NSi_3$  unit is much greater than that of the  $OSi_2$  unit (bending force constants:  $OSi_2 = 9.6 \text{ N m}^{-1}$ ,  $NSi_3 = 97.3 \text{ N m}^{-1}$  [11]). This explains why the introduction of a limited amount of nitrogen results in a relatively strong enhancement of the network rigidity. It is also interesting to notice that the incorporation of nitrogen leads to a substantial deviation from existing relations between the hardness and glass-transition temperatures [12]. For instance for composition K1 with a glass transition temperature of  $953 \text{ }^\circ\text{C}$  [13] a hardness around  $7.5 \text{ GPa}$  is expected whereas it turns out to be much higher ( $9.3 \text{ GPa}$ ). This relation is based on the assumption that  $(c_{p,\text{melt}} - c_{p,\text{glasS}})$  is equal for different glasses, which is viable for most oxide glasses [12]. It describes the amount of energy involved in transforming a rigid glass in a plastic pseudo-melt at the measurement temperature. In the oxynitride glasses this energy increases upon

nitrogen incorporation [14], which offers a plausible explanation for the unusually high hardness.

It can also be noted that the replacement of  $\text{SiO}_2$  by  $\text{Y}_2\text{O}_3$  leads to an increase of the hardness. This increase suggests the formation of very strong covalent O-Y-O cross-linking bonds, as has been previously noted by Becher et al. [1]. In practice the observed trends imply that the addition of silicon nitride to the system is in two ways beneficial. Firstly, there is a direct influence of the  $\text{NSi}_3$  groups on the hardness. Secondly, the addition of nitrogen shifts the glass-forming region more to the alumina- and yttria-rich side of the system, which allows a further increase of the hardness by addition of a greater quantity of yttria and alumina [3]. In that respect there is room for improvement of the hardness of these glasses.

#### *The elastic recovery parameter ( $\delta$ )*

In crystalline systems a substantial amount of effort has been dedicated to explaining the various parameters that are used to describe the ISE in terms of materials characteristics. It is assumed that the elasticity as well as the viscosity of the material influences the extent of the ISE [15]. Other processes like fracture and (in crystals) slip are also known to contribute the indentation process and the ISE [6,8]. A distinct influence of the environment (e.g. the presence of water) has also been noted for vitreous silica [7,16]. Based on the notorious susceptibility of this material to subcritical crack growth we believe that this behaviour might be related to fracture related processes although this was not explicitly stated in the original paper of Hirao et al. [16].

Although there is only a limited amount of data available for other glass systems the ISE appears to be present in most glasses [7,17]. The absolute decrease of the hardness with the load is lower than in most ceramics, due to the relatively low hardness, which is probably the reason that the effect has not received as much attention in glasses as in ceramics. Nevertheless this investigation shows similar  $\delta$ -values as can be found as in ceramics, indicating that the similar mechanisms are active in glasses. The current tests show only a limited effect of the composition on the  $\delta$ -values, if any at all. It appears that the  $\delta$ -values increase towards the borders of the glass forming region, whereas the lowest values can be found in the center. However, in order to interpret these results more information on the ISE in a wider range of glass systems is needed, since only a relatively small variation in e.g. the viscosity and Young's modulus can be achieved in a single system. Moreover we need a better understanding of the relevant mechanisms that contribute to the plasticity of the material.



### 9.4 The influence of the modifier cation

Seven samples were prepared, based on the central composition  $\text{Ln}_{15.2}\text{Si}_{14.7}\text{Al}_{8.7}\text{O}_{54.1}\text{N}_{7.4}$  in which the type of lanthanide ion is varied (Y, La, Ce, Sm, Eu, Gd, Tb, Yb). As starting materials were used  $\text{Y}_2\text{O}_3$ ,  $\text{La}_2\text{O}_3$ ,  $\text{CeO}_2$ ,  $\text{Sm}_2\text{O}_3$ ,  $\text{Eu}_2\text{O}_3$ ,  $\text{Gd}_2\text{O}_3$ ,  $\text{Tb}_5\text{O}_7$ ,  $\text{Yb}_2\text{O}_3$ ,  $\text{SiO}_2$ ,  $\text{Al}_2\text{O}_3$  and  $\text{Si}_3\text{N}_4$ . The raw materials were mixed in a ball mill using isopropanol as a dispersion medium. The dried mixtures were fired at temperatures between 1600 and 1700 °C. The glasses were fired in a vertical tube furnace. These results (Table 9.3) clearly show that there is a trend of increasing hardness with decreasing size of the modifier cation (Fig. 9.5). This can be attributed to a slight increase of the covalence of the Ln-O bond and to a (larger) increase of the cationic field strength.

Table 9.3 *Chemical composition of glasses L1-L2 ionic radius of the modifier cation (IR) measured load-independent hardness ( $H_v^0$ ) and elastic recovery parameter  $\delta$ .*

Sample	Composition	IR [pm]	$H_v^0$ [GPa]	$\delta$ [ $\mu\text{m}$ ]
K1	Y-Si-Al-O-N	104.0	9.3	1.5
L1	Tb-Si-Al-O-N	106.3	8.69	1.1
L2	Gd-Si-Al-O-N	107.8	9.2	1.5
L3	Ce-Si-Al-O-N	115.0	7.6	1.5
L4	La-Si-Al-O-N	117.2	8.2	1.3
L5	Eu-Si-Al-O-N	135.0	6.3	1.6

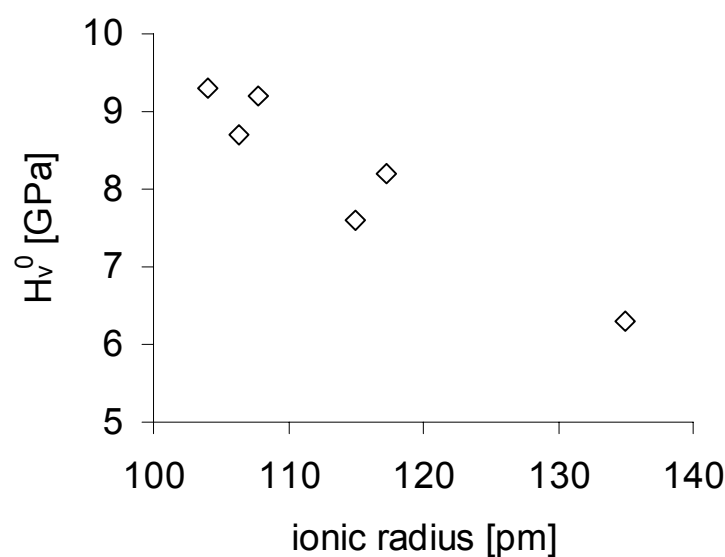


Fig. 9.5 *Load independent hardness of  $\text{Ln}_{15.2}\text{Si}_{14.7}\text{Al}_{8.7}\text{O}_{54.1}\text{N}_{7.4}$  glasses as a function of the ionic radius of the lanthanide ion.*

## 9.5 Conclusions

It has clearly been shown that the ISE has to be taken into account when measuring the load-independent hardness of Y-Si-Al-O-N glasses. Measurements at relatively low loads will lead to an apparent hardness, which is significantly higher than the load-independent hardness and renders comparison with other measurements at different loads unreliable. Measuring the hardness of materials with different compositions or at comparable low loads can lead to a misinterpretation of trends since the ISE may vary with the composition or material. In our load-dependent studies it is shown that the addition of nitrogen increases the hardness of Y-Si-Al-O-N glasses over the whole load range and thus the load-independent hardness. Compositional variations have shown a clear hardness increase by the incorporation of nitrogen. Nitrogen not only increases the load-independent hardness, but also allows greater quantities of yttria and alumina to be incorporated into the glass matrix, which has an additional hardness increasing effect.

## References

1. R. Ramesh, E. Nestor, M.J. Pomeroy and S. Hampshire, *J. Eur. Ceram. Soc.* 17[1] (1997) 1933-1939
2. P.F. Becher, S.B. Waters, C.G. Westmoreland and L. Riester, *J. Am. Ceram. Soc.* 85 [4] (2002) 897-902
3. S. Hampshire, E. Nestor, R. Flynn, J.-L. Besson, T. Rouxel, H. Lemerrier, P. Goursat, M. Sebai, D.P. Thompson and K. Liddell, *J. Eur. Ceram. Soc.* 14 (1994) 261-273
4. H. Bückle, In: *Science of hardness testing and its research applications*, (American Society for Metals, 1971) 453-491
5. P.M. Sargent, In: *Microindentation techniques in materials science and engineering* (American Society for Testing and Materials, 1985) 160-174
6. S.J. Bull, T.F. Page and E.H. Yoffe, *Phil. Mag. Lett* 59[6] (1989) 281-288
7. H. Li and R.C. Bradt, *J. Non-Cryst. Sol.* 146 (1992) 197-212
8. J.B. Quinn and G.D. Quinn, *J. Mater. Sci.* 32 (1997) 4331-4346
9. H.-J. Weiss, *Phys. Stat. Sol. (a)* 99 (1987) 491-501
10. H. Lemerrier, R. Ramesh, J.-L. Besson, K. Liddell, D.P. Thompson and S. Hampshire, *Key engineering materials*, Vols. 132-136 (1997) 814-817
11. S. Sakka, *J. Non-Cryst. Sol.* 181(1995) 215-224

12. F.J. Baltá Calleja, D.S. Sanditov and V.P. Privalko, *J. Mater. Sci.* 37 (2002) 4507-4516
13. Y. Menke, V. Peltier-Baron and S. Hampshire, *J. Non-Cryst. Sol.* 276 (2000) 145-150
14. J. Rocherulle, M. Matecki and Y. Delugeard, *J. Non-Cryst. Sol.* 238 (1998) 51-56
15. P.M. Sargent and T.F. Page, *J. Mater. Sci.* 20 (1985) 2388-2398
16. K. Hirao and M. Tomozawa, *J. Am. Ceram. Soc.* 70 [7] (1987) 497-502
17. J. Gong, W. Si and Z. Guan, *J. Non-Cryst. Sol.* 282 (2001) 325-328

# Chapter X

---

## Subcritical crack growth and power law exponent of Y-Si-Al-O(-N) glasses in aqueous environment

*The subcritical crack growth resistance in water of a Y-Si-Al-O and Y-Si-Al-O-N glass is investigated with three point bending experiments. It has been shown that the SCG behaviour of the Y-Si-Al-O-N glass differs significantly from that of the Y-Si-Al-O glass. This is reflected by the power law exponent  $n$ , conventionally used to indicate the susceptibility to subcritical crack growth, which is 21 for the Y-Si-Al-O glass and 63 for the Y-Si-Al-O-N glass. Implications of this observation are discussed.*

## 10.1 Introduction

Y-Si-Al-O-N glasses are renowned for their high resistance against water-induced subcritical crack growth (SCG) [1,2]. This makes these glasses, together with their overall high mechanical thermal and chemical durability, a sensible alternative for applications where the glasses have to sustain mechanical loading under aggressive chemical or thermal conditions. One can think of joining applications [3] or scratch resistant or chemical resistant applications [4].

However, as much has been investigated on the Y-Si-Al-O-N glasses, as little is known on the properties of the corresponding Y-Si-Al-O glasses. It is therefore the aim of this investigation to assert whether the high SCG resistance of Y-Si-Al-O-N glasses can be attributed to the incorporation of nitrogen or if it simply is a basal property of the Y-Si-Al-O glass matrix.

For that goal a Y-Si-Al-O-N glass has been prepared as well as a Y-Si-Al-O glass. Their slow crack growth resistance has been determined. In order to validate the used method a commercial borosilicate glass has been included in this investigation.

## 10.2 Experimental

The two glasses prepared in this investigation are  $Y_{3.5}Si_{17}Al_{3.5}O_{76}$  and  $Y_{15.2}Si_{14.7}Al_{8.7}O_{54.1}N_{7.4}$ . The change of the cationic composition reflects the shift of the glass-forming region with the nitrogen content. For both compositions, data on the mechanical properties are already available from other authors [5,6]. The borosilicate glass (Scott Duran<sup>®</sup>) was used as received. The Y-Si-Al-O(-N) glasses were prepared from  $Y_2O_3$  (Shin Etsu),  $SiO_2$  (amorphous, 99.7%, Al<sub>2</sub>O<sub>3</sub> (Taimei 4N) and  $Si_3N_4$  (Akzo Nobel P95H). Batches of 50 g powder were mixed by ball milling (isopropanol,  $Si_3N_4$  balls), dried and placed in a graphite crucible with BN powder lining to prevent sticking. The glasses were molten for one hour at temperatures of 1600 °C (Y-Si-Al-O) and 1700 °C (Y-Si-Al-O-N) in an electrical furnace under a nitrogen atmosphere. The glasses were rapidly cooled down by retracting the crucibles from the furnace. They were then placed in an annealing furnace operating at 800°C (Y-Si-Al-O) and 900 °C (Y-Si-Al-O-N) after which they cooled down slowly to room temperature. The surface of glass ingots was ground down to dispose of the oxide scale, which had formed during the cooling process. The density of the glasses was determined (Archimedes) and the Young's modulus (Ultrasonic pulse-echo measurements). The hardness was determined as a function of the load (P = 100, 200, 300, 500, 1000, 2000 g). The load dependent data were converted to and load independent hardness ( $H_v^0$ )

and an elastic recovery parameter ( $\delta$ ) in order to compensate for the indentation size effect according to the relation [Chapter IX,7,8].

$$H_v = H_v^0 \left( 1 + \frac{\delta}{d_m} \right)^2 \quad (1)$$

The Y-Si-Al-O(-N) glass ingots were then further diamond cut to bending bars with a height and width of 2 and 3 mm, respectively, and a length of 14 mm. The borosilicate glass was cut into specimens with a dimension of 2x4x20 mm. A Vickers indent was made on the back of the specimen in order to provide an initiating point for the crack. For the Y-Si-Al-O(-N) glasses an indentation load of 1000 g was used. For the borosilicate glass this was 500 g. The bars were immediately after indentation tested in deionised water in a three point bending configuration (10 mm span) in which the stress rate ( $\dot{\sigma}$ ) was varied. After breaking, the bar was examined with an optical microscope to determine whether the crack initiated from the indent. If this was not the case the datapoint was rejected.

Two experimental set-ups were used to determine the failure stress. Higher stress rates were achieved with a conventional testing machine (TesT). These experiments were executed at a constant crosshead velocity and from the logged data the stress rate was determined. For low stress rates another set-up was used in which the weight of a water-filled container is transferred via a lever construction to the sample. By slowly filling the container with water a constant increase of the loading force can be achieved (Fig. 10.1).

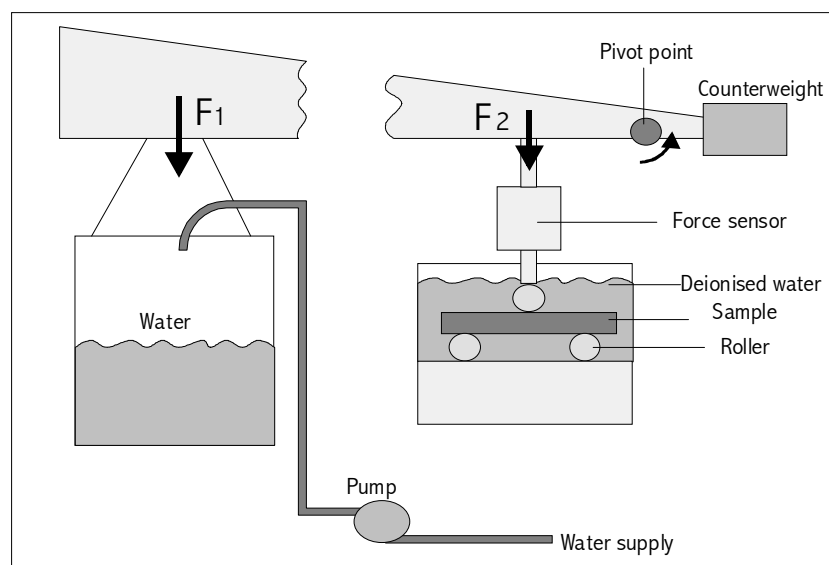


Fig. 10.1 Used experimental set-up for measuring SCG at low stress rates.

The relation between the failure stress and the stress rate is given by [9]:

$$\sigma_f = A'(n'+1)\dot{\sigma}^{\frac{1}{n'+1}} \quad (2)$$

The SCG parameter  $n'$  was determined by plotting the stress rate versus the failure stress on a double logarithmic scale and determining the slope by linear regression. The  $n'$  value for indented specimens can be translated to the power law exponent  $n$  by [9]:

$$n' = \frac{3}{4}n + \frac{1}{2} \quad (3)$$

The power law exponent describes the susceptibility to subcritical crack growth. An increase of the  $n$ -value implies an increased resistance against subcritical crack growth.

### 10.3 Results and discussion

Both the Y-Si-Al-O and the Y-Si-Al-O-N glass were completely transparent though greyish in appearance, which is common for these materials. Figure 10.2 and 10.3 show the raw data for the strength measurements, while table 10.1 gives an overview of the investigated properties of the three glasses. From the data it becomes immediately apparent that the mechanical performance improves going from the borosilicate to the oxide to the oxynitride glass. In the case of the Y-Si-Al-O glass one would expect the glass network to be further developed than in the case of the borosilicate glass. The reason for this lays in the addition of both aluminium and yttrium. The tetrahedral as well as the octahedral coordinated aluminium complexes can provide charge compensation for  $Y^{3+}$  thereby reducing the amount of non-bridging oxygen in the glass. The network modifying ability of Y is further limited since the Y-O bond has only a small ionic character. Apparently this enhanced rigidity of the network contributes to an increase of the mechanical properties such as the hardness and the Young's modulus. When  $Si_3N_4$  is added to this system the rigidity of the network is further increased by the ability of nitrogen to form three covalent bonds with silicon. This seems to be consistent with a substantial increase of the mechanical properties. However, some care must be taken when directly comparing these values because of the changing levels of yttrium and aluminum.

The values of  $n$  show a large difference between the oxide and oxynitride glasses. The value of  $n=15$ , obtained for the borosilicate glass corresponds exactly to the findings of Fett et al. [10], thus showing the viability of the used method. This is a normal value for silicate-based glasses: e.g. soda-lime glass gives a value of  $n = 17.9$  [9]. The value for the Y-Si-Al-O glass is already quite high ( $n = 21$ ), this possibly is a result of the high degree of cross-linkage in these glasses. However, the power law exponent for the Y-Si-Al-O-N glass is much higher than that of conventional silicate glasses ( $n=63$ ), and the value even approaches that of  $\text{Si}_3\text{N}_4$  itself.

Table 10.1 *Density ( $\rho$ ), Young's modulus ( $E$ ), intrinsic hardness ( $Hv^0$ ), elastic recovery parameter ( $\delta$ ), number of bend specimens ( $N$ ) and  $n$ -value (with a 90% confidence interval) for the glasses studied in this investigation. The density and the Young's modulus are compared with literature data.*

	$\rho$ [g/cm <sup>3</sup> ]	$E$ [Mpa]	$Hv^0$ [Gpa]	$\delta$ [ $\mu\text{m}$ ]	$N$	$n$ (90% conf)
Schott Duran ®	2.505	60	5.6	0.8	63	15 (13- 19)
Y-Si-Al-O	3.588 (3.572 [5])	110 (112 [5])	8.0	1.0	72	21 (16- 29)
Y-Si-Al-O-N	3.985 (3.97 [6])	145 (146 [6])	9.6	1.1	72	63 (33- 404)

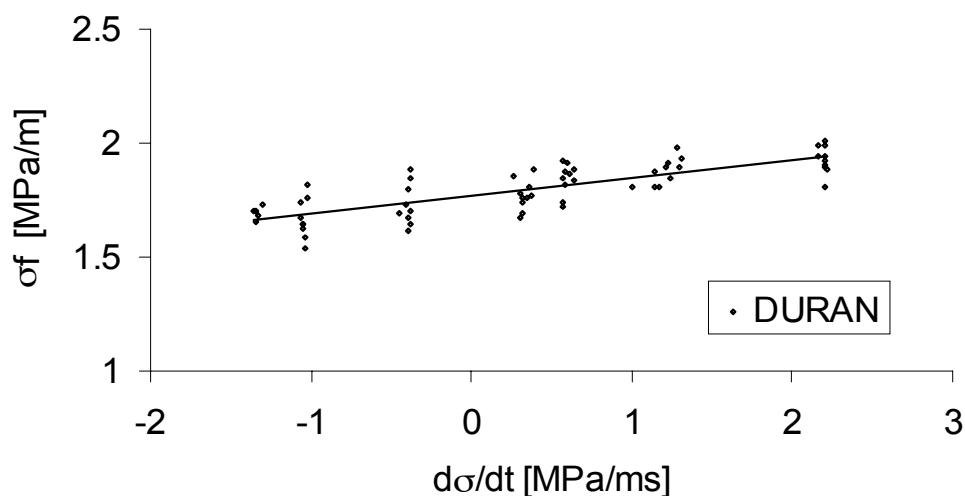


Fig. 10.2 *Failure stress versus stress rate for the Schott Duran borosilicate glass. Samples tested in three point bending in water*



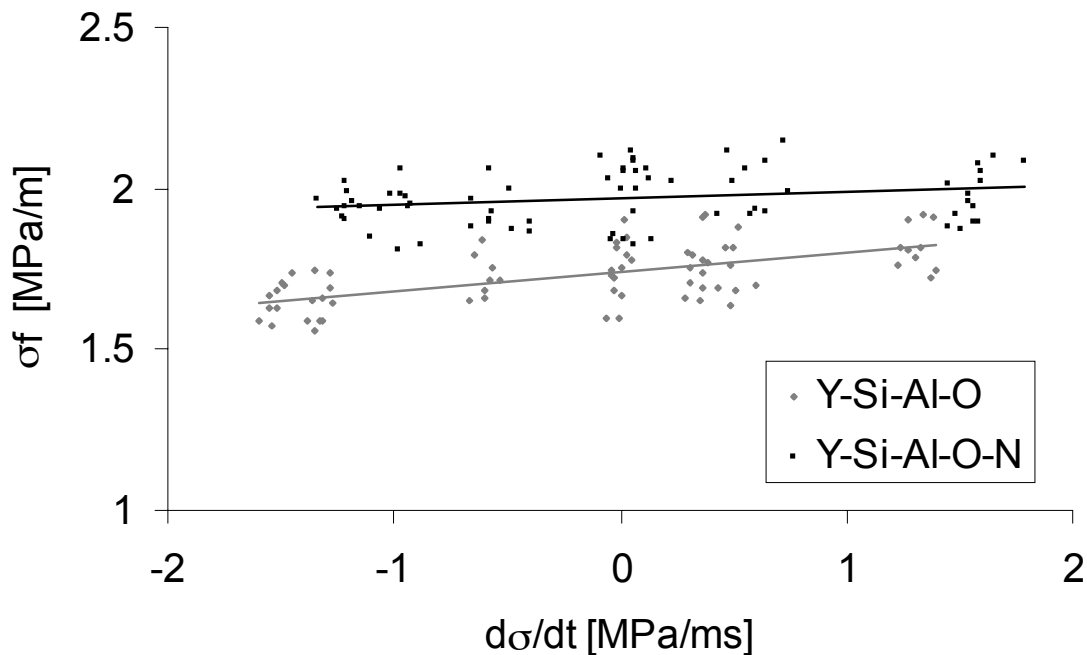


Fig. 10.3 Failure stress versus stress rate for the Y-Si-Al-O and Y-Si-Al-O-N glass. Samples tested in three point bending in water.

The atomistic model of SCG in glass predicts that bond rupture takes place in a number of steps [11]. Firstly a chemically reactive Si-O site or kink is formed under the applied stress. Water then reacts with the kink to finally break the bond. The number of kink sites along the crack front is the limiting factor to the fracture rate. In order to become a reactive centre, charge has to be transferred from the silicon site to the neighbouring oxygen (or nitrogen) ion. This process is less likely to occur with Si-N bonds than with Si-O bonds due to the larger covalence of the former.

We therefore expect the water assisted crack to propagate by the breaking of Si-O bonds not by rupture of Si-N bonds. This in itself cannot explain the large increase of the resistance to slow crack growth since approximately 85% of the bonding is still performed by oxygen and the crack would experience little hindrance by the present nitrogen. Bhatnagar et al. measured a high value for the average work of bond rupture in Y-Si-Al-O-N glass. Assuming that the crack propagates through breaking of Si-O bonds, it can be stated that the presence of nitrogen reduces the susceptibility of the Si-O bonds to water attack.

Michalske and Bunker argue the primary attack of a water molecule takes place on silicon on a distorted site [12]. This distortion of the tetrahedral angles of Si occurs when a three- and fourfold [-Si-O-] ring structure in the glass is elongated and puckered by the applied stress like shown in figure 10.4 [13].

Therefore the crack propagation rate can be correlated to the number of  $[-\text{Si-O}]_3$  and  $[-\text{Si-O}]_4$  rings present in the glass. The absence of these ring structures can lead to a substantial increase of the SCG resistance. This has been observed in the case of tellurite glasses, which display  $n$ -values ranging from 50-70 [14].

In Y-Si-Al-O-N glasses these ring structures are expected to be present, since they can be found in many crystalline (oxy)nitrides. However, the incorporation of nitrogen in the direct vicinity of these rings or in these rings themselves would lead to a substantial increase of the resistance to deformation since the bending energies of nitrogen and oxygen differ considerably (bending force constants:  $\text{OSi}_2 = 9.6 \text{ N m}^{-1}$ ,  $\text{NSi}_3 = 97.3 \text{ N m}^{-1}$  [15]). The rings can therefore not produce effective kink sites at the low stress levels associated with subcritical crack growth.

The incorporated nitrogen thus inhibits the formation of chemically active centres. This can explain why the incorporation of a relatively low percentage of nitrogen leads to such a dramatic increase of the resistance against subcritical crack growth.

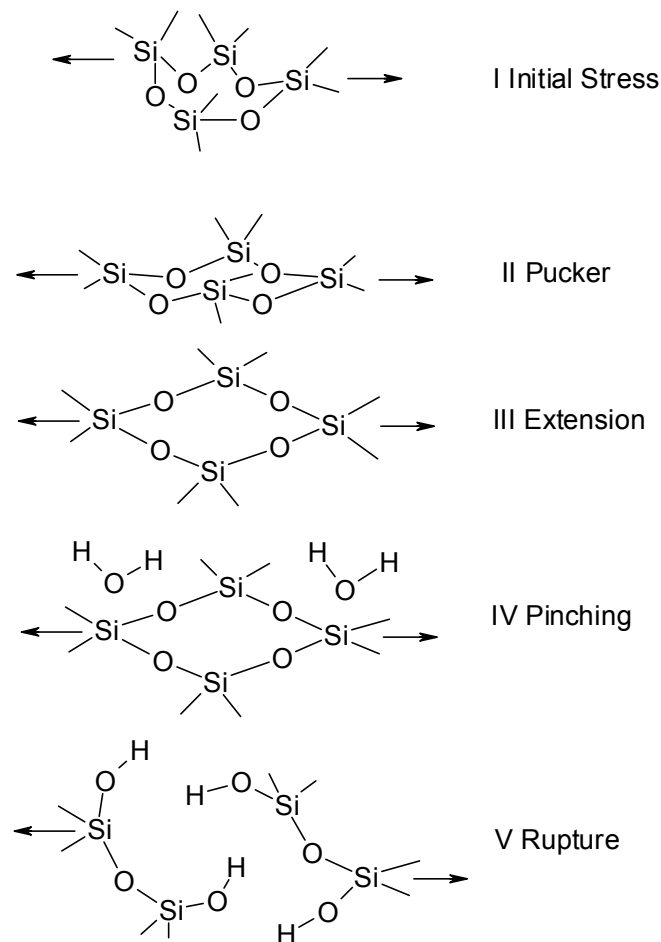


*Fig.10.4 The five stages of ring deformation and water-assisted rupture according to Michalske and Bunker [12].*

## 10.4 Conclusions

This investigation has shown that Y-Si-Al-O glasses display a good resistance against subcritical crack growth in a water environment. However, the SCG resistance of Y-Si-Al-O-N glass is by far superior to that of Y-Si-Al-O indicating that the incorporated nitrogen intervenes with one of the critical steps of the slow crack growth mechanism. It also shows that more information on the structure of these glasses, especially on the presence of three membered –Si-O-rings in the glass is required in order to understand this anomalous behaviour.

## References

1. D.N. Coon, J. Non-Cryst. Sol. 226 (1998) 281-286
2. A. Bhatnagar, M. Hoffman and R. H. Dauskardt, J. Am. Ceram. Soc. 83 [3] (2000) 385-396
3. L.M. Weldon, M.J. Pomeroy and S. Hampshire, J. Eur. Ceram. Soc. 17 (1997) 1941-1947
4. R.E. Loehman, Treatise on materials science and technology, vol 26 glass IV, Academic Press (1985) 119-151
5. A. Makishima, Y. Tamura and T. Sakaino, J. Am. Ceram. Soc. 61 [5-6] (1978).247-249
6. Y. Menke, V. Peltier-Baron and S. Hampshire, J. Non-Cryst. Sol. 276 (2000) 145-150
7. S.J. Bull, T.F. Page and E.Y. Hoffe, Phil. Mag. Lett. 59[6] (1989) 281-288
8. D. de. Graaf, M. Bracisiewicz, H.T. Hintzen, M. Sopicka-Lizer and G. de With, *accepted by J. Mater. Sci.*
9. B. Lawn, 'Fracture of brittle solids', Cambridge University Press, 2<sup>nd</sup> ed. (1993).
10. T. Fett, K. Germdonk, A. Grossmüller, K. Keller and D. Mutz, J. Mater. Sci. 26 (1991) 253-257
11. R.E. Cook and E.G. Liniger, J. Am. Ceram. Soc. 76[5] (1993) 1096-1105
12. T.A. Michalski and B.C. Bunker, J. Appl. Phys 56[10] (1984) 2686-2693
13. J.K. West and L.L. Hench, J. Mater. Sci.29 (1994) 5808-5816
14. S. Yoshida, J. Matsuoka and N. Soga, J. Non-Cryst. Sol. 279 (2001) 44-50
15. S. Sakka J. Non-Cryst. Sol. 181(1995) 215-224

# Chapter XI

---

## Thermal and elastic properties of rare-earth containing Si-Al-O-N glasses

*In this chapter the elastic properties (Elastic modulus, shear modulus, Poisson ratio) and the thermal properties (thermal diffusivity, heat capacity, thermal conductivity) of RE-Si-Al-O-N glasses are studied as a function of the nitrogen content and the rare-earth ion (RE = Y, La, Ce, Eu, Tb, Gd). The results are evaluated in terms of (local) structure. It was found that although the nitrogen strongly enhances the resistance against deformation, the effect on the thermal properties is limited, the reason being the lack of a strongly developed silicate network.*

## 11.1 Introduction

Rare-earth containing Si-Al-O-N glasses have received a substantial amount of attention of the past decade, the main reason being the excellent mechanical durability of these systems [1]. It has been widely established that the incorporation of a relatively small amount of nitrogen leads to a significant change of the glass network, and therefore to a strong change of the mechanical properties. This is e.g. visible for the susceptibility to subcritical crack growth, which virtually disappears upon nitrogen incorporation [2] or the fracture toughness which is increased by nitrogen incorporation [3]. Although it has been shown that nitrogen tends to incorporate in a threefold coordination with silicon and that the Si-N bond is slightly more covalent than the Si-O bond, it is not exactly understood how this attributes to the sometimes unexpected behavior of these glasses.

Despite the amount of investigations that have been dedicated towards the mechanical properties of these glasses and the effect that nitrogen and the different lanthanides have thereon [4,5], the thermal properties and especially the thermal conduction have received relatively little attention. This is a pity because for many applications knowledge on the thermal conduction is very important. Moreover, the theories on heat conduction in solids by lattice vibrations have been established for a long time and have shown to yield valuable information on the internal structure of a material. This is particularly true in crystals [6] but many of the developed concepts can also be applied to disordered solids [7].

This chapter is dedicated to the elastic and thermal properties of RE-Si-Al-O-N glasses. Special attention is focused on the effect of nitrogen incorporation and rare earth replacement. The goal of this work is not only to derive information on the thermal and elastic properties of these glasses but more importantly to gain a better insight in the bond structure and its relation to the properties of these glasses.

## 11.2 Experimental

The glasses were prepared from  $Y_2O_3$ ,  $Gd_2O_3$ ,  $CeO_2$ ,  $La_2O_3$ ,  $Tb_4O_7$ ,  $Eu_2O_3$ ,  $SiO_2$  and  $Al_2O_3$  as starting materials. Nitrogen was added to the system in the form of  $Si_3N_4$ . The compositions are listed in table 11.1. Although trivalent europium is added, it is shown to reduce to the divalent state during the preparation of the glasses [Chapter IV, 8] whereas the other rare earths are expected to be present in the trivalent state.

Table 11.1 *Compositions (weighed-out) of the glasses prepared in this investigation.*

	RE	Si	Al	O	N	$M_A$ *10 <sup>3</sup>	$\Gamma_{RE}$
	[at%]	[at%]	[at%]	[at%]	[at%]	[kg/mol]	[pm]
Y(1)	15.2	14.7	8.7	54.1	7.4	29.68	104.0
Y(2)	15.0	14.4	8.6	57.7	4.3	29.52	104.0
Y(3)	14.8	14.3	8.5	60.3	2.1	29.42	104.0
La	15.2	14.7	8.7	54.1	7.4	37.28	117.2
Ce	15.2	14.7	8.7	54.1	7.4	37.47	115.0
Eu	15.2	14.7	8.7	54.1	7.4	39.28	135.0
Gd	15.2	14.7	8.7	54.1	7.4	40.08	107.8
Tb	15.2	14.7	8.7	54.1	7.4	40.32	106.8

The raw materials were mixed by ball-milling in isopropanol using agate balls. The resulting mixtures were dried and fired in a vertical tube furnace at 1700 °C for 1 hr in a nitrogen atmosphere. A graphite crucible was used which was powder-lined with hexagonal-BN to prevent sticking. After the furnace was cooled down to 1600 °C, the hot samples rapidly extracted from the furnace and placed in an annealing furnace operating in air at 800-900 °C depending on the composition. This annealing step is necessary to obtain stress- and crack-free samples. The thin oxide scale that had formed on the samples during cooling and annealing was removed by grinding the surface. In order to ensure that the glasses were amorphous the glasses were characterized using XRD.

The glass was then cut in to specimens for testing. Pieces of 1-2 g were used to measure the density ( $\rho$  [kg m<sup>-3</sup>]) using the Archimedes method in distilled water. Ultrasonic pulse echo measurements were used to determine the transversal ( $v_t$  [m/s]) and longitudinal sound velocity ( $v_l$  [m/s]). From these velocities the Poisson ratio ( $\nu$  [-]), Young's modulus ( $E$  [GPa]) and bulk modulus ( $G$  [GPa]) can be derived using equations 1-3.

$$\nu = \frac{v_l^2 - 2v_t^2}{2(v_l^2 - v_t^2)} \quad (1)$$

$$E = 2\rho(1+\nu)v_l^2 \quad (2)$$

$$G = \frac{E}{2(1+\nu)} \quad (3)$$

Since glasses are isotropic the following approach can be used to derive the Debye temperature as reported by Anderson [9]. The longitudinal and transversal sound velocities are averaged ( $v_s$  [m/s]) using equation 4 and the averaged values are inserted in equation 5 to yield the Debye temperature.

$$v_s = \left( \frac{1}{3} \left[ \frac{1}{v_l^3} + \frac{2}{v_t^3} \right]^{-\frac{1}{3}} \right) \quad (4)$$

$$\Theta = \frac{h v_s}{2k} \left( \frac{8}{\frac{4}{3}\pi} \cdot \frac{N_A \rho}{M_A} \right)^{\frac{1}{3}} \quad (5)$$

in which  $h$  is Planck's constant ( $6.626 \cdot 10^{-34}$  J s),  $k$  Boltzmann's constant ( $1.381 \cdot 10^{-23}$  J K<sup>-1</sup>),  $N_A$  Avogadro's number ( $6.023 \cdot 10^{23}$  mol<sup>-1</sup>) and  $M_A$  [kg mol<sup>-1</sup>] the average atomic mass.

The thermal diffusivity was measured using the photo-flash method. The diffusivity was measured on disks measuring 0.50 mm in thickness ( $d$ ) and 8.0 mm in diameter. The disks were given an optical finish using diamond wheels. In order to prevent the signal passing through the sample the front and backside were coated first with a 50  $\mu$ m gold coating and afterwards with a carbon dispersion. The thermal diffusivity ( $a$  [m<sup>2</sup> s<sup>-1</sup>]) was determined from:

$$a = \frac{W_x d^2}{\pi^2 t_x} \quad (6)$$

in which  $t_x$  is the time from the initiation of the pulse and  $W_x(t)$  is a dynamic correction factor to account for the heat losses. From the thermal diffusivity and the average sound velocity (which equals the mean phonon velocity) the phonon free path ( $l_{tot}$  [m]) can be determined using the relation.

$$a = \frac{1}{3} v_s l_{tot} \quad (7)$$

### 11.3 Results and Discussion

#### *Young's modulus*

It is well known that the incorporation of nitrogen into an oxide glass leads to an increase in the elastic modulus [10]. Such effects has also been observed in this investigation. In earlier work the change has been ascribed to enhanced degree of crosslinking in oxynitride glasses [1]. Although the coordination of nitrogen (3) is higher than that of oxygen (2) the number of bonds does not increase since nitrogen and oxygen are exchanged in a ratio of 2 to 3. Indeed the decrease of the molar volume upon nitrogen incorporation suggests the elimination of some free volume and thus to a higher number of bonds per unit volume. However, this effect is relatively small and should not lead to changes of the observed magnitude.

In oxide glasses one approach that has been proven to be very useful in understanding and predicting the elastic properties of a glass are the ionic models of Makishima and Mackenzie [11], which are based on earlier work by Sun, Huggins [12,13] and Gilman [14].

It would go to far to explain all the details of this approach but it is based on the fact that the elasticity of a single bond is related to its dissociation energy. The elastic modulus of a glass can therefore be derived from a summation of the dissociation energy of the individual bonds. Since the dissociation energies of the individual bonds in a glass are not known one has to turn to crystalline reference materials in which the type of bonding is similar as in the glasses.

Makishima and Mackenzie showed that by choosing suitable reference materials the elastic properties of a glass can be predicted with a reasonable to good accuracy. We have chosen to use  $\text{SiO}_2$  (cristobalite) and  $\text{Si}_3\text{N}_4$  (alpha) to represent the Si-O and the Si-N bond.  $\text{Si}_3\text{N}_4$  might not be the ideal reference material since in the glasses the coordination of silicon with more than one nitrogen atom is highly unlikely [15,16]. In table 11.2 we have calculated some of the relevant parameters for  $\text{SiO}_2$  and  $\text{Si}_3\text{N}_4$  [17]. The elastic modulus is then given by [11]:

$$E \approx 2V_t G = 2 \frac{\rho}{M} \sum_i V_i x_i \sum_i G_{v,i} x_i \quad (8)$$

where  $\rho$  [ $\text{kg m}^{-3}$ ] and  $M$  [ $\text{kg mol}^{-1}$ ] are the density and the molar mass of the glass.



Table 11.2 *Density ( $\rho$ ) dissociation energy ( $\Delta G$ ), packing density ( $V$ ) and single bond strength (SBS) of  $\text{SiO}_2$  and  $\text{Si}_3\text{N}_4$ .*

		$\text{SiO}_2$	$\text{Si}_3\text{N}_4$ ( $\text{SiN}_{4/3}$ )
$\rho$	[g/cm <sup>3</sup> ]	2.3	3.4
$\Delta G_i$	[kJ/mol]	1723	3686 (1229)
$\Delta G_{v,i}$	[kJ/cm <sup>3</sup> ]	66.5	90.4 (90.4)
$V_i$	[cm <sup>3</sup> /mol]	14.0	51.0 (17.0)
SBS	[kJ/moll]	430	307

$\Delta G_f(\text{SiO}_{2(\text{cr})}) = -854.509 \text{ kJ mol}^{-1}$ ,  $\Delta G_f(\text{Si}_3\text{N}_{4(\text{cr})}) = -647.343 \text{ kJ mol}^{-1}$ ,  $\Delta G_f(\text{O}_{(\text{g})}) = 231.736 \text{ kJ mol}^{-1}$ ,  $\Delta G_f(\text{N}_{(\text{g})}) = 455.540 \text{ kJ mol}^{-1}$  and  $\Delta G_f(\text{Si}_{(\text{g})}) = 405.528 \text{ kJ mol}^{-1}$ ,  $r_{\text{O}} = 41 \text{ pm}$ ,  $r_{\text{N}} = 171 \text{ pm}$ ,  $r_{\text{Si}} = 140 \text{ pm}$ .

From these parameters we can conclude that the elastic modulus increases somewhat, due to the nitrogen incorporation but this is entirely due to an increase of the bond density since the single bond strength (SBS [12]) of Si-N is actually predicted to be lower than that of Si-O. Therefore straightforward application of the expressions of Makishima and Mackenzie always leads to a too low prediction of the elastic modulus as was previously observed by other authors [18,19] as well as in this work (table 11.3).

Table 11.3 *Key properties of RE-Si-Al-O-N glasses as a function of the nitrogen content*

	$\rho$ [kg/m <sup>3</sup> ]	$v_t$ [m/s]	$v_l$ [m/s]	$v_s$ [m/s]	$\theta_{293}$ [K]	$E (E_{\text{calc}})^*$ [GPa]	$G$ [GPa]	$\nu$ [-]	$a_{293}$ [10 <sup>-8</sup> m <sup>2</sup> /s]	$l_{\text{tot}}$ [Å]
Y(1)	4000	3758	6891	4191	537	146 (113)	56.5	0.29	36	2.6
Y(2)	3938	3500	7014	3927	502	129 (106)	48.3	0.33	34	2.6
Y(3)	3914	3456	6955	3878	495	125 (101)	46.8	0.34	33	2.6
La	4561	3006	6415	3384	420	112	41.2	0.36	28	2.5
Ce	4737	3063	6249	3440	432	119	44.4	0.34	28	2.4
Eu	4755	2794	5088	3115	385	95	37.1	0.28	20	1.9
Gd	5137	3076	5875	3441	434	127	48.6	0.31	29	2.5
Tb	4880	3125	5975	3496	433	125	47.7	0.31	29	2.5

\*(..) calculated values according to Makishima and Mackenzie [11].

This does not mean that the bond strengths calculated with the method of Sun are unreliable. An extensive analysis by Murakami and Sakka of the Si-O and Si-N bonds shows that the stretching force constant of Si-O and Si-N in oxynitride glasses ( $K_{r,\text{Si-O}} = 737 \text{ N m}^{-1}$  and  $K_{r,\text{Si-N}} = 507 \text{ N m}^{-1}$ ) [20, 15] are indicating lower bond strength for Si-N bonding.

In the ionic model of Makishima and Mackenzie, the potential energy of the system is determined by the interatomic distances and it does not take bond angles into account. This approximation is valid for oxide glasses. Since the bending force constants of the  $\text{O}(-\text{Si}\equiv)_2$  units are very low ( $K_{\theta,\text{O}} = 9.60 \text{ N m}^{-1}$  [20]), these bonds easily align themselves with the force, leaving the bond length as the predominant factor. For the  $\text{N}(-\text{Si}\equiv)_3$  units, which have a much higher bending force constant ( $K_{\theta,\text{N}} = 97.3 \text{ N m}^{-1}$  [20]), a substantial angular contribution to the potential energy is expected. This directionality explains both the high elastic modulus of oxynitride glasses as well the failure to explain this increase in terms of bond strength and by the model of Makishima and Mackenzie.

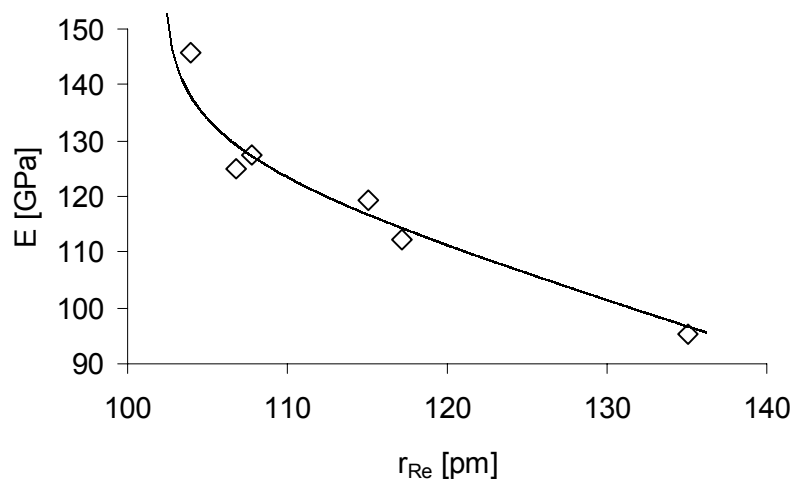


Fig. 11.1 *Young's modulus vs. ionic radius of the rare-earth ion (Line serves as a guide for the eye only).*

When the size of the lanthanide ion is increased the elastic modulus decreases (Fig. 11.1), as is the case in oxide glasses [21]. As the size of the rare-earth ion decreases the RE-O bonding gradually becomes less ionic which leads to a higher elastic modulus in compliance with the theory of Makishima and Mackenzie. Of course, the average coordination of the lanthanide is also expected to increase with the ionic radius, which should lead to further degradation of the elastic modulus.

*Poisson's ratio*

The Poisson's ratio ( $\nu$ ) decreases upon nitrogen incorporation (Table 11.3). The Poisson's ratio is defined as the ratio between lateral and longitudinal strain and reflects the ability of a structure to resist deformation in the plane perpendicular to the primary force. A decrease of the Poisson's ratio in a glass is therefore usually associated with an increase of the bonding density since this increases the lateral rigidity [22]. Although the bond density does not substantially increase upon nitrogen incorporation (as was discussed earlier) we can intuitively understand why the directional bonding of nitrogen would lead to more efficient resistance against lateral deformation, with respect to the longitudinal deformation.

For the different lanthanides we also observe a difference in the Poisson's ratio. The general trend is an increase of the Poisson's ratio with an increase of the ionic radius of the lanthanide suggesting that the packing of the glass becomes looser when the radius of the rare-earth ion is increased (Fig. 11.2). Surprisingly a very low value is observed for the Eu-Si-Al-O-N glass. This perhaps is the result of the different oxidation state of europium (2+ instead of 3+) and the somewhat lower nitrogen content due to the reduction.

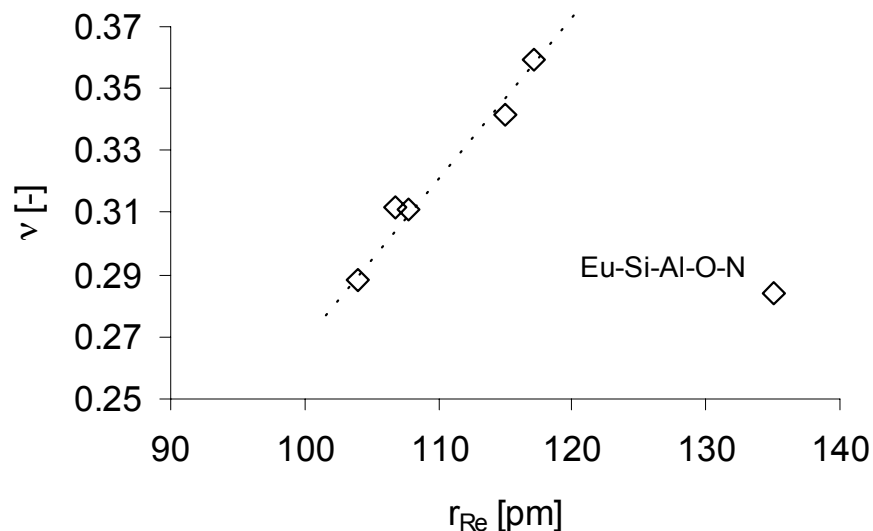


Figure 11.2 *Poisson's ratio versus ionic radius of the rare earth ion*

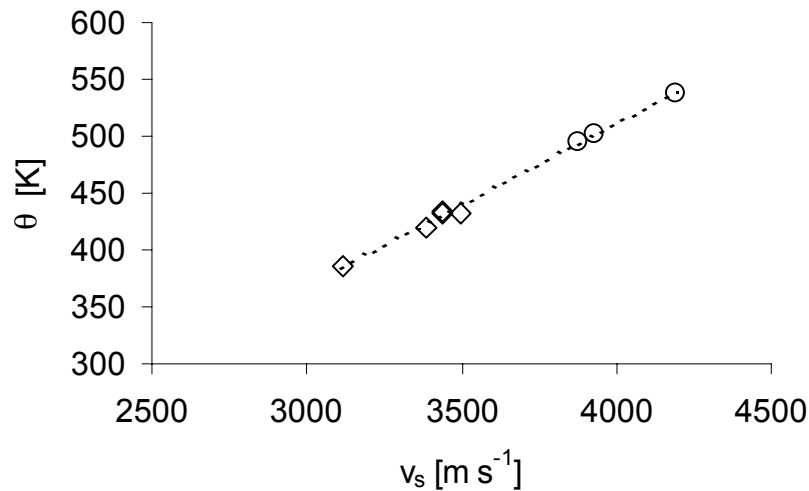


Fig. 11.3 Debye temperature versus average velocity of sound (◇ RE-Si-Al-O-N, ○ Y-Si-Al-O-N)

### Debye temperature

The Debye temperature of these glasses is relatively high as compared to other glass systems like telluride glasses [23] and aluminosilicate glasses [24] and increases with the nitrogen content. An increase of the Debye temperature with the nitrogen content was previously also observed for the Mg-Y-Si-Al-O-N glass system [25]. Since  $\rho/M_A$  only marginally changes as a function of the chemical composition, the Debye temperature is by approximation linearly dependent on  $v_s$  as can be seen in figure 11.3.

### Thermal diffusivity

According to eq. 7 the thermal diffusivity is governed by the free path and the velocity of the phonons. With the exception of Eu-Si-Al-O-N glasses, the mean free path does not change much over the measured range, which leaves the thermal diffusivity almost linearly dependent on  $v_s$ . Nevertheless, despite having Young's moduli and Debye temperatures, which surpass most glass systems, the thermal diffusivities are amongst the lowest ever reported [26]. This implies that the mean free path of these systems is very low. Indeed when compared with the scarce data on free paths in glasses it becomes apparent that the free path in these glasses is much lower than that in most glasses such as vitreous silica ( $l_{\text{tot},298} = 8.1 \text{ \AA}$  [27]) and crown glasses ( $l_{\text{tot},298} = 4.1 \text{ \AA}$ ) [27]. In ceramics, the phonon free path can be lowered to a minimum of few lattice spacings by

introducing imperfections [28,7]. In our glasses the phonon free path is even lower, nearly the size  $a$  of a single silica tetrahedron.

Since glasses are by nature homogenous isotropic materials some of the scattering mechanisms, which play a role in ceramics, (e.g. grain boundary scattering) can be disregarded [29]. Therefore the phonon free path is primarily dependent on the amount of scattering centers and their scattering power, which is related to the deviation in atomic mass and the force constants of the scattering centers [7].

In silicate glasses heat is expected to be transferred through the strongly interlinked silicate network. Figure 11.4 shows, that the thermal diffusivity for most silicate glasses is determined by the silica content of the glass. Therefore the low conductivity of the RE-Si-Al-O-N glasses can be attributed to the high amount of scattering centers or inversely to the low amount of silica, which leads to the short phonon free path. Within this larger trend we can see As a secondary effect the elastic properties and the mass of the other ions (Al, Si, N) do influence the phonon velocity and the phonon free path and thus the thermal diffusivity, but this effect is by far inferior to the former.

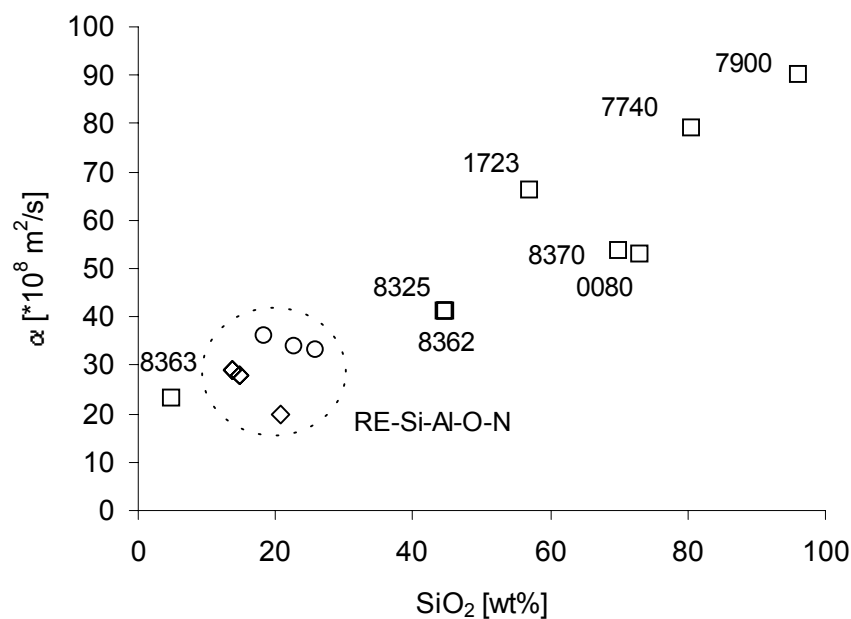


Fig. 11.4 *Thermal diffusivity various glasses as a function of the silica content. Comparison between the RE-Si-Al-O-N glasses prepared in this investigation and literature values on Corning silicate glasses( $\square$ ) [26]. ( $\diamond$  RE-Si-Al-O-N,  $\circ$  Y-Si-Al-O-N)*

*Heat capacity and thermal conductivity*

The thermal diffusivity is an important parameter since it describes the velocity of temperature averaging in a material. It is related to the thermal conductivity ( $k$ ) via equation 9.

$$k = a\rho_m C_v \quad (9)$$

So if we can estimate the heat capacity at constant volume ( $C_V$ ) we can calculate the thermal conductivity at room temperature. Inaba et al. [30] have provided a semi-empirical relation between the one dimensional Debye temperature ( $\theta_{D1} = \theta/0.3$ ) and the heat capacity at constant volume ( $C_P$ ) which allows us to predict the  $C_P(T)$  curve. Their work shows that for a wide variety of glass systems this one-dimensional equation is preferable over the standard Debye equation.

$$C_p = 3R \left[ 1 - \exp\left(-5 \frac{T}{\theta_{D1}}\right) \right] \quad (10)$$

The difference between  $C_P$  and  $C_V$  is given by:

$$C_P - C_V = \frac{9\alpha^2 V_m T}{\beta_T} \quad (11)$$

in which  $\alpha$  [ $\text{K}^{-1}$ ] is the linear thermal expansion coefficient,  $V_M$  is the molar volume [ $\text{m}^3 \text{mol}^{-1}$ ],  $T$  is the temperature [ $\text{K}$ ] and  $\beta_T$  the isothermal compressibility [ $\text{Pa}^{-1}$ ]. This quantity is assumed to be very small for glasses at moderate temperatures so that  $C_P = C_V$ . Indeed the work of Rocherulle et al [25]. shows that for Mg-Y-Si-Al-O-(N) glasses the difference between  $C_P$  and  $C_V$  is less than one percent even at 50 degrees below the glass transition temperature. In figure 11.5 the  $C_P(T)$  curves are plotted for the Y-Si-Al-O-N glasses. It shows that the introduction of nitrogen leads to a small decrease of the  $C_p$  over the whole temperature range as a consequence of the increase in the Debye temperature.

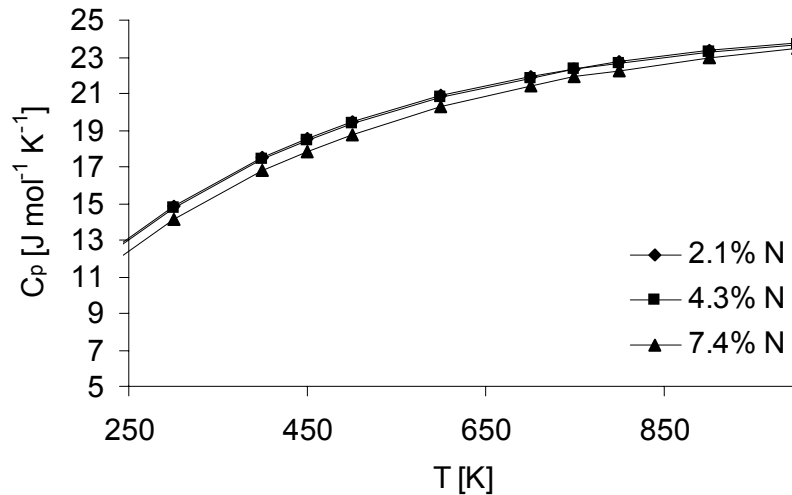


Fig. 11.5 Calculated  $C_p(T)$  curves for glasses Y(1), Y(2) and Y(3).

Table 11.4 Calculated heat capacity and thermal conductivity (at room temperature) of the glasses studied in this investigation

glass	$\rho_M$ $\cdot 10^{-4}$ [m <sup>3</sup> /mol]	$C_p$ [J/ mol K]	$\kappa$ [W/m K]	glass	$\rho_M$ $\cdot 10^{-4}$ [m <sup>3</sup> /mol]	$C_p$ [J/ mol K]	$\kappa$ [W/m K]
Y(1)	13.5	14.8	0.684	La	12.2	16.3	0.560
Y(2)	13.3	14.7	0.667	Ce	12.6	16.1	0.569
Y(3)	13.3	14.1	0.651	Eu	12.1	17.1	0.415
				Gd	12.8	16.0	0.596
				Tb	12.1	16.1	0.566

Since neither the thermal diffusivity nor the heat capacity is strongly altered by the nitrogen incorporation the thermal conductivity of these glasses changes little with the nitrogen content (Table 11.4). As a whole the thermal conductivity of these glasses is very low compared to other glasses. This can be ascribed to the short phonon free path of the glasses as a result of the lack of a strongly developed silicate network. This is visible in figure 11.6, where the thermal conductivity of the RE-Si-Al-O-N glasses is compared to data for other silicate based glasses [31].

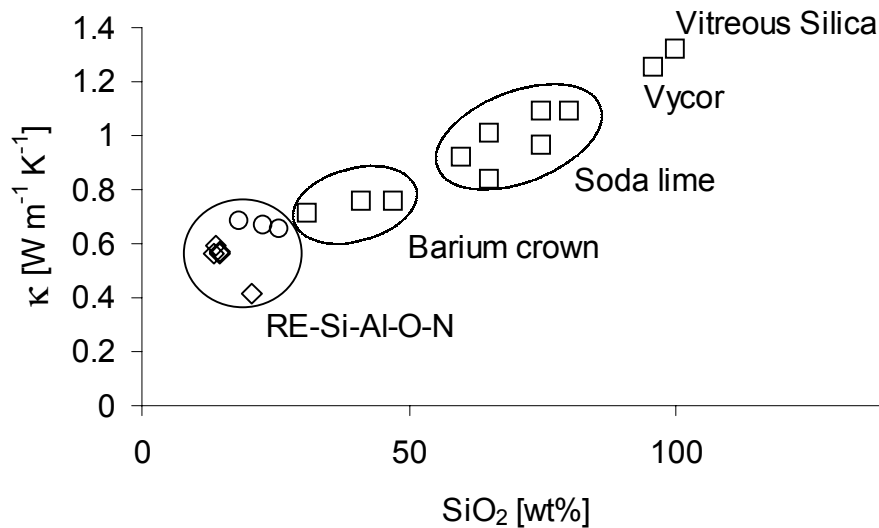


Fig. 11.6. Room temperature thermal conductivity of various glasses as a function of the silica content [31] ( $\diamond$  Ln-Si-Al-O-N,  $\circ$  Y-Si-Al-O-N).

## 11.4 Conclusions

These results show a clear and consistent picture of the constitution and properties of RE-Si-Al-O-N glasses. It confirms that the assumptions of Sakka et al. are correct and that it is the rigidity of the  $\text{NSi}_3$  unit that determines the elastic properties of oxynitride glasses rather than the stretching force constants of the Si-N bonds.

The elastic properties of the glasses are further determined by the oxidation state, the size and the covalence of the RE-O bonding. Since these properties vary in a regular fashion across the rare earth series as does the ionic radius, it usually suffices to display them as a function of the ionic radius or the cationic field strength to show the trends. However, the real behavior is expected to be a complex function of the above-mentioned arguments.

The changes of thermal properties of the RE-Si-Al-O-N glasses with the composition can be well understood by the effect of the different constituents on the rigidity of the glass matrix (and thus on the phonon velocity) and on the phonon free path. As a whole the thermal conductivity of the RE-Si-Al-O-N glasses is very low. This can be ascribed to the lack of a well-developed silicate network.



## References

1. R.E. Loehman, In: Treatise on materials science and technology, vol 26 glass IV (Academic Press, 1985) 119-151
2. D.N. Coon, *J. Non-Cryst. Sol.* 226 (1998) 281-286
3. A. Bhatnagar, M.J. Hoffman and R.H. Dauskardt, *J. Am. Ceram. Soc.* 83 [3] (2000) 585-596
4. R. Ramesh, E. Nestor, M.J. Pomeroy and S. Hampshire, *J. Eur. Ceram. Soc.* 17 (1997) 1933-1939
5. Y. Murakami and H. Yamamoto, *J. Ceram. Soc. Jpn.* 102 (1994) 231-236
6. R. Peierls, *Ann. Phys.* 5[3] (1929) 1055-1101
7. W.G. Klemens, In: Solid state physics vol 7 (Academic Press, 1958) 1-97
8. D. de Graaf, H.T. Hintzen, S. Hampshire and G. de With, *J. Eur. Ceram. Soc* 23 (2003) 1093-1097
9. O.L. Anderson, *J. Phys. Chem. Sol.* 24 (1963) 909-917
10. S. Hampshire, E. Nestor, R. Flynn, J.L. Besson, T. Rouxel, H. Lemerrier, P. Goursat, M. Sebai, D.P. Thompson and K. Liddell, *J. Eur. Ceram. Soc.* 14 (1994) 261-273
11. A. Makishima and J.D. Mackenzie, *J. Non-Cryst. Sol.* 12 (1973) 35-45
12. K.-H. Sun, *J. Am. Ceram. Soc.* 30 [9] (1947) 277-281
13. M.L. Huggins and K.-H. Sun, *J. Phys. Chem.* 50 (1946) 319-328
14. J.J. Gilman In: Progress in ceramic science, vol 1, (Pergamon Press, 1961) 146-155
15. S. Sakka, *J. Non-Cryst. Sol.* 181 (1995) 215-224
16. P.F. McMillan, R.K. Sato and B.T. Poe, *J. Non-Cryst. Sol.* 224 (1998) 267-276
17. M.W. Chase, Jr, C.A. Davies, J.R. Downey, Jr, D.J. Frurip, R.A. McDonald and A.N. Syverud, JANAF thermochemical tables 3rd ed. Vol 14 (Am. Chem. Soc. and Am. Inst. of Phys, 1985)
18. J. Rocherulle, C. Ecolivet, M. Poulain, P. Verdier and Y. Laurent, *J. Non-Cryst. Sol.* 108 (1989) 187-193
19. C. Schrimpf and G. H. Frischat, *J. Non-Cryst. Sol.* 56 (1983) 153-159
20. M. Murakami and S. Sakka, *J. Non-Cryst. Sol.* 101 (1988) 271-279
21. J.E. Shelby and J.T. Kohli, *J. Am. Ceram. Soc.* 73[1] (1990) 39-42
22. B. Bridge, N.D. Patel and D.N. Waters, *Phys. Stat. Sol. (a)* 77 (1983) 655-667
23. R. El-Mallawany, *Mater. Chem. and Phys.* [60] (1999) 103-131
24. J.A. Sampaio, M.L., S. Gama, A.A. Coelho, J.A. Eiras and I.A. Santos, *J. Non-Cryst. Sol.* 304 (2002) 293-298 .

25. J. Rocherulle, M. Matecki, Y. Delugeard, *J. Non-Cryst. Sol.* (1998) 51-56
26. Y.S. Touloukan, R. W. Powell, C.H. Ho and M.C. Nicolau, *Thermophysical properties of matter Vol 10, Thermal diffusivity* (1973) 577-580
27. C. Kittel, *Phys. Rev.* 75 [6] (1949) 972-974
28. W.D. Kingery, *J. Am. Ceram. Soc.* 38 [7] (1955) 251-255
29. F.R. Charvat and W.D. Kingery, *J. Am. Ceram. Soc.* 40 [9] (1957) 306-315
30. S.Inaba, S. Oda, K. Morinaga, *J. Non-Cryst. Sol.* In press
31. R.C. Weast and S.M. Selby, *Handbook of chemistry and physics* 48th ed (the Chemical Rubber Co, 1957), E6-E9

*Perfect as is the manufacture of glass for all ordinary purposes, and extensive the scale upon which its production is carried on, yet there is scarcely any substance in which it is so difficult to unite what is required to satisfy the wants of science.*

*Michael Faraday, 1830*

## Summary

---

Glasses have always played an important role in our civilisation and are expected to do so in the future. Some applications of glass are obvious such as container and windows glasses. Other applications are less obvious such as glass components for telecommunication or fuel cells. These applications are less visible for the general public since they are not produced in bulk and are usually hidden inside a device. These technical glasses are becoming increasingly important. As novel applications become more and more demanding in terms of glass properties the need for new glasses is growing. In this work we create glasses in which part of the oxygen is replaced by nitrogen and create oxynitride glasses with novel properties.

By replacing oxygen for nitrogen in a glass forming system, the basic advantages of a glass are preserved. It is transparent and relatively easy to shape and machine. But as previous work (as well as this thesis) shows, almost all properties of the glass are affected by the nitrogen incorporation. More specifically the chemical, mechanical and thermal durability of the glass increases which makes this a very interesting system for (future) applications.

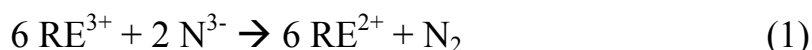
This thesis describes a broad explorative study towards the properties of one of the oxynitride systems, the RE-Si-Al-O-N glasses, RE being a rare earth ion. Goal of this work is to create a global understanding of the properties that can be achieved in these systems and to serve as a basis for more application driven research. However, in order to describe and explain the properties of these glasses, one has to have a detailed understanding of the chemistry and the structure of the materials. Therefore a large portion of this thesis deals with those aspects.

Apart from the effect that nitrogen poses on these systems, one important focal point of this investigation is on the rare earths, the reason being that the properties of these glasses are as much affected by the modifier cations (in this case rare-earth ions) as by the incorporation of nitrogen.

### *Chemistry*

Since the synthesis of Si-Al-O-N glasses requires a different atmosphere than oxide glass synthesis, the chemical equilibria in the glass change. In order to prevent oxidation of the glass during synthesis of oxynitride glasses the presence of oxygen in the furnace atmosphere has to be prevented. That has as a

consequence that many of the transition metal oxides, which are present as contamination in the raw materials, can spontaneously reduce to the metallic state and form (nano-sized) segregates in the glass. This has been observed in the case of iron in this work. Although the iron levels in the glass are too low to have a notable effect on the properties of the glasses, the transparency is adversely affected due to diffraction by the iron particles. This is the cause of the grey colour, which is so often observed for Si-Al-O-N glasses and it can only be prevented by the removal of iron from the glasses. A second effect is caused by the presence of nitrogen in the glass. Nitrogen can react during the synthesis with a number of rare earths according to the general reaction



The formed nitrogen gas then evolves from the melt. This reaction has for instance been observed for europium, samarium and ytterbium. The lowering of the oxidation state of these rare earths has a strong effect on the properties of the glass. As a secondary effect the nitrogen content of the glass is lowered, which also affects the properties of the glass.

### *Structure*

Nitrogen is incorporated on a bridging position. That means that nitrogen tends to bind with silicon as does oxygen. There are however some fundamental differences between the Si-O and the Si-N binding. Firstly nitrogen can bind three silicon atoms whereas oxygen can bind only two. This leads to a somewhat higher degree of cross-linking in the glass. The main effect is originating from the somewhat higher covalence of the Si-N bond as compared to the Si-O bond. The Si-N bond is not exactly stronger than the Si-O bond, however the  $\text{NSi}_3$  unit is much stiffer than the  $\text{OSi}_2$  unit. This enhances the rigidity of the glass network.

With luminescence spectroscopy new information was acquired on the position and the role that the rare earths play in these systems. Conventionally it is assumed that modifier cations occupy one type of sites in the glass. Due to the randomness of the glass network this site is not well defined as in crystalline matrices; it is therefore better to speak about a site distribution. However both for the divalent europium as for the trivalent cerium different types of emission were observed, suggesting that not one but multiple site distributions simultaneously exist in the glass. The main selection criterion for the population of these sites appears to be the size of the rare-earth. A large cation will

preferably occupy the larger sites. When there are no more large sites available, the excess will start to incorporate on the smaller sites. When there is a competition between two or more different cations the ions will be distributed over these sites according to their relative size.

Using the emission of  $Tb^{3+}$  we have been able to study the distribution of the rare earth ions in the glass. From the measurements we can conclude that the rare earths are even on a microscopic level homogeneously distributed in the glass and do not form segregates or domains with different rare earth concentrations.

### *Properties*

Because nitrogen enhances the rigidity of the glass network, the mechanical properties of the glasses are altered. It becomes increasingly difficult to deform or break. This results in an increased elastic modulus and hardness. Surprisingly the incorporation of nitrogen also leads to a strong increase of the resistance to subcritical crack growth. The reasons for this increase are unclear, but it appears that nitrogen interferes with one of the critical steps in the crack growth mechanism.

The effects of the different rare earth cations on the properties of the Si-Al-O-N glasses are mainly as expected from their behaviour in oxide glasses. As the size of the rare-earth ion decreases the bond density increases, as does the RE-O bond strength. Therefore the highest mechanical durability can be found for the smaller RE ions such as yttrium and gadolinium. Due to the reaction with the incorporated nitrogen some of the RE-ions are in a lower oxidation state in Si-Al-O-N glasses as they are in most oxide glasses. Since the ionic radius of the divalent state is larger than that of the trivalent state, the mechanical durability of the glasses is lower than expected.

The optical properties of the base glass remains virtually unaffected by the incorporation of nitrogen. However the enhanced reducing capacity of the Si-Al-O-N glasses allow some RE-ions to be stable in a lower oxidation state than is usually the case in oxide glasses, which makes these glasses an interesting medium to obtain e.g.  $Eu^{2+}$  luminescence.

The thermal conductivity of the glasses is only marginally affected by the nitrogen incorporation. In theory the thermal conductivity of these glasses should increase as a result of the increased rigidity of the glass matrix. This is indeed the case, but the effect is negligible as compared to the changes that can be obtained by variation of the overall composition.



## Samenvatting

---

Glas als materiaal heeft altijd een belangrijke rol in onze samenleving gespeeld, en de verwachting is dat dit in de toekomst niet anders zal zijn. Sommige toepassingen van glas zijn algemeen bekend zoals glazen voor vensters of containers. Andere toepassingen zijn minder bekend zoals componenten voor telecommunicatie toepassingen of glazen afdichtingen voor brandstofcellen. Deze glazen zijn min of meer onzichtbaar voor het gewone publiek, omdat het hier om een relatief kleine hoeveelheid glas gaat, dat bovendien nog eens vaak verstopt zit in een apparaat. Deze ‘technische’ glazen worden steeds belangrijker, echter de nieuwe toepassingen worden ook steeds veeleisender waar het gaat om de eigenschappen van de glazen. In deze studie maken wij oxynitride glazen door een gedeelte van het zuurstof in het glas te vervangen door stikstof. Op deze manier proberen wij tot glazen te komen met nieuwe of verbeterde eigenschappen.

Door zuurstof in een glas te vervangen door stikstof blijven de belangrijkste karakteristieken van een glas hetzelfde. Het blijft transparant en relatief makkelijk te vormen en te bewerken. Maar zoals blijkt uit andere onderzoeken (en dit proefschrift), veranderen de eigenschappen van de glazen sterk. Vooral de resistentie tegen hoge temperaturen, chemische aantasting en mechanische belasting nemen sterk toe. Dit maakt het glas zeer interessant voor (toekomstige) toepassingen.

In dit onderzoek wordt een breed scala aan eigenschappen bestudeerd van één van de oxynitride systemen, de RE-Si-Al-O-N glazen, waar bij RE een zeldzame aardion is. Het doel van dit werk is om een globaal overzicht te krijgen van de eigenschappen van deze systemen en zo de basis te leggen voor meer toepassingsgericht onderzoek. Echter om te kunnen begrijpen waarom een bepaald glas een bepaalde eigenschap heeft is het ook van belang om informatie te hebben over de chemie en de structuur van het glas. Daarom is een aanzienlijk deel van dit proefschrift gewijd aan die aspecten.

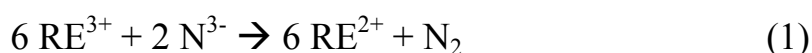
Behalve aan stikstof wordt er ook veel aandacht besteed aan de rol die de zeldzame aarden in dit systeem spelen. De reden hiervoor is dat de eigenschappen van een glas minstens even afhankelijk zijn van de zgn. modifierende kationen (in dit geval de zeldzame aarden) als van de inbouw van stikstof.



## Chemie

Omdat de synthese van Si-Al-O-N glazen plaatsvindt in een andere atmosfeer dan voor de synthese van oxidische glazen kunnen de chemische evenwichten in het glas verschuiven. Om ervoor te zorgen dat het glas niet oxideert tijdens het smelten moet de aanwezigheid van zuurstof in de ovenatmosfeer voorkomen worden. Een gevolg hiervan is dat veel overgangs metaal oxiden, die aanwezig zijn als een verontreiniging in de grondstoffen, spontaan kunnen reduceren tot de metallische vorm. Daardoor ontstaan metaal deeltjes in het glas. Dit gedrag is waargenomen voor ijzer in dit onderzoek. Omdat het ijzergehalte in de glazen zeer laag is worden de meeste eigenschappen van het glas niet beïnvloed door deze deeltjes. Echter omdat licht verstrooid wordt door de deeltjes daalt de transparantie van de glazen aanzienlijk. Dit is de oorzaak van de grijze kleur van Si-Al-O-N glazen. Deze kleuring kan alleen voorkomen worden door te zorgen dat de glazen vrij van ijzer zijn.

Een tweede effect wordt veroorzaakt door de aanwezige stikstof in het glas. Stikstof kan tijdens het smelten van het glas met een aantal zeldzame aarden reageren volgens de algemene reactie:



Het stikstof gas wat hierbij vrij komt vervliegt. Deze reactie is waargenomen voor europium, samarium en ytterbium. Doordat de oxidatietoestand van het zeldzame aardion lager wordt (2+ ipv. 3+) veranderen de eigenschappen van het glas sterk. Door de consumptie van stikstof door deze reactie is de uiteindelijke stikstofconcentratie in de glazen lager, wat een duidelijk effect op de eigenschappen heeft.

## Structuur

Stikstof bouwt in op een bruggende positie in het glas. Dit betekent dat stikstof (net als zuurstof) verbindingen vormt met silicium. Er zijn echter een aantal fundamentele verschillen tussen de Si-O en Si-N bindingen. Ten eerste kan stikstof drie silicium atomen aan zich binden terwijl zuurstof een coördinatie van twee heeft met silicium. Dit zorgt ervoor dat de bindingsdichtheid in het glas licht toeneemt. Echter het belangrijkste effect wordt veroorzaakt door de hogere covalentie van de Si-N binding ten opzichte van de Si-O binding. De Si-N binding is niet bepaald sterker dan de Si-O binding, maar de  $\text{NSi}_3$  eenheid is is

veel stijver dan de  $\text{OSi}_2$  eenheid. Dit leidt tot een hogere rigiditeit van de glasstructuur.

Het luminescentie onderzoek in dit proefschrift heeft geleid tot nieuw inzicht in de rol die de zeldzame aarden in deze systemen spelen. Normaal wordt aangenomen dat de modificerende kationen één soort plaats innemen in het glas. Door de wanordelijke natuur van glazen zijn deze sites niet zo goed gedefinieerd als in kristallijne materialen, de omringing kan enigszins verschillen van plaats tot plaats. Het is daarom beter om te spreken over een ‘site populatie’. In dit onderzoek is echter voor zowel voor divalent europium als trivalent cerium verschillende soort emissie waargenomen wat erop duidt dat er meerdere soorten populaties naast elkaar in een glas kunnen bestaan. De grootte van het kation bepaalt welke populatie gevuld wordt. Een groot kation zal de populatie met de grootste sites het eerst vullen. Wanneer deze volledig gevuld zijn, zullen de overgebleven kationen gedwongen worden op kleinere sites in te bouwen. Zo zal ook in het geval van competitie tussen verschillende kationen de verdeling over de verschillende populaties bepaald worden door de onderlinge grootte.

Door het bestuderen van de emissie van  $\text{Tb}^{3+}$  in de glazen hebben wij ook informatie verkregen over de distributie van de zeldzame aardionen in het glas. Uit de metingen kunnen wij concluderen dat de zeldzame aarden ook op een microscopisch niveau uniform verdeelt zijn in het glas en dat er geen sprake is van concentratieverschillen door segregatie of domein vorming.

### *Eigenschappen*

Omdat de rigiditeit van het glas netwerk wordt versterkt door de aanwezige stikstof veranderen de mechanische eigenschappen van het glas. Met toenemend stikstofgehalte wordt het moeilijker om het glas te deformeren of te breken. De elasticiteit neemt af en de hardheid neemt toe. De weerstand tegen langzame scheurgroei neemt verrassenderwijs zeer sterk toe. Wij hebben nog dit niet helemaal kunnen verklaren, omdat het mechanisme achter langzame scheurgroei nog onduidelijk is, maar het lijkt erop alsof het aanwezige stikstof interfereert met een van de kritieke stappen in het mechanisme.

Het effect van de verschillende zeldzame aarden op de eigenschappen van de glazen is hoofdzakelijk hetzelfde als in oxidische glazen. Een kleiner kation resulteert in een hogere bindingsdichtheid en een sterkere RE-O binding. Daardoor neemt de mechanische resistentie toe naarmate de straal van het zeldzame aardion afneemt. Zoals eerder vermeld bevinden sommige zeldzame aarden zich in een lagere oxidatietoestand door een reactie met de aanwezige

stikstof. Doordat een ion in de tweewaardige toestand een grotere straal heeft dan in de driewaardige toestand neemt de rigiditeit van het glas af.

De optische eigenschappen van het basisglas veranderen niet of nauwelijks door de inbouw van stikstof. Omdat de Si-Al-O-N glazen zeer reducerend zijn, zijn enkele zeldzame aard ionen stabiel in een lagere oxidatietoestand dan in de meeste oxidische glazen. Dit maakt deze systemen een aantrekkelijk medium om bijvoorbeeld  $\text{Eu}^{2+}$  luminescentie op te wekken.

De thermische geleiding van de glazen verandert nauwelijks door de stikstofinbouw. In theorie zou de geleiding toe moeten nemen door de toename van de rigiditeit van het glas netwerk. Dit gebeurt inderdaad, maar het effect is miniem vergeleken bij de invloed van de andere componenten.

## Dankwoord

---

Toen ik voor het eerst een proefschrift onder ogen kreeg, verbaasde ik mij over het dankwoord. De hoeveelheid mensen die daarop verscheen leek nauwelijks toepasbaar op een enkel promotieonderzoek en eerder afkomstig van een project ter grootte van zeg de Kanaaltunnel. Nu ik terugkijk op mijn promotie begin ik te beseffen hoeveel mensen er direct en indirect betrokken zijn bij een promotie; hoe vaak je een beroep op mensen moet doen



en hoe je volkomen vast kan komen te zitten als zij bijvoorbeeld een keertje op vakantie zijn. Om onconventioneel te beginnen zou ik graag *Ron Hoekstra* en *Ria Weijers* willen bedanken die een rebelse puber hebben weten te interesseren in de chemie en dus direct verantwoordelijk mogen worden gehouden voor mijn aanwezigheid hier op de TU/e.

Verder zijn er natuurlijk mijn (ex)collega's van de groep Vaste Stof en Materiaalchemie:

*Huub van der Palen, Anneke Delsing, Niek Lousberg, Marco Hendrix, Hans Heijligers* en *Sacha Kodentsov*, die ervoor zorgen dat wij daadwerkelijk onderzoek kunnen doen. Zonder kundige ondersteuning is een apparaat slechts een dure vorm van labdecoratie, iets wat helaas te vaak vergeten wordt.

Mijn begeleider *Bert Hintzen*, omdat hij minstens even eigenwijs is als ik. Maar vooral omdat hij mij heeft laten zien hoe je met relatief weinig middelen innovatief en relevant wetenschappelijk onderzoek kan doen.

*Joost van Krevel* voor al de keren dat ik hem wreed verstoord heb in zijn overpeinzingen om domme vragen over luminescentie te stellen.

*Giel Bastin* voor zijn inbreng in het EPMA gedeelte en de begeleiding van een aantal studenten. Door zijn zorg ben ik in ieder geval goed georiënteerd mijn promotie doorgekomen.

*Ruud Metselaar* die mij op een aantal congressen onder zijn vleugels heeft genomen en als constante factor op de achtergrond van mijn onderzoek aanwezig is geweest.

*Bert de With* voor het promotorschap, de vele discussies en het inhoudelijk becommentariëren van mijn werk.

*Xaviera Reynhout, Sjoerd Stelwagen, Aarnoud Dommissie, Raoul Martens, Lianne van der Linde, Alexandra Oberndorff-Laska, Marek Bracissiewicz en Tomasz Kepa.* Als studenten hebben zij een belangrijke bijdrage aan dit werk geleverd, en ik hoop dat zij daar net zoveel van geleerd hebben als ik. Ik wens hun veel succes in de toekomst.

*Linda van Loon-Nunen en Imanda Scholten-Kamstra* die (behalve het feit dat het beiden notoire theedrinkers zijn) gemeen hebben dat ze begrijpen dat de sfeer essentieel is voor het functioneren van een groep en daar beiden op geheel eigen wijze invulling aan geven en gegeven hebben.

Tenslotte zijn er nog mijn mede AIO's (en OIO's) met wie ik een zeer plezierige tijd gehad heb, ook buiten het werk.

Ook heb ik het geluk gehad om gedurende mijn promotie samen te werken met een aantal buitenlandse instellingen, waar ik zelfs te gast heb mogen zijn. Daarom.

*Stuart Hampshire, Valerie Peltier-Baron, Yvonne Menke and your colleagues in Limerick,* thank you for your very warm welcome in a cold Ireland and thank you for keeping me out of (too much) trouble, but foremost, thank you for introducing me to the Si-Al-O-N glasses.

*Kandalam Ramanujachary,* thank you for all the work you've done. I thoroughly enjoyed our late-night conversations at the coffee corner.

*Malgorzata Sopicka-Lizer,* thank you for trusting your students with me. I just hope that you didn't expect them to come back.

Onderzoek kost natuurlijk geld en daarom zou ik ook *TNO* willen bedanken voor de financiële ondersteuning van dit project.

En tenslotte is er nog het thuisfront.

*Karin Seijdell* voor haar geduld en vertrouwen. Het is lastig met iemand samen te wonen die af en toe vergeet thuis te komen voor het eten omdat 'hij net midden in een interessante berekening zat'.

*Tijger* en *Bunny* wiens eindeloos gelam, gedoezel en gedut aanstekelijk werkt. Zij hebben er zo voor gezorgd dat ik mijn promotie op een uiterst relaxte manier heb kunnen afronden.

## List of Publications

---

1. D. de Graaf, H.T. Hintzen, J.W.H. v. Krevel, G. de With, R. Metselaar, V. Baron, Y. Menke, en S. Hampshire; “Beter glas door stikstof”, KGK 10 (2000) 21-25
2. D. de Graaf, H.T. Hintzen, J.W.H. v. Krevel, G. de With, R. Metselaar, V. Baron, Y. Menke and S. Hampshire, “The dependence of the optical properties of (Eu,Y)-Si-Al-O-N glasses on their chemical composition”, proceedings of the XVIII<sup>th</sup> International congress on glass, Amsterdam (2000)
3. D. de Graaf, A. Dommissie, X.E.E. Reynhout, G.F. Bastin en H.T. Hintzen, “Analyse van ultralichte elementen in Sialon glas door middel van EPMA/WDS” KGK 2 (2001) 15-18
4. D. de Graaf, H.T. Hintzen, R. Metselaar & G. de With, “Unusual Eu<sup>2+</sup> and Ce<sup>3+</sup> luminescence in M-Si-Al-O-N (M = Sc, Y, La, Gd) glasses”, proceedings of the XIX<sup>th</sup> International congress on glass, Edinburgh (2001)
5. D. de Graaf, H.T. Hintzen, R. Metselaar and G. de With, “Unusual luminescence phenomena in Ce(III)-doped M-Si-Al-O-N glasses (M = Sc, Y, Gd, La)”, Key Engineering Materials, Volume 206-213, Issue III (2001) 2065-2068
6. M. Braciszewicz. D. de Graaf, H.T. Hintzen. M. Sopicka-Lizer, “Load-dependence of the microhardness of Y-Si-Al-O-N glasses measured by Vickers indentation”, Polish Ceramic Bulletin 66/2 (2001). 664-669
7. D. de Graaf, R. Metselaar, H.T. Hintzen, G. de With, “Unusual long-wavelength excitation and emission in Eu<sup>2+</sup> and Ce<sup>3+</sup> doped M-Si-Al-O-N glasses (M = Sc, Y, La, Gd)”, Optoelectronics - Materials & Technology in the Information Age, Ceramic Transactions, Volume 126 (2002) 31-36
8. D. de Graaf, H.T. Hintzen, S. Hampshire and G. de With, “Long wavelength Eu<sup>2+</sup> emission in Eu-doped-Y-Si-Al-O-N glasses”. J. Eur. Ceram. Soc. 23 (2003) 1093-1097
9. D. de Graaf, H.T. Hintzen, G. de With., “The influence of the composition on the luminescence of Ce(III) –Ln-Si-Al-O-N glasses (Ln = Sc,Y,La,Gd), J. Lum. 104 (2003) 131-136
10. D. de Graaf, S.J. Stelwagen, H.T. Hintzen and G. de With, “Tb<sup>3+</sup> luminescence as a tool to study lanthanide clustering in oxynitride glasses”, J. Non-Cryst. Sol. 325 (2003) 29-33

11. D. de Graaf, S. Le Rol, H.T. Hintzen, L. Le Gendre and G. de With, "Reduction of lanthanide ions in Si-Al-O-N glasses" *Key Engineering materials Accepted*
12. D. de Graaf, M. Braciszewicz, H.T. Hintzen, M. Sopicka-Lizer and G. de With, "The influence of the composition on (the load-dependence of) the microhardness of Y-Si-Al-O-N glasses as measured by Vickers indentation", *J. Mater. Sci. Accepted*
13. H.T. Hintzen, J.W.H. van Krevel, D. de Graaf, R. Metselaar, Y. Menke and S. Hampshire, "Evidence for the presence of  $\text{Eu}^{2+}$  in (Y,Eu)-Si-Al-O-N glass by luminescence spectroscopy", *J. Mater. Sci. Lett. Accepted*

### Submitted/in preparation

14. D. de Graaf, S. le Rol, H.T. Hintzen, L. le Gendre and G. de With, "Mixed oxidation states of Yb and Sm in Si-Al-O-N glasses", *J. Mater. Chem. submitted*
15. D. de Graaf, H.T. Hintzen, G. de With, K.V. Ramanujachary C. Lanci and S.E. Lofland, "Quantitative determination of  $\text{Eu}^{2+}$  and  $\text{Eu}^{3+}$  content in (Eu,Y)-Si-Al-O-N glasses by magnetic measurements", *Solid State Comm. submitted*
16. D. de Graaf, H.T. Hintzen and G. de With, "The origin of ironsilicides in Si-Al-O-N glasses", *in preparation*
17. D. de Graaf, H.T. Hintzen and G. de With, "Subcritical crack growth and power law exponent of Y-Si-Al-O(-N) glasses in aqueous environment", *in preparation*
18. D. de Graaf, H.T. Hintzen and G. de With, "Optical properties of rare-earth oxynitride glasses: a review", *in preparation*

### Other

19. De Mantel van Lucas, een historische reconstructie van het pigment smalt, VPRO Noorderlicht 12 Dec 2001 (*TV-documentary*)
20. M.A.H. Donners, J.J.M.G Dortmans, G. de With and D. de Graaf, "Minima in the strength of MnZn ferrites", *J. Mater. Res.* 16 (2001) 3575

*see also*

M.A.H. Donners, J.J.M.G Dortmans, G. de With and D. de Graaf, "Erratum to Minima in the strength of MnZn ferrites", *J. Mater. Res.* 18 [8] (2003) 1

## Curriculum Vitae

---

Dennis de Graaf is geboren op 29 juli 1974 te Purmerend. Hij behaalde zijn VWO diploma in 1993 aan het Murmellius Gymnasium te Alkmaar. In dat zelfde jaar begon hij met zijn studie scheikundige technologie aan de Technische Universiteit Eindhoven. Tijdens de studie heeft hij zich toegelegd op het gebied van vaste stof en materiaalchemie door middel van een interne stage met als onderwerp langzame scheurgroei in MnZn ferrieten. Verder heeft hij in het kader van zijn industriële stage bij Philips Centrum voor Fabricagetechnieken onderzoek gedaan naar de interacties tussen een glassmelt en (gecoate) stempels voor het persen van televisiebeeldschermen. Tijdens zijn afstuderen heeft hij onderzoek gedaan naar de synthese en eigenschappen van (Eu,Y)-Si-Al-O-N glazen. Deze opdracht is gedeeltelijk uitgevoerd in Ierland aan de Universiteit van Limerick en gedeeltelijk aan de Technische Universiteit Eindhoven binnen de groep Vaste Stof en Materiaalchemie (SVM). In november 1999 heeft hij deze studie afgesloten. Aansluitend is hij een promotie begonnen aan de Technische Universiteit Eindhoven, wat geresulteerd heeft in dit proefschrift.

Dennis de Graaf was born on July the 29<sup>th</sup> 1974 in Purmerend. He received his secondary education at the Murmellius Gymnasium in Alkmaar, from which he graduated in 1993. In the same year he started his study chemical technology at Eindhoven University of Technology. During this study he has introduced to the field of solid state and materials chemistry by an internship on slow crack growth in MnZn-ferrites. He further performed a traineeship at the Philips Center for Manufacturing Technology on the interactions between a hot glass melt and a (coated) pressing plunger used for the fabrication of TV-screens. During his master project he worked on the synthesis and properties of (Eu,Y)-Si-Al-O-N glasses. This project was partially performed at the University of Limerick (Ireland) and partially at the group Solid-State and Materials Chemistry (SVM) of Eindhoven University of Technology. In November 1999 he completed his masters studies, after which he started his graduation project at Eindhoven University of Technology, which has resulted in this thesis.



Stellingen behorende bij het proefschrift

**Chemistry, Structure and Properties of Rare-Earth Containing  
Si-Al-O-N Glasses**

Dennis de Graaf

- 1.) The adaptation of the electrostatic model of Makishima and Mackenzie by Rocherulle et al. for oxynitride glasses is not physically correct as they suggest. Disregarding black hole conditions, AlN with a packing factor of 1.0284 is an impossibility, which reduces this model to an elaborate fitting procedure rather than a serious modeling attempt.

*J. Rocherulle, C. Ecolivet, M. Poulain, P. Verdier and Y. Laurent, Elastic moduli of oxynitride glasses: Extension of Makishima and Mackenzie's theory, J. Non-Cryst. Sol. 108 (1989) 187-193*

- 2.) The multitude of reactions which can occur in an oxynitride glass melt, plus the uncertainty in the composition of the furnace atmosphere, should urge researchers to caution when it comes to drawing conclusions based on relatively simple thermodynamic calculations.

*D.R. Messier and E.J. Deguire, Thermal decomposition in the system Si-Y-Al-O-N, J. Am. Ceram. Soc. 67 (1984) 602-605*

- 3.) In EPMA(WDS) on non-electrically conducting materials, two wrongs can make a right.

*P.F. McMillan, R.K. Sato and B.T. Poe, Structural characterization of Si-Al-O-N glasses, J. Non-Cryst. Sol. 224 (1998) 267-276*

- 4.) Luminescence spectroscopy is an enlightening technique to investigate the local structure of solids and should therefore be applied more to investigate the structure of glasses.

*J. Rakovan and G. Waychunas, Luminescence in minerals, The Mineralogical Record 27 (1996) 7-19*

- 5.) Trying is the first step towards failure.  
*Homer Simpson*
- 6.) It is my firm belief that nature tends to favor relatively simple solutions for complex problems whereas modern modeling seems to be more involved with finding very complex solutions for relatively simple problems.
- 7.) The design of foolproof research equipment will only encourage researchers to use them in a foolish way.
- 8.) For most car owners the main problem with the public transport is not its speed, cost or reliability, but its lack of social status.
- 9.) Politics are too serious a matter to be left to the politicians.  
*Charles de Gaulle, 1890-1970*
- 10.) Efforts towards a sustainable “hydrogen economy” should be focused on hydrogen production, transport and storage. Application (hydrogen-driven cars, buses etc.) is only of secondary importance.  
*Worldwide, 48% of hydrogen is produced from natural gas, 30% from oil, 8% from coal, and the remaining (4%) via water electrolysis (source U.S. Department of Energy)*
- 11.) Because of the accumulation of high debts by governments, companies and individuals alike, the term “capitalism” can better be replaced by “debtalism” to describe the present day western societies.
- 12.) Sift through the internet and you’ll find argumentation for every view imaginable, and indeed, unimaginable. The challenge for the next generation of search engines is to find that, which is refereed, factual and trustworthy.
- 13.) The chemical faculties should realize that it is still the fiery and explosive demonstrations, which appeal the most to students. Any activity to attract new students should therefore at least contain an explosive component.